Footwall basal thrust, Sakatti Cu-Ni-PGE deposit, Northern Finland

Matti Vuorisalo
University of Turku
Department of Geography and Geology
Bedrock geology
June 2021

University of Turku

Department of Geography and Geology, Geology section

Vuorisalo, Matti: Footwall basal thrust, Sakatti Cu-Ni-PGE deposit, Northern Finland

MSc thesis, 78 p + 6 appendices pp.

Geology and mineralogy

June 2021

The Sakatti Cu-Ni-PGE deposit, located ~20 km northeast from the municipality of Sodankylä, has been formerly investigated mainly for its economic potential, while the structural character of the deposit has been left in the background. An example of this is the minor amount of oriented drill cores that would have penetrated and reached the essential geological structures. The present study focuses on the footwall basal thrust, a major geological structure in the deposit.

The first main objective of this study was the kinematic interpretation of the thrust, which was investigated based on the observed geological structures and deformation trends in the rocks above and below the thrust. Data about the deformation and kinematics related to the thrust were gathered by analyzing dipmeter-data, drill core and thin section observations and by conducting a study that focused on stratigraphic separations and unit continuations.

According to new observations and interpretations the rock units were displaced towards SW during progressive D_1-D_2 phases, which consisted of overthrusting and subsequent overturned folding. The overthrusting took place along SW-vergent thrust faults, to which the footwall basal thrust probably belonged. During D_3 phase the thrust and the rock units were ductilely deformed in NNW-SSE compression that resulted in buckling of the thrust and rock units against a competent ultramafic body, which formed a large-scale open fold. The buckling was observed as NW-dipping rock units and structures west of the axial trace of the large scale fold, while on the eastern side all units and structures dip to NE.

Later, a renewed NNW-SSE compression displaced the rock units and the footwall basal thrust within one domain towards SSE by lateral strike-slip movement during a brittle D_4 phase. A model is presented for this phase, in which SE-NW directed vertical faults are conjugate fault planes for the displacements.

Local stratigraphy in Sakatti has not been yet correlated to any regional stratigraphic groups, although discovery of such a correlation would increase our understanding of the geological history of the deposit. Therefore, the second main objective of this study was to stratigraphically classify the rock units above and below the footwall basal thrust. The whole rock analysis, thin section studies and observations indicated that the metasedimentary rocks below the thrust correlate well with the upper parts of the Sodankylä Group, while the overlying ultramafic rocks do not seem to correspond to the Savukoski Group but rather to the Kevitsa intrusion.

Turun yliopisto

Maantieteen ja geologian laitos, Geologian osasto

Vuorisalo, Matti: Footwall basal thrust, Sakatti Cu-Ni-PGE deposit, Northern Finland

Pro gradu – tutkielma, 78 s. + 6 liites.

Geologia ja mineralogia

Kesäkuu 2021

Noin kaksikymmentä kilometriä Sodankylästä koilliseen sijaitsevaa Sakatin esiintymää on aiemmin tutkittu lähinnä sen taloudellisen potentiaalin kannalta, jolloin esiintymän rakenteen ja rakennekehityksen tutkimus on jäänyt vähemmälle huomiolle. Tästä syystä suuri osa kairasydämistä on suuntaamattomia ja vain osa kairauksista yltää rakenteisiin, jotka ovat saattaneet olla merkittäviä esiintymän kehittymisessä. Tässä työssä keskitytään yhteen rakenteeseen, joka Sakatissa tunnetaan nimellä jalkapuolen pohjaruhje.

Tutkimuksen ensimmäinen päätavoite oli pohjaruhjeen kinematiikka, jota selvitettiin pohjaruhjeen molemmilta puolilta havaittujen geologisten rakenteiden ja deformaatiotrendien avulla. Tutkimusaineisto koostui kairareikädatasta, ohuthiehavainnoista sekä stratigrafisessa erottelussa havaituista ominaisuuksista ja yksiköiden jatkuvuuksista.

Aineiston ja siihen perustuvan tulkinnan perusteella kivilajiyksiköt siirtyivät kohti lounasta ylityönnön ja myöhemmän ylikääntyneen poimutuksen aikana, jotka yhdessä muodostavat progressiiviset D_1-D_2-deformaatiovaiheet. Ylityöntö tapahtui lounaaseen pitkin ylityöntösiirroksia, joihin pohjaruhje todennäköisesti kuuluu. D_3-vaiheen aikana pohjaruhje ja kivilajiyksiköt deformoituivat duktiilisti NNW–SSE-suuntaisessa kompressiossa, joka taivutti pohjaruhjeen ja kivilajiyksiköt kompetenttia ultramafista pakettia vasten muodostaen nykyisen suuren, avoimen poimun. Poimurakenne ilmenee luodetta kohti kaatuvina kivilajiyksikköinä ja rakenteina suuren poimun akselitason länsipuolella, ja koilliseen kaatuvina rakenteina sen itäpuolella.

D_4-vaiheen NNW–SSE-kompression aikana pohjaruhje ja kivilajiyksiköt liikkuivat kahden hauraan siirroksen rajaamina kohti eteläkaakkoa. Tälle deformaatiovaiheelle esitettiin malli, jonka mukaan siirrokset ovat toistensa konjugaatteja.

Sakatin esiintymää ei ole vielä pystytty osoittamaan kuuluvaksi mihinkään Keski-Lapin vihreäkivivyöhykkeen stratigrafisista yksiköistä, vaikka se auttaisi esiintymän geologisen historian ymmärtämistä. Siksi tämän tutkimuksen toinen päätavoite oli pohjaruhjeen lähellä olevien kivilajien stratigrafinen luokittelu. Kokokivianalyysit ja ohuthietutkimukset osoittavat, että pohjaruhjeen alapuolella olevat metasedimentit muistuttavat hyvin paljon Sodankylän ryhmän ylimpiä kivilajiyksiköitä. Pohjaruhjeen yläpuolella olevat kivilajiyksiköt eivät kuitenkaan vertaudu selvästi Savukosken ryhmän kiviin, vaan muistuttavat paremminkin Kevitsan intruusion kivilajeja.

Table of contents

1. Introduction

1.1 Sakatti Cu-Ni-PGE Deposit

The Sakatti Cu-Ni-PGE deposit, currently held by AA Sakatti Mining Oy, is located ~20 km northeast from the municipality of Sodankylä in Northern Finland (fig. 6) and forms one of the most significant Cu-Ni sulphide discoveries in Finland and globally (Brownscombe et al. 2015). It was discovered in 2009 by the Anglo American Exploration Finland Team that was led by Jim Coppard (Brownscombe et al. 2015). The main deposit is hosted by a large ultramafic body, while there are two smaller satellite ultramafic bodies that also host ore mineralizations (Brownscombe et al. 2015). The ultramafic bodies are surrounded by volcanic and metasedimentary rocks, which have not yet been successfully correlated to any regional stratigraphic group. The deposit has been formerly investigated mainly geochemically and petrographically, while its structural characteristics have not been studied in detail. One reason for this is the lack of outcrops in Sakatti, as the deposit is situated below the Viiankiaapa swamp. Thus, the overall data about the deposit and geological structures has mainly been obtained by drilling, while geophysical research has supplemented the data. Since 2017 most of the drill cores have been oriented, which has enabled detailed structural investigation to be performed for drill cores. This study aims at advancing the structural comprehension of the deposit, although concentrating on a single dominating structure, called the footwall basal thrust.

1.2 Study zone

The study zone covers a ~1.5 x 1.5 x 1.0 km large zone (figs. 6 & 11) that is penetrated by drill cores that comprise the material of this study. The drill cores only reveal small windows to the subsurface bedrock, thus in reality covering much smaller area than the above-mentioned study zone itself. However, as surface data is not available, the drill cores offer useful data to interpret the subsurface geology and geological structures.

1.3 The footwall basal thrust

The footwall basal thrust is situated in great depths below the main ultramafic body and above the underlying metasedimentary rocks, and its status in the regional geological context is unknown. The term footwall is given to the thrust as it is located on the footwall side of the main deposit. It is characterized by thick clayish rubble zone in fault core and associated fault rocks and fragments from the surrounding rock units. Luukas (Anglo American internal reports) modelled it as a two-parts northwards dipping thrust with a listric fault shape. Its kinematic history, relative age and impact on the deposit

and structures in Sakatti are yet unknown. As the data used in this study is only consisted of very limited drill hole data, certain assumptions had to be made about the footwall basal thrust: 1) By definition, the footwall basal thrust follows the contact between the ultramafic main body and underlying metasedimentary rocks, although in reality it is possible that the thrust does not follow the contact continuously; 2) The footwall basal thrust has parallel orientation with the underlying metasedimentary rocks and with dominating planar structures in the study zone and near the thrust. These assumptions were not treated as rules, but they formed the initial basis investigated and discussed further in this study.

1.4 Structures and drill core logging

Only a minor proportion of a target of interest is penetrated by drill holes, which produces difficulties in geological interpretation of a study zone. In addition, since drilling projects typically aim at finding economically profitable mineral deposits, the geological structures are sometimes left in the background, even if they commonly control the deposit. In the present case of Sakatti this is exemplified by the small amount of oriented drill cores penetrating and reaching essential geological structures, such as the footwall basal thrust. The thrust is technically difficult to penetrate in drilling, which is also one reason for the small amount of oriented drill cores that have penetrated the thrust. As the only measurable ductile structures near the thrust occurred within the metasedimentary rocks, which only covered relatively small sections below the main ultramafic body, the data obtained by the measurements is limited. Furthermore, rubble zones and broken drill core intervals complicated the investigation. The structural data was complemented by investigating the non-oriented drill cores of which several reach the footwall basal thrust and metasedimentary rocks. Their structural investigation included a special method that will be presented next. The management and interpretation of the structural data obtained by the measurements also included a profound dipmeter-data management and analysis.

Dipmeter-data

Measured structural data can be analyzed in several manners, such as stereoplot analysis, fracture density analysis or by drawing sketches during drill core logging. Another advantageous method is illustrated in figure 1, where dip and dip azimuth values are separately plotted in relation to compressed vertical scale (Fossen, 2010). The diagrams facilitate the identification of geological structures and their nature. Sudden changes in dip or dip azimuth values usually refer to a presence of faults, which separate

different blocks where the foliation is differently oriented, whereas progressive and rapid changes in local rock intervals are called cusps and are related to fault related drags (fig. 1, Fossen, 2010). In addition, anomalous values close to fractures or deformation bands can reveal a fault (Fossen, 2010). The dipmeter-data obtained in this study was analyzed by using the above-mentioned method, which turned out to be extremely useful and provided valuable information about the deformation.

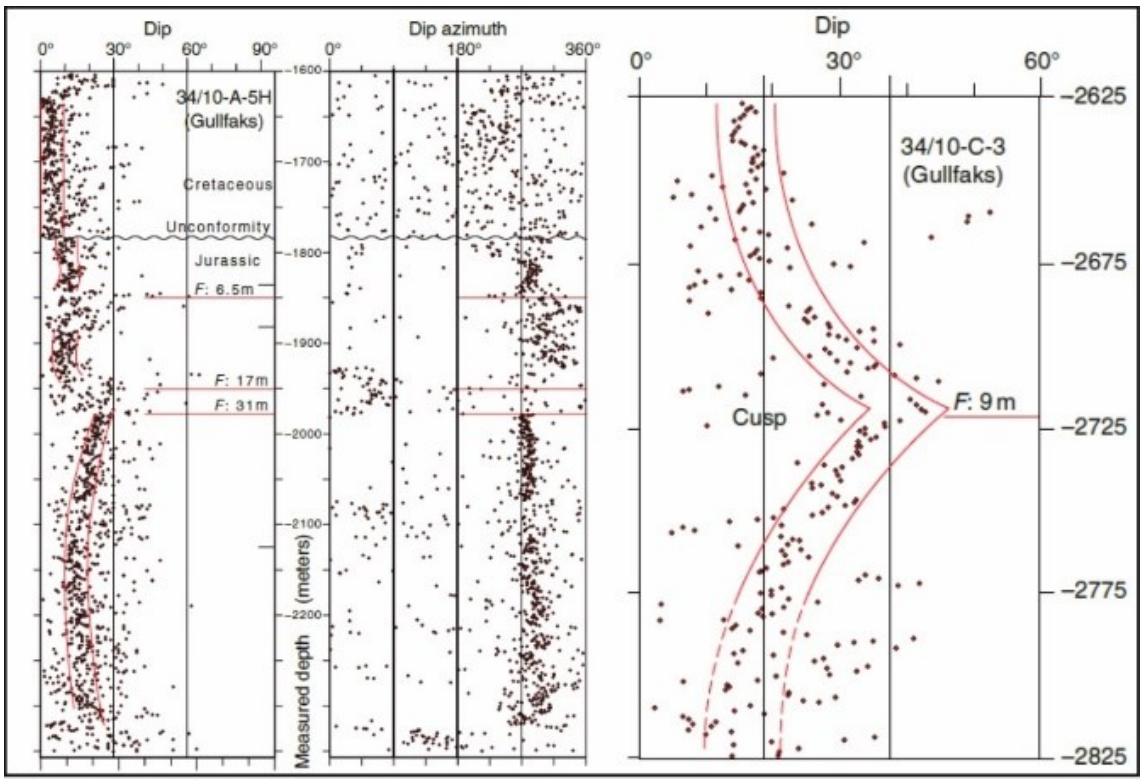

Figure 1. One advantageous method for analyzing and interpreting dipmeter-data presented. The vertical scale in y-axis is compressed and the dip and dip azimuth values are plotted separately in relation to depth. The diagrams on left and center describe how faults (red lines) are identified from the diagrams. The diagram on the right identifies a ductile drag around a fault. Modified after Fossen (2010).

Stratigraphic separation study and stratigraphic correlation

Non-oriented drill cores were utilized in the structural investigation by conducting a stratigraphic separation study, where each non-oriented and oriented drill core was first described and characterized by lithology, then divided in stratigraphic units and finally demonstrated in several cross sections. In cross sections, the repeated or missing sections were detected on purpose to identify faults and comprehend unit continuations and deformation (fig. 2). Unusual repeated or missing sections observed in an area whose stratigraphy is known are results from drilling through a fault (Fossen, 2010). Typically, although not exclusively, reverse faults are observed as repeated sections in drill cores while normal faults result in omission of stratigraphical units and create stratigraphical gaps (fig. 2, Fossen, 2010). A stratigraphic separation study can also

provide information about the amount of fault displacement. Some of the faults observed in the study were also detected during core logging, and for that reason their positions in stratigraphic columns and drill core were recorded during core logging and compared with the faults observed in the stratigraphic separation study.

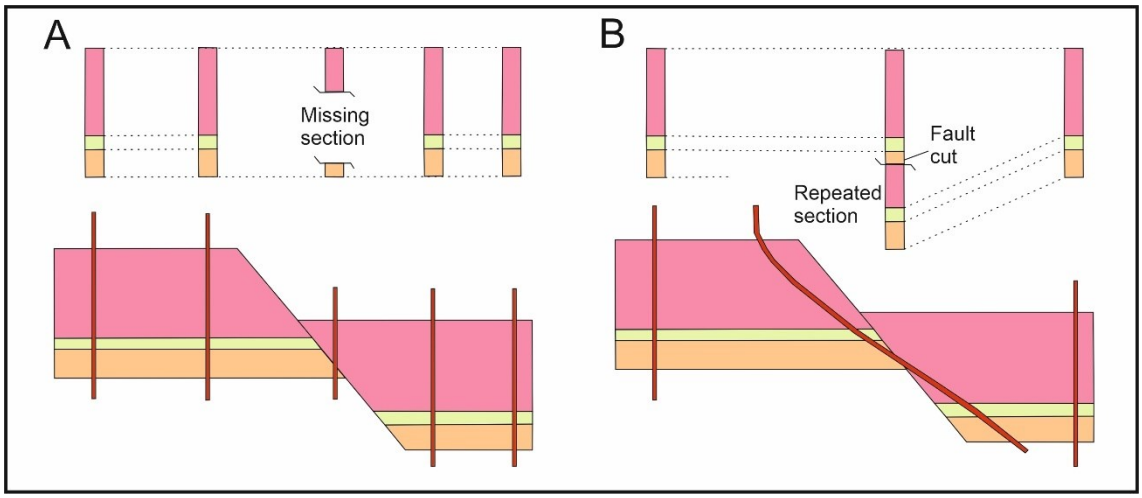

Figure 2. A method for investigating stratigraphic separations illustrated in two cases. A: Missing section in vertically oriented drill holes (red lines) indicates a presence of a normal fault. B: Repeated section in an inclined drill hole that is less steep than a fault also indicates a presence of a normal fault. Repeated sections usually infer to a presence of a reverse fault. Modified after Fossen (2010).

1.5 Earlier studies

Since its discovery, several studies have been performed of the Sakatti deposit. Brownscombe et al. (2015) and Brownscombe (2015) presented the main features of the Sakatti deposit, mainly focusing on geochemical signatures, rock units and petrography in ultramafic rocks, but additionally presented a model for the formation of the Sakatti deposit. Previously, the ultramafic bodies in Sakatti have been thought to belong to the Savukoski Group as they are surrounded by the Sodankylä and Savukoski Groups in the geological map (fig. 6), of which the latter has been reported to contain ultramafic volcanic rocks in its upper parts (in e.g., Lehtonen et al. 1998). In the study of Brownscombe (2015) the ultramafic bodies hosting the mineralizations were further compared with regional stratigraphic units and intrusions. He concluded that the Savukoski Group exhibits distinctively different ε_{Nd} values from those values calculated for the Sakatti intrusion that does not support their close genetic relationship. Instead of the Savukoski Group, the Kevitsa intrusion was described as more similar to the Sakatti intrusion and a shared genetic history between them was suggested (Brownscombe (2015).

The petrology and geochemistry of the rock units in the Sakatti deposit were comprehensively investigated in the studies of Halkoaho (Anglo American internal

reports, 2014, 2015 & 2019). Those studies provided essential information about the mineralogy and geochemical signatures of rock units. However, they did not particularly focus on the metasedimentary rocks, although some samples were geochemically analyzed. Since no later studies exist about the metasedimentary rocks close to the study zone, this study is the first attempt to describe and correlate them with regional stratigraphic units, although the observations made in the studies of Halkoaho (Anglo American internal reports, 2014, 2015 & 2019) need to be recognized in this context. However, several regional stratigraphical studies have been performed in the CLGB and in Sodankylä region, of which particularly the studies of Lehtonen et al. (1998), Hanski & Huhma (2005) and reports of Räsänen (1996, 2008 & 2018) provided useful data for comparison. In addition, a recently published report about the Sodankylä Group metasediments (Köykkä & Luukas, 2021) offered new and useful data for the stratigraphic correlation.

The most comprehensive structural studies performed in Sakatti include mainly the Anglo American internal reports of Luukas (2016, 2017 & 2018), in which lithological and fault models for the Sakatti deposit are presented. These studies also provided the initial information about the footwall basal thrust, while its detailed structural characterization is at the grassroots level. The deformation history interpreted in this study will be compared with the regional tectonic history and regional structural investigations, of which the studies of Evins & Laajoki (2002) and Lahtinen & Huhma (2019) are especially important.

1.6 Research questions

The footwall basal thrust has possibly had a major influence on the surrounding rock units and on the deposit. Comprehension of the local kinematic history and metamorphic conditions during the deformation would be vital in interpreting the significance of the footwall basal thrust to the deposit and surrounding rocks. Thus, in this project one of the two main objectives is

1) the kinematic interpretation of the footwall basal thrust, which is investigated based on the ductile structural trends observed in the rocks above and below the footwall basal thrust.

Moreover, as mentioned the rocks in the Sakatti deposit have not been successfully correlated to any regional stratigraphic group or intrusion. According to present hypothesis and a geological map (fig. 6), the metasedimentary rocks represent the Sodankylä Group, while the ultramafic rocks would belong to the Savukoski Group.

Verification of this hypothesis would promote geological understanding of the whole deposit and of the relation between the deposit and the ultramafic and metasedimentary rocks. The second main objective of this study focuses on this subject, which is

2) to test whether the metasedimentary rocks below the footwall basal thrust truly correlate with the Sodankylä Group rocks and whether the ultramafic and mafic rocks above the footwall basal thrust correlate correspondingly with the Savukoski Group rocks.

The project is performed as a contract work for AA Sakatti Mining Oy owned by Anglo American Ltd, who funded the study. The study was planned in collaboration between the Geological Survey of Finland, the University of Turku and the AA Sakatti Mining Oy.

2. Geological background

2.1 Overview

The Sakatti Cu-Ni-PGE deposit, geologically situated within the Fennoscandian Shield and Paleoproterozoic Central Lapland Greenstone Belt (figs. 3-5), has a complex geological history that has been under debate since its discovery. The greenstone belt records a depositional evolution of both sedimentary and volcanic rocks that commenced with the deposition of erupted volcanic material on to the Archean basement at ~2440 Ma and terminated after ~1880 Ma when the latest sediments were deposited after the Lapland-Kola orogeny (Hanski & Huhma, 2005). Several tectonic events have had an impact on the area, by generating structural systems such as fault zones and orogenic belts that pose fundamental features that affect the geology of Central Lapland and on the deposit itself.

2.*2* The Fennoscandian Shield

In greater scale, the bedrock in Sodankylä region belongs to the Fennoscandian Shield, as does the entire bedrock of Finland and parts of bedrock in Sweden, Norway and Kola Peninsula. The Fennoscandian Shield (fig. 3) further continues buried below younger sedimentary rocks towards southwest, and it is a crustal segment part of the East European Craton (EEC) where the other segments are Sarmatia in south and Volgo-Uralia in east (Gorbatschev & Bogdanova, 1993; Bogdanova et al. 2008; Lahtinen et al. 2011). From global geological perspective, the shield could be connected to other ancient shields in Canada, South Africa and Australia based on its geological features, of which greenstone belts and significant mineral resources are examples (Lahtinen et

al. 2011). Furthermore, the Fennoscandian Shield connects the cratons of Laurentia and NE Europe, which may have been parts of an ancient supercontinent during Late Archean-Early Proterozoic (Gorbatschev & Bogdanova, 1993). Its geographical borders and main units can be observed from the maps in figures 3 and 4.

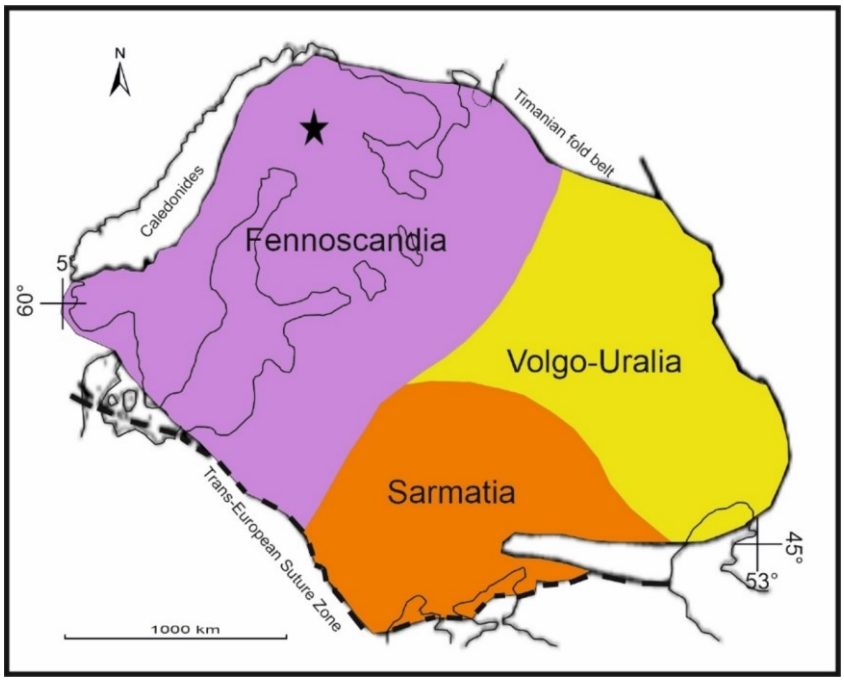

Figure 3. Geographical location of the East European Craton (EEC) exhibited with its shields. Modified after Gorbatschev & Bogdanova (1993). Sakatti deposit is marked with a star. WGS 84 was used as a reference coordinate system.

The Fennoscandian Shield (figs. 3-4) is composed of geological domains formed during the Archean and Proterozoic Eons, which in general are younging from northeast to southwest (Gaál & Gorbatschev, 1987). The Archean crust dominates in the northeast and can be divided into the Karelia and Kola blocks, of which the Karelia block sometimes has been subdivided further into Belomorian and Karelian Provinces (Gaál & Gorbatschev, 1987; R. Gorbatschev & Bogdanova, 1993; Vaasjoki et al. 2005). During the Proterozoic Eon, the Svecofennian domain, the Transscandinavian Igneous Belt (TIB) and the Sveconorwegian domain were accreted, of which the Svecofennian domain covers most of the central and southern parts of the Fennoscandian Shield and a great part of Finnish bedrock as well (Gorbatschev & Bogdanova, 1993). The Svecofennian domain and TIB formed during the Paleoproterozoic Era while the Sveconorwegian domain, covering only a minor part of the shield in the southwest, is Mesoproterozoic in age (Gorbatschev & Bogdanova, 1993). In the study zone especially the rocks of the Archean Karelia block and the Paleoproterozoic rocks dominate (fig. 4), and the tectonic events related to their crustal evolution were of major importance in creating the present geological units in the area.

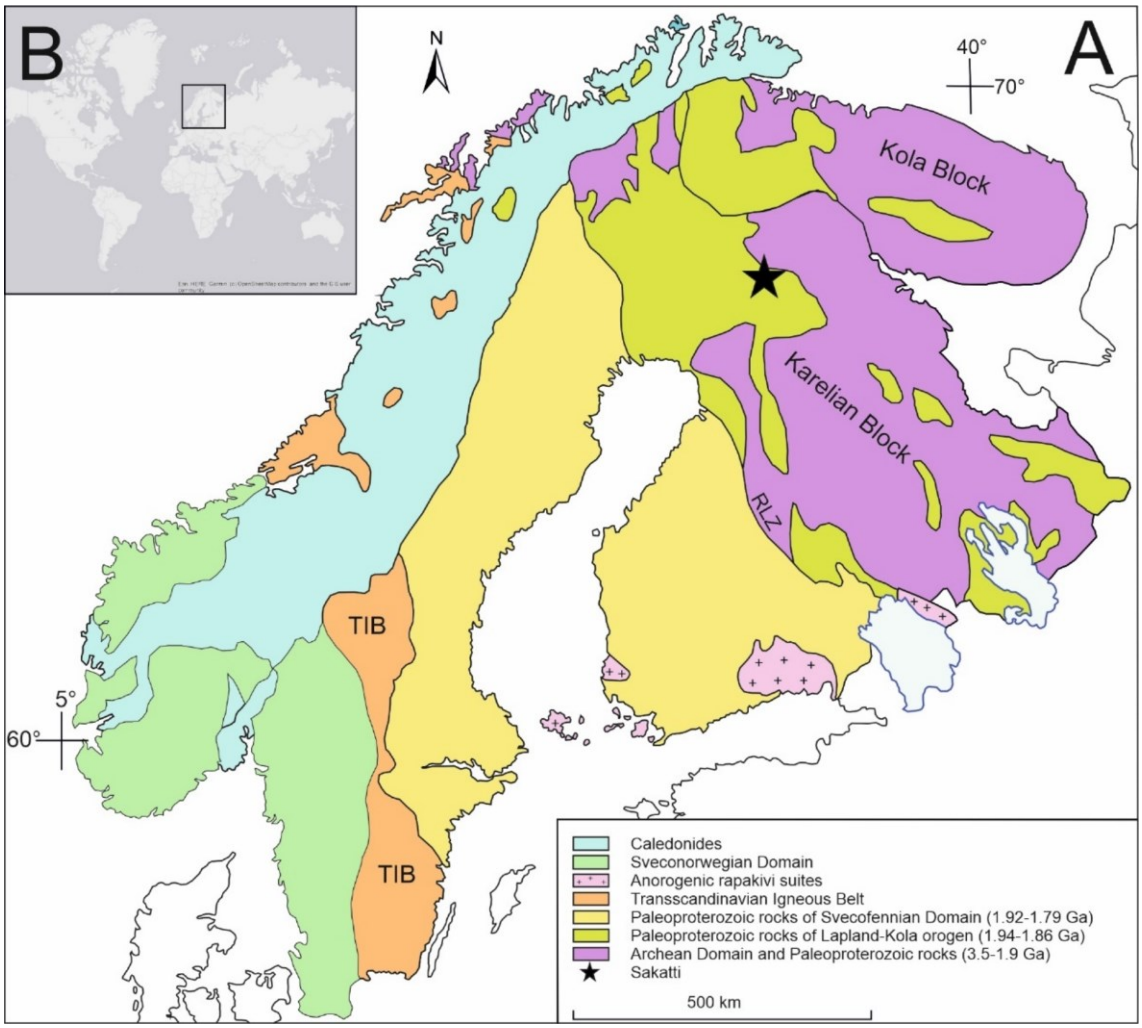

Figure 4. A: The Fennoscandian Shield and its provinces presented as a simplified version based on Koistinen et al. (2001) with a division used by Vaasjoki et al. (2005). B: An index map based on publicly available google imagery basemap pointing the area A in global scale. Abbreviations: RLZ = Raahe-Ladoga Zone, TIB = Transscandinavian Igneous Belt. Coordinates are given according to the WGS 84.

2.3 Geological units in Northern Finland

In northern Finland, there are several major geological units formed during certain tectonic events that took place during the formation of Fennoscandian bedrock. These major geological units include the Archean gneisses and granites, the Paleoproterozoic supracrustal belts, the Central Lapland Granitoid Complex (CLGC), the Lapland Granulite Belt (LGB) and the layered mafic-ultramafic intrusions (Hanski & Huhma, 2005), which are all located close to the Sakatti deposit (fig. 5). Paleoproterozoic supracrustal belts comprise the Central Lapland Greenstone Belt (CLGB), the Peräpohja belt (PB) and the Kuusamo belt (KB), which represent the sedimentation and magmatism active during rifting episodes 2500-1920 Ma. In Sodankylä region, the CLGB, the layered mafic-ultramafic intrusions and related granitoids are the dominating units.

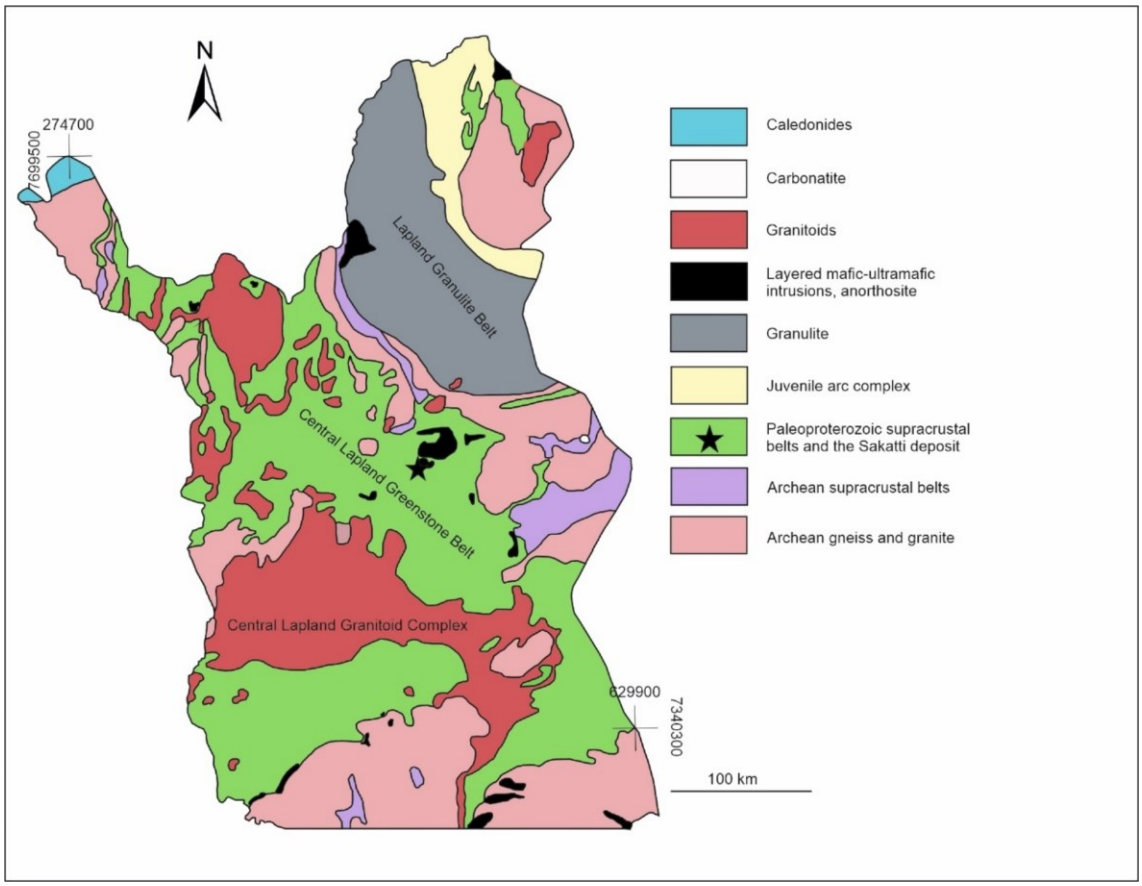

Figure 5. Major geological units in northern Finland in geochronological order. The Sakatti deposit is located within the CLGB near layered mafic-ultramafic intrusions and Archean gneisses and granites. Modified after Hanski & Huhma, 2005. Coordinates are given in EUREF-FIN.

2.4 Tectonic history

Most of the tectonic events described in this chapter have affected the study zone and the CLGB by promoting depositional processes and by deforming rock units. The tectonic events that occurred during the Archean (Saamian and Lopian orogeny) and Proterozoic Eons (rifting stage, Lapland-Kola orogeny and Svecofennian orogeny) are comprehended as the most essential events with respect to the present geology in the study zone. Paleoproterozoic mafic-ultramafic intrusions, LGB, CLGC of 2.1 Ga continental breakup origin, pieces of Archean bedrock and the CLGB of rifting stage origin constitute the main components affected the study zone.

2.4.1 Archean

The development of the bedrock in northern Finland and in Sodankylä region commenced already during Early Archean. The Archean tectonic events are not well comprehended and thus there is no precise tectonic model concerning those events (Sorjonen & Luukkonen, 2005). However, according to the geochronological studies the oldest rocks in Finland are TTG rocks and gneisses with ages ranging from 3.1 to 3.5

Ga and they are situated in the northeast of the Fennoscandian Shield (Sorjonen & Luukkonen, 2005). These rocks occur as widely dispersed and isolated terrains (Vaasjoki et al. 2005) and acted as source material for later sedimentary rocks ultimately deformed during 2.9-2.7 Ga in the Lopian cycle, characterized by low-grade metamorphic granitoid-greenstone complexes (Sorjonen & Luukkonen, 2005). This cycle probably consisted of accretions of exotic terranes and of a subsequent major collisional event approximately at 2.7 Ga between the Belomorian terrain and some preceded Karelian block elements (Sorjonen & Luukkonen, 2005; Hölttä et al. 2012). It also influenced the area probably by secular and various changes towards the Proterozoic, with varying polarities in tectonism, and was combined by coeval volcanism and tonalitic plutons during 2.75-2.73 Ga (Sorjonen & Luukkonen, 2005; Hölttä et al. 2012). Before the Lopian cycle, the Saamian cycle occurred during 3.1-2.9 Ga that is represented by high-grade metamorphic migmatites and granitoids (Sorjonen & Luukkonen, 2005). Both cycles are regarded as main contributors in creation of the Archean areas of northern Finland. In Sodankylä region, the Archean rocks are exposed as domes in Möykkelmä and Tojottamanselkä (Brownscombe, 2016). These domes belong to the gneissic basement of the Archean Pomokaira terrane, which underlies the CLGB (in e.g., Brownscombe, 2016).

2.4.2 Paleoproterozoic rifting stage

The Proterozoic Eon commenced with the emplacement of mantle plume-related layered gabbro-norite intrusions during 2.5-2.44 Ga (Heaman, 1997), which was thereafter followed by rifting of the Archean continent or continents within the Fennoscandian Shield (Hanski & Huhma, 2005; Lahtinen et al. 2008). During rifting, deposition of quartzite-dolomite-basalt-pelite transgressive succession was ongoing in a probably intra-cratonic basin, which was accompanied by periodic volcanism of komatiitic, picritic and mafic-ultramafic lavas, and intrusions of tholeiitic mafic dykes and sills (e.g., Hanski & Huhma, 2005; Lahtinen et al. 2011). These sedimentary and volcanic successions led to the formation of the CLGB that forms an intrinsic part of the geology in Sakatti and in Central Lapland generally, and thus the belt will be under further discussion with respect to its major features and lithostratigraphic units.

Lahtinen et al. (2008) divided the rifting episodes into three successive stages: 1) Onset of global rifting with the emplacement of layered gabbro-norite plutons during 2.505-2.44 Ga (Heaman, 1997). During this stage sedimentation took place in lacustrine basins; 2) Tectonic inversion at 2.44-2.33 Ga during which the previously uplifted flood

basalts were first dissected by rifting with southwest directed propagation and were later affected by erosion and weathering (Melezhik, 2006); 3) Repeated intraplate rifting during 2.33-2.06 Ga that led to the openings of the ancient Kola Ocean and the Svecofennian Sea. During this stage, subaerial volcanism, accumulation of polymictic conglomerates, marine sediments, red beds and black shales characterized the sedimentation environment (Melezhik, 1999; Melezhik et al. 2005; Lahtinen et al. 2008). The rifting stage was further described by Köykkä et al. (2019) who divided the evolution of basin into five stages consisting of initial rifting/early syn-rift, syn-rift, syn-rift to early post-rift, passive margin stage and foreland basin system. The events and basin evolution stages related to the formation of the Sodankylä and Savukoski Group metasediments will be described briefly when presenting the stratigraphical units in the CLGB (chapter 2.6).

2.4.3 Lapland-Kola orogeny

The rifting stage was terminated by the Lapland-Kola orogeny (1.94-1.86 Ga) and Svecofennian orogeny (1.92-1.76 Ga), of which the latter is divided into four orogenies named as Lapland-Savo, Fennian, Svecobaltic and Nordic orogenies (e.g., Vaasjoki et al. 2005; Lahtinen et al. 2008; Lahtinen et al. 2011). These events led to the closure of an ancient ocean and to the deformation and metamorphism of earlier geological units in Northern Lapland (Vaasjoki et al. 2005). Lapland-Kola orogen consisted of reworked Late Archean terranes with limited preservations of juvenile crust from the Paleoproterozoic Era (Daly et al. 2001), while the Svecofennian domain covers extensive areas of Paleoproterozoic crust (e.g., Lahtinen et al. 2005). Important tectonic regions during the Lapland-Kola orogeny were a collisional foreland in the present NE, the NW-SE oriented cryptic suture of eclogites in between the ancient plates and a retroarc foreland in the SW with a retroarc basin represented by Lapland Granulite Belt (LGB) and Umba Granulite Belt (Lahtinen & Huhma, 2019). The NE part consisted mostly of the Kola Archean continent and Paleoproterozoic cover rocks while the SW part was represented by the Karelian Archean continent, Inari Arc and Paleoproterozoic cover rocks (Lahtinen & Huhma, 2019).

Deformational evolution during the Lapland-Kola orogeny exhibits, according to the recent study by Lahtinen and Huhma (2019), an exhumed continent-continent collision zone. It consists of three deformation phases, of which the first includes NE-SW shortening with SW-vergent thrusting that occurred possibly synchronously with the E-vergent thin-skinned thrusting in CLGC (Lahtinen & Huhma, 2019). This is

comprehended as the main thrusting and peak metamorphism stage at 1.92-1.91 Ga that led to the uplifting of the Kittilä allochthon as well (for references see Lahtinen & Huhma, 2019). The first deformation phase also created mostly isolated recumbent folds with a strong shearing along the fold limbs and folding of foliation (Lahtinen & Huhma, 2019). After this peak tectonometamorphic stage began the exhumation stage (1.9-1.89 Ga) observed as granulite crosscutting post-collisional appinites, S-type granites and anatectic veins (Lahtinen & Huhma, 2019). The second phase with renewed SW-NE shortening occurred after 1.89 Ga and resulted in a weak foliation, crustal duplexing and tight to open folding with upright or slightly inclined position, and to the exhumation of LGB (for references see Lahtinen & Huhma, 2019). The third and final phase with the main shortening direction from NNW to SSE event is understood as an evolving event where structures reactivated later in younger events (Lahtinen & Huhma, 2019). It created conical radial and orocline features and buckling of previously formed structures formed by the change in the main shortening direction (Lahtinen & Huhma, 2019). Common structures formed during this event were gentle-open to close folds where the axial traces are suborthogonal to the main foliation and the fold plunge directions depend on the dip of the main foliation (Lahtinen & Huhma, 2019).

2.4.4 Svecofennian orogeny

The Svecofennian rocks constitute a major part of the Paleoproterozoic crust in central and southwestern parts of the Svecofennian Domain, and the Svecofennian orogeny left its traces also to northern Fennoscandia seen in its crustal blocks and related deformation and metamorphism (e.g., Lahtinen et al. 2009; Lahtinen et al. 2015b). These near orthogonal accretionary events infer to amalgamation of crustal blocks with Archaean Karelia, where the Lapland-Savo, Fennia, Svecobaltic and Nordic orogenies led to accretions of the crustal blocks (Lahtinen et al. 2009; Lahtinen et al. 2015b). The Lapland-Savo orogeny in northern part of the Svecofennian Domain includes the collision between the Archaean Karelian and Norrbotten cratons with E-vergent thrusting, as well as the shortening and the obduction of Kittilä allochthon upon the Archaean Karelian (e.g., Lahtinen et al. 2015a). Before this orogeny, after 2.1 Ga, a triple-point continental breakup led to the formation of a NNW-SSE directed passive margin and an aulacogen known as the CLGC later overprinted by several tectonic events (Lahtinen et al. 2015a). The Fennia orogeny for its part marks a change in plate motions to north and southward subductions between the Keitele-Karelia collage and the Bergslagen microcontinent (Lahtinen et al. 2009). This event took place far south from the area of main interest. Transpressional collision during the Svecobaltic orogeny

between Sarmatia and Fennoscandia resulted in E-W directed shear zones and large-scale thrusting in Southern Finland and Sweden 1.83-1.80 Ga (Lahtinen et al. 2009). The final Nordic orogeny is not yet well comprehended, but it has commonly been understood as an advancing Andean type orogeny that led to the intrusion of a batholith chain of TIB (Lahtinen et al. 2009).

2.5 Central Lapland Greenstone Belt (CLGB)

The CLGB (fig. 5) represents depositional evolution in an opening sea during Paleoproterozoic prolonged extensional event and following collisional event and their subsequent outgrowths (Hanski & Huhma, 2005). The stratigraphic units of the CLGB (fig. 8A) will be described in the next chapter. The CLGB forms a part of one of the largest Paleoproterozoic greenstone belts that continues further in Russian Karelia, Northern Norway and Sweden, and is surrounded by the CLGC in south, Archaean granites and gneisses and supracrustal belts, the LGB in the north and layered mafic-ultramafic intrusions (fig. 5, Hanski & Huhma, 2005). This belt plunges beneath the LGB and runs parallel to its southwestern borders and is underlain by the Archean basement gneisses (Hanski & Huhma, 2005). The Svecofennian collisional event in the southwest and the thrusting of the LGB in the northeast during the Lapland-Kola orogeny deformed and metamorphosed its units, where the degree of metamorphism generally increases towards the CLGC (fig. 10, Hanski & Huhma, 2005). The dominating degree of metamorphism varies within the CLGB (fig. 10), but the Sakatti deposit is located within a region of greenschist facies metamorphism (fig. 9, Brownscombe, 2015). According to the study of Sorjonen-Ward et al. (1997), the CLGB acted as a foreland fold and thrust belt for two convergent systems with opposing polarities in SW and NE.

Lehtonen et al. (1998) created a lithostratigraphic division for the Paleoproterozoic supracrustal rocks in the CLGB, where Salla, Onkamo, Sodankylä, Savukoski, Kittilä, Lainio and Kumpu Groups constituted the stratigraphic units in the geochronological order from oldest to youngest. These units were further described by Hanski & Huhma (2005) who concentrated on the details at the group level, while Lehtonen et al. (1998) focused on the type of formations in each of these groups. The Onkamo Group was changed to Kuusamo Group and Lainio and Kumpu Groups were united and named as Kumpu Group by Huhma et al. (2018). In this study the approach of Hanski & Huhma (2005) will be followed with previously mentioned modifications. Each lithostratigraphic unit in the CLGB represents a certain geological environment and they

will be next presented with respect to the lithology and the tectonic environment they represent. The Sodankylä and Savukoski Groups will be under special focus since they presumably constitute the lithostratigraphy in the vicinity of the Sakatti deposit (fig. 6).

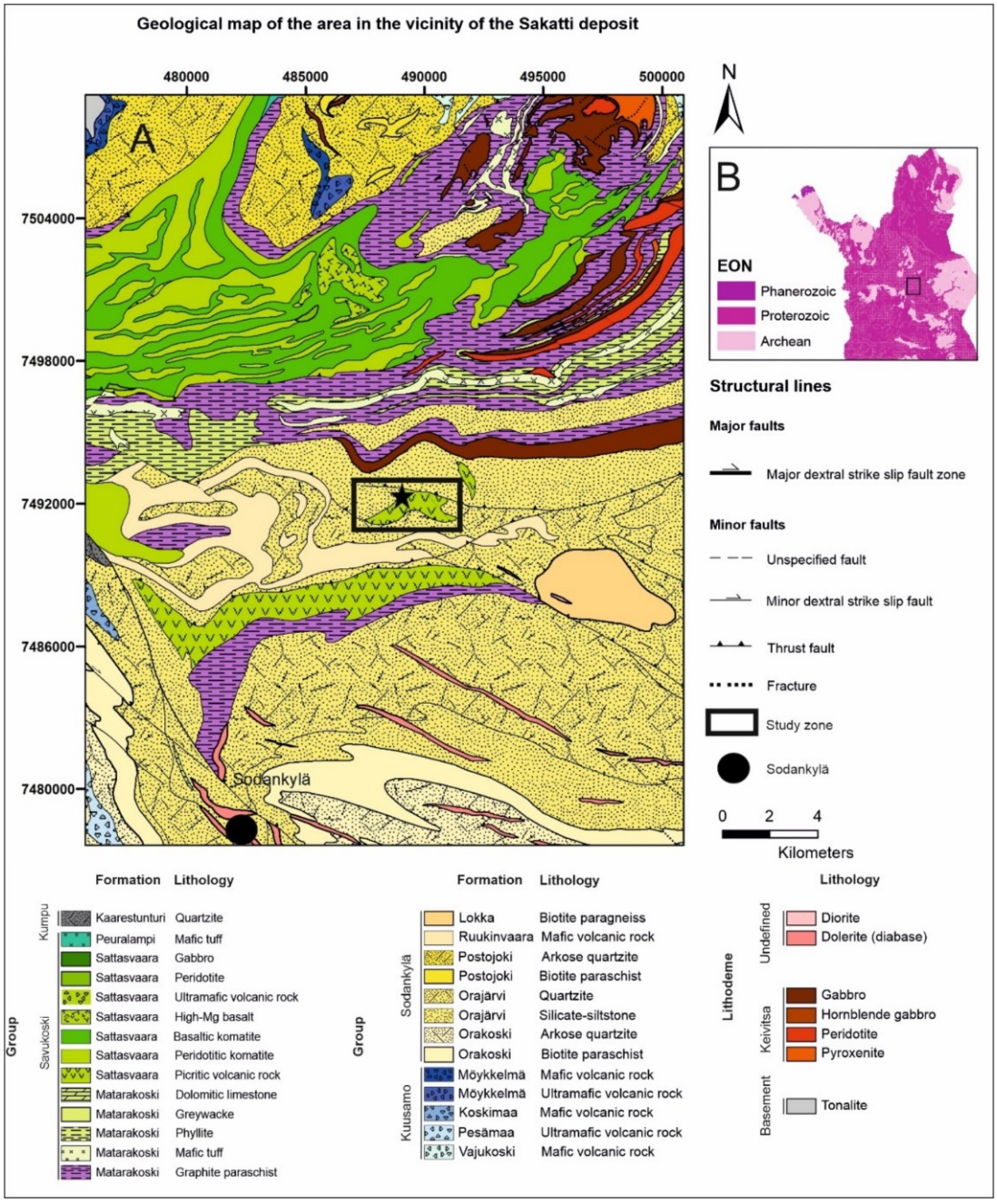

Figure 6. A: A Geological map of the northern Sodankylä region after the publicly available map The Bedrock of Finland 1:200 000 (GTK). B: An index map after publicly available map The Bedrock of Finland 1:1 000 000 indicating the area of the geological map A with respect to the age of bedrock. In the geological map the Sakatti deposit is located at the border between the Savukoski and Sodankylä Groups and between the Sattasvaara Formation picritic volcanic rocks and Orajärvi Formation silicate-siltstones. Structural position is in between the two N-vergent thrust faults. Coordinates are given in EUREF-FIN.

2.6 Stratigraphic units of the CLGB

2.6.1 The Salla Group

The lowermost unit of the CLGB, the Salla Group, overlies the Archean basement (fig. 7) and is consisted mostly of intermediate to felsic metavolcanic rocks that were erupted onto the rifted Archean basement and may cover a thickness of 2 km (Hanski & Huhma, 2005). This group is found especially in the southeastern part of the CLGB (fig. 8) but also in the vicinity of the partially coeval Akanvaara and Koitelainen layered intrusions near Sodankylä region (Hanski & Huhma, 2005). Characteristic for this group is that even though the rocks have been overprinted by greenschist facies regional metamorphism, primary volcanic structures like welding in ash flows are often observed in the extrusive rocks of this group (Hanski & Huhma, 2005). Eruption occurred in subaerial conditions, which is supported by the scarcity of intervening epiclastic metasedimentary rocks and the typical volcanic structures (Hanski & Huhma, 2005). Geochemically the rocks of this group are between basaltic andesites to rhyolites with a strong crustal contamination, which took place before the fractional crystallization that generated the ultimate composition (Hanski & Huhma, 2005).

2.6.2 The Kuusamo Group

The Kuusamo Group (or Onkamo Group) is situated above the lavas of the Salla Group (fig. 7), although this has been observed only in the Salla area. According to the study of Manninen (1991) the contact between these units was erosive and it graded upwards to a 10 m thick sericite schist unit while the lower parts composed of conglomerates. However, thirty kilometres north from Sodankylä, the Kuusamo Group metavolcanic rocks lie on the Archean basement and below the quartzites of the Sodankylä Group (Hanski & Huhma, 2005). The rocks of the Kuusamo Group occur in a wide area and close to the Sakatti deposit as well (fig. 8). An observation in the contact between the Salla Group and 2.44 Ga old Koitelainen and Akanvaara intrusions, where the latter ones cut the former but not the Kuusamo Group, enabled its dating (Manninen & Huhma, 2001). The Kuusamo Group consists mostly of subaerial amygdaloidal tholeiitic-komatiitic metavolcanites, but the rock types depend on whether they are found in the Salla area or in Möykkelmä (Hanski & Huhma, 2005). In the latter one the mafic and ultramafic rocks alternate, where pyroclastic komatiites and andesitic lavas with Archean gneiss xenoliths are followed by more primitive mafic rocks when advancing upwards (Hanski & Huhma, 2005). These rocks, like the rocks of the Salla Group, displayed crustal contamination and both groups could be understood as representing the same magmatic episode with relatively small difference in age (Hanski

& Huhma, 2005). Since komatiites and ultramafic-mafic rocks generally have been found in Sakatti and in the vicinity of the Sodankylä Group quartzites, their possible relation to the Kuusamo Group was considered in this study.

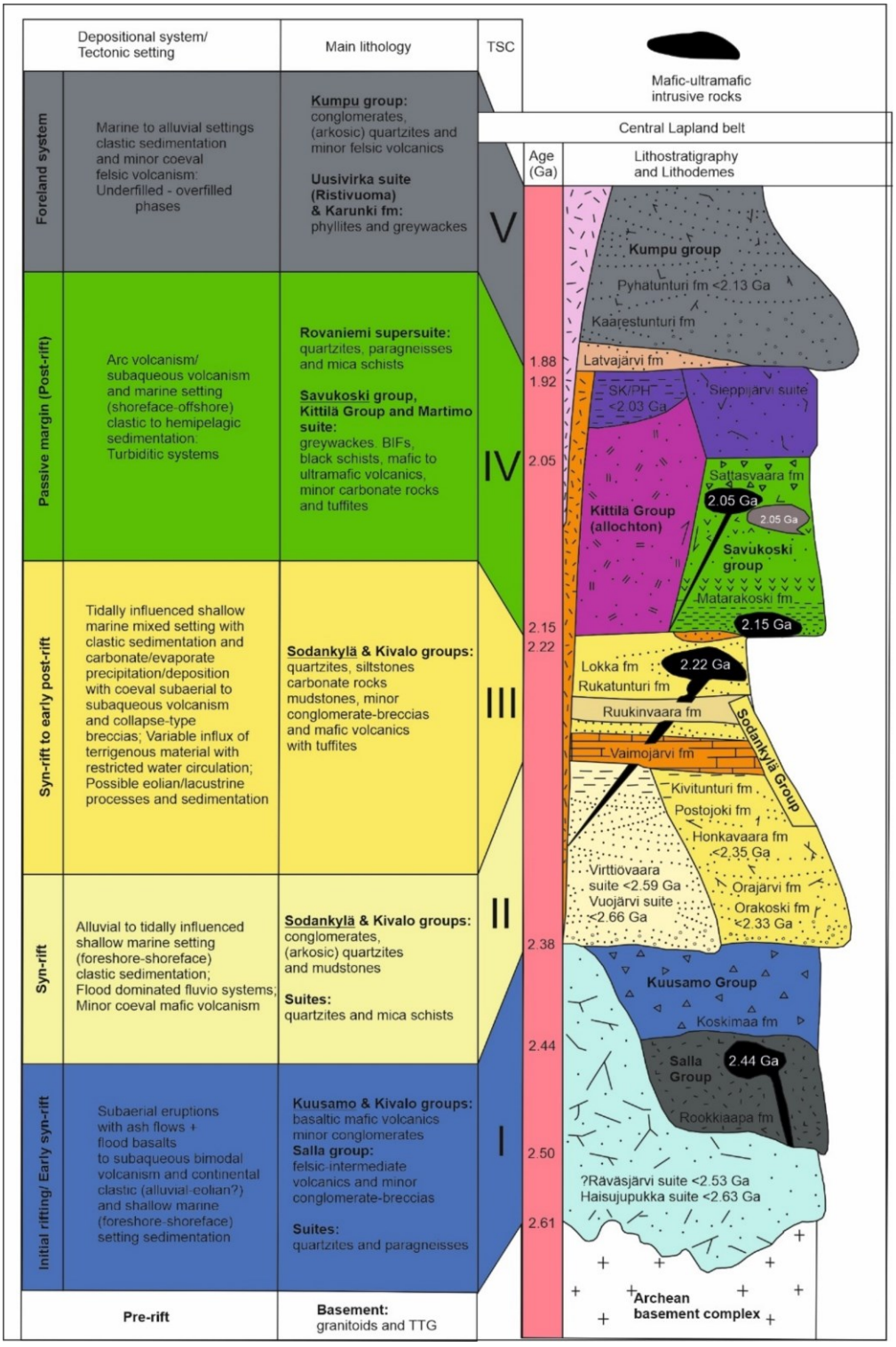

Fig. 7. Stratigraphic column of the CLGB. The most essential stratigraphic groups for this study are highlighted in bold. Some of the original age determinations were left out and the colours in the column mainly follow the colour scheme used in the geological map presented in figure 6. Modified after Köykkä et al. 2019.

2.6.3 The Sodankylä Group

Hanski & Huhma (2005) interpreted the Sodankylä Group as a succession of epiclastic sedimentary rocks, carbonate rocks, stromatolitic structures and mafic metavolcanic rocks that represent a more tranquil period with respect to tectonism and magmatism. It is overlain by the Savukoski Group and underlain by either the Archaean basement gneisses or the Salla or the Kuusamo Group rocks depending on the location (Hanski & Huhma, 2005). The rocks of this group occur in a wide area but especially on the eastern and southern side of the Kittilä Group (fig. 8). Orthoquartzites, clast to matrix supported conglomerates, mica schists and sericite quartzites are common rock types, which contain sedimentary structures such as cross-bedding, graded bedding, mud cracks and herringbone structures that were comprehended as representing a tidal environment (Nikula, 1988; Hanski & Huhma, 2005; Köykkä et al. 2019). The volcanic rocks are crustally contaminated tholeiitic amygdaloidal mafic basalts and basaltic andesites (Hanski & Huhma, 2005). 2.2 Ga minimum age for the rocks has been estimated by the presence of 2.2 Ga hypabyssal mafic-ultramafic sills which do not cut overlying units (Hanski & Huhma, 2005). The isotope analyses of detrital Zr samples from the quartzites pointed to Archean provenance (Hanski & Huhma, 2005). These details assisted in relative dating of other stratigraphic units and in correlating the period with corresponding periods seen in other related greenstone belts, such as the Peräpohja Belt (Rastas et al. 2001).

The abundance of quartzites in the Sodankylä Group indicates widening of a depositional basin after periods of volcanism and deposition of the Salla and Kuusamo Group volcanic rocks (Hanski & Huhma, 2005). Lower parts of this group have been interpreted as syn-rift stage sediments deposited in a shallow marine setting and in a basin that was controlled by active faults along the rift margin where the sedimentation took place (Köykkä et al. 2019). As for the upper parts of the Sodankylä Group, it was interpreted as representing syn-rift to early post-rift stage characterized by thick carbonate successions and evaporites precipitated in a restricted basin system and a tidal influenced depositional environment in an epeiric sea (Köykkä et al. 2019). Red-beds and anhydrite/gypsum with collapse type breccias are interesting indicators of these geological environments, although so far only indirectly evidenced from the Peräpohja and Kuusamo Belts (for references see Köykkä et al. 2019). Records of albitization and Na metasomatism have been made in the PB and possibly in the CLGB and KB as well, and their possible link to evaporite deposits and remobilization has been recognized (Köykkä et al. 2019). Recently, evidenced evaporite layers have been found in the

CLGB as well, which were interpreted as slip surface platforms for propagating thrust faults (Haverinen, 2020). These matters will be carefully considered in the stratigraphical correlation and structural investigation performed in this study.

2.6.4 The Savukoski Group

Deepening of the basin continued after the deposition of the Sodankylä Group rocks, when the deposition of fine-grained metasedimentary rocks of the Savukoski Group took place (Hanski & Huhma, 2005). This group comprises phyllites, black schists and mafic tuffites in lower parts of the unit, while komatiitic and picritic volcanic rocks cover the upper parts (Hanski & Huhma, 2005). The Savukoski Group rocks are present close to the Sakatti deposit together with the Sodankylä Group rocks, while in larger scale they occur in a broad area and surround the Kittilä Group (fig. 8). The presence of graphite and sulphide bearing schists is an important indicator since from the older rock sequences in the CLGB these have not been found (Hanski & Huhma, 2005). According to Haverinen (2020), evaporite successions deposited after the deposition of black schists in a closing basin. The contact with the underlying Sodankylä Group is concordant and gradual while the upper contact with the Kittilä Group has been interpreted as tectonic (fig. 7, Hanski & Huhma, 2005).

The komatiitic and picritic rocks commonly exhibit pillow structures and they may occur as agglomerates, massive lavas and lapilli tuffs that differ from the older Kuusamo Group komatiites and picrites by the environment where eruptions occurred (Hanski & Huhma, 2005). The ultramafic-mafic rocks of the Savukoski Group can be geochemically divided into two series of komatiites and picrites, which both evolved from MgO-rich parental magma to basaltic rocks. They however differ from each other based on their TiO_2 contents that are higher in komatiites (Hanski et al. 2001). Differences are also observed in the REE patterns and high-field strength element (HFSE) contents so that the komatiites are strongly LREE depleted and moderately HREE depleted while the picrites are enriched in both LREE and HFSE (Lehtonen et al. 1998; Hanski & Huhma, 2005).

Crosscutting intrusive rocks, such as the 2.06 Ga Kevitsa intrusion, determined the minimum age for the deposition of the Savukoski Group metasediments (Hanski & Huhma, 2005). According to the recent study by Köykkä et al. (2019), the deposition of the rocks of this group represents a passive margin stage (2.1-1.92 Ga), when the aulacogens (CLGC) developed and the basin was deepened during long term thermal subsidence when gravity-driven sandstones, subaqueous volcanic rocks and hemi-

pelagic sediments were deposited with mainly Paleoproterozoic provenance. The hemi-pelagic sediments of the Matarakoski Formation are especially under scope in this study since in the stratigraphic column of the CLGB they overlie the Sodankylä Group metasediments (fig. 7).

2.6.5 The Kittilä Group

The Kittilä Group metavolcanic rocks overlie the Savukoski Group rocks (fig. 7) and are overlain by the rocks of the Kumpu Group, and the group has been estimated to cover ~6 kilometres of thickness (Hanski & Huhma, 2005). The rocks of this group can be found in the Kittilä greenstone complex west from the Sodankylä region (fig. 8). In addition to metavolcanic rocks, this unit comprises sedimentary sequences such as phyllites, metagreywackes and minor carbonate rocks and BIF formations (Hanski & Huhma, 2005). Its contact with the Savukoski Group seems to be tectonic, since the southern contact follows the E-W trending Sirkka line and in the east a thrust zone (fig. 8) runs close to the complex (for references see Hanski & Huhma, 2005). The metavolcanic rocks are either primitive tholeiitic basalts whose volcanic structures indicate submarine eruptions, or more evolved tholeiitic basalts and andesites, which together with sulphur isotope analyses support oceanic geotectonic environment (Hanski & Huhma, 2005). These rocks are in concordance with the model proposed by Hanski (1997), in which a sliver of allochthonous oceanic crust was uplifted upon the Archaean rocks from the east (Hanski & Huhma, 2005; Hanski et al. 2018). According to age determinations made for the tholeiitic lava samples the age of these rocks would be ~1.98 Ga (Hanski & Huhma, 2005).

2.6.6 The Kumpu Group

The Kumpu Group overlies with angular unconformity the Kittilä Group and Savukoski Group rocks (fig. 7). They are composed of molasse-like quartzites and conglomerates and they record a stratigraphic break in the lithostratigraphy (Hanski & Huhma, 2005). Kumpu Group has outcrops for instance in Levi and in Kaarestunturi in the Sodankylä region, and it comprises thickness of 200-2000 meters of sedimentary rocks deposited after 1.88 Ga according to the age determinations and field observations (Hanski & Huhma, 2005). Common characters for the rocks of the Kumpu Group are the red-brown tint due to hematite pigment, clasts from the underlying lithostratigraphical units and occasional undeformed quartzites with primary clastic texture (Hanski & Huhma, 2005). The rocks of this group probably deposited in fluvial environments with alluvial fans and braided river deposits (for references, see Hanski & Huhma, 2005).

2.6.7 Ultramafic intrusions

In addition to the Kuusamo and Savukoski Group ultramafic rock sequences, several ultramafic-mafic intrusions occur within the CLGB (fig. 8). They comprise at least three magmatic phases: 1) The 2.44 Ga Koitelainen and Akanvaara intrusions, which intruded when the extensive rifting initiated (in e.g., Mutanen, 1997; Hanski & Huhma, 2005). The Koitelainen intrusion is found at the contact between the Salla Group and Archean basement to the northeast of the Sakatti deposit and Sodankylä (fig. 8), while the Akanvaara intrusion is present ~80 km to the east of Sodankylä (Hanski & Huhma, 2005) ; 2) The 2.22 Ga gabbro-wehrlite sills (Haaskalehto-type intrusions), that intruded into the Sodankylä Group sediments during short-lived magmatic stage and extension, are especially abundant in the southern margin of the CLGB where they roughly follow the CLGB margin (fig. 8) and can sometimes occur as hundreds of meters thick layers (in e.g., Lehtonen et al., 1997; Hanski & Huhma, 2005); 3) The 2.05 Ga intrusions include several tens of meters thick smaller intrusions that particularly occur within the Savukoski Group (Hanski & Huhma, 2005). The Kevitsa intrusion belongs to this group, although its thickness has been estimated to cover more than 2 km (Mutanen, 1997). It has been recently compared in detail with the Sakatti deposit in the study of Brownscombe (2015), where it was concluded that they are rather similar. The Kevitsa intrusion of all above mentioned intrusions is located closest to the Sakatti deposit (fig. 8) and it is possible that they have common genesis (Brownscombe, 2015).

2.7 Major structures

There are several major geological structures in northern Lapland (fig. 8) that have had impact on the geological units and have been active several times during tectonic history. The most important structures and their significance in Central Lapland and in Sodankylä region are presented below.

The Sirkka shear zone (SSZ, fig. 8) is one of the major structures in northern Finland and it runs along the southern boundary of the Kittilä greenstone area and follows the southwestern border of the CLGB towards southeast (in e.g., Evins & Laajoki, 2002). According to the study of Nironen (2017) this shear zone comprises several southwards dipping and northwards verging thrusts and fold structures that were formed at 1.88 Ga. In overall, the thrusts are mainly low-angle thrusts (Berthelsen & Marker, 1986) while steeper thrusts have been recorded as well (Nironen, 2017). In the southern border of the CLGB at the Sirkka shear zone (fig. 8), the Kittilä Group underthrusts the Savukoski Group (for references see Hölttä et al. 2007). Since the shear zone is cut by plutonic

rocks of 1.88-1.8 Ga age, the displacements and reactivations may have developed during 1.9-1.8 Ga interval (Berthelsen & Marker, 1986). These reactivations include sinistral strike-slip movements along NE-SW directed major faults, which can be detected also in figure 8 close to the Kittilä Group-Savukoski Group contact. The SSZ is present in the Sodankylä region 15 km west of the Sakatti deposit, where it dips towards SW (fig. 8). The northwards dipping thrust faults in Sakatti may be related to the SSZ, as they seem to be connected (fig. 8).

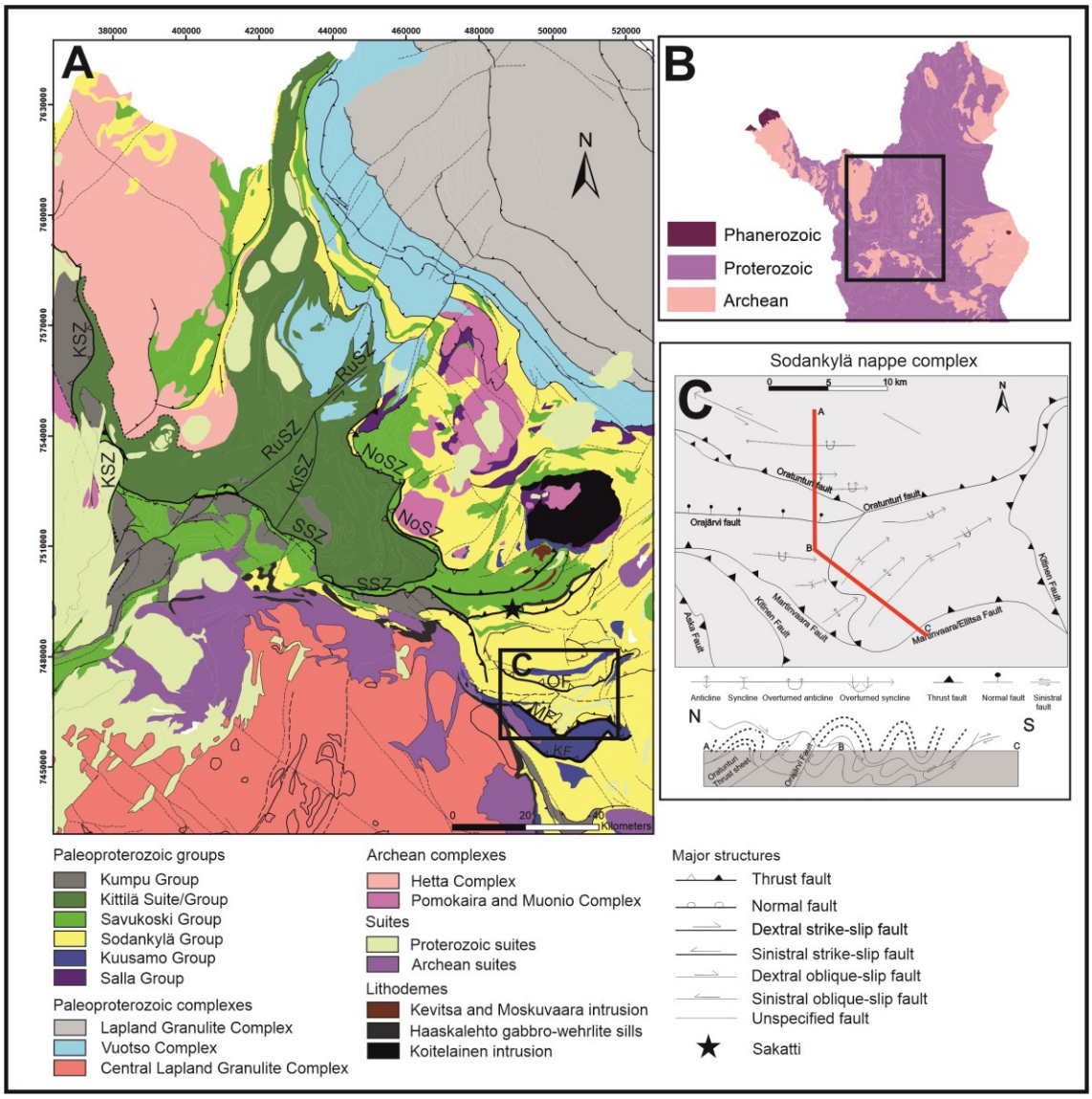

Figure 8. A: Generalized geological map of the CLGB showing the locations of its stratigraphic units and major geological structures after the publicly available map The Bedrock of Finland 1:1 000 000 (GTK). Abbreviations: SSZ= Sirkka Shear Zone, KSZ= Kolari Shear Zone, RuSZ= Ruoppapalo Shear Zone, NoSZ= Nolppio Shear Zone, KiSZ= Kiistala Shear Zone, OF= Oratunturi Fault, MF= Martinvaara Fault. B: An index map marks the area of the map A. C: A structural map and cross section of the Sodankylä Nappe complex that is located ~10 km south of the Sakatti deposit. Modified after Evins & Laajoki (2002). Coordinates are given in EUREF-FIN.

Close to the Finnish-Swedish border located Kolari Shear Zone (KSZ, fig. 8) is an approximately NNE-trending large-scale structure that is consisted of several westwards

dipping thrusts (fig. 8). The KSZ has been referred to represent a 1.8 Ga old post-peak metamorphic thrusting event related to the Kolari Fe-Cu-Au deposits (Niiranen et al. 2007). It has been interpreted as a northern continuation of the N-S trending Pajala shear zone, which for its part represents a major sinistral strike-slip zone (Berthelsen & Marker, 1986). In addition, according to the interpretation of Väisänen (2002) it has accommodated NNE-vergent thrusting and later E-vergent thrusting thus representing a transpressional shear zone.

According to the interpretation of Evins & Laajoki (2002), a complex thrust duplex overlies the Archaean basement in the Sodankylä region (fig. 8C). The complex is called the Sodankylä nappe, which is consisted of the Oratunturi, Martinvaara, Ellitsa and Leviäaapa thrust sheets (fig. 8C, Evins & Laajoki, 2002). According to the same study the formation of the nappe created extent folding and comprised at least three deformational phases where (i) the D_1 is the axial planar schistosity to coeval southwards verging thrusting, (ii) the D_2 is represented by large-scale upright NE-trending folds in south and crenulation in north and (iii) the D_3 is observed as faults with sinistral displacements and local NW-trending folds. Evins and Laajoki also concluded that based on the internal nappe-like structure (fig. 8C) the CLGB represents a foreland fold and thrust belt to the LGB, which is concordant with the study of Sorjonen and Luukkonen (1997) and with more recent studies such as the study of Lahtinen & Huhma (2019). However, the deformation events vary slightly from the ones presented by Lahtinen & Huhma (2019).

The NE-SW and NW-SE trending curving shear zones that surround the Kittilä Group (fig. 8A) define the Nolppio shear zone (NoSZ), which runs northwest of the Sodankylä region as NE or SW-dipping thrust faults and related folds (Väisänen, 2002; Hölttä et al. 2007). It is associated with E-vergent thrusting and asymmetric folding that are related to the uplift of the Kittilä allochthon over the older stratigraphical units at 1.92 Ga during the Svecofennian accretions (Väisänen, 2002; Hölttä et al. 2007). The E-vergent thrusting displaced the Kittilä Group rocks over and under the Savukoski Group along the thrust faults of the NoSZ (Molnar et al. 2018). Related structures near this shear zone are usually gently dipping proposed to represent overthrusting (for references, see Väisänen, 2002). The thrust faults in the NoSZ occasionally exhibit opposing polarities, which is typical for this zone (fig. 8A) and has been referred to be possibly related to two simultaneously operating and competing tectonic forces (for references, see Molnar et al. (2018).

The Kiistala (KiSZ) and Ruoppapalo (RuSZ) shear zones (fig. 8A) represent NE trending strike-slip zones that crosscut the Kittilä Group rocks and other older stratigraphic units and deformed the earlier large-scale folds (Nironen, 2017). According to the study of Nironen (2017) the KiSZ formed as a transfer zone during thrusting from N-NNE at 1.92 Ga (for references see Nironen, 2017). Apparently, the shear senses in these zones have changed from sinistral to dextral during several reactivations (Patison, 2007).

In Central Finland and in Sakatti, later 1.79-1.76 Ga old E-W, NNW-SSE and ENE-WSW trending extensional fractures and faults (fig. 8) crosscut the older structures and units and they are usually observed only from the aeromagnetic maps (Lahtinen & Huhma, 2019). They are considered to represent radial fractures formed by far-field effects during NNE-SSW shortening and to be related to the 1.79-1.76 Ga granites (Lahtinen & Huhma, 2019). According to the geological 3D-model of the Sakatti these faults crosscut the whole deposit.

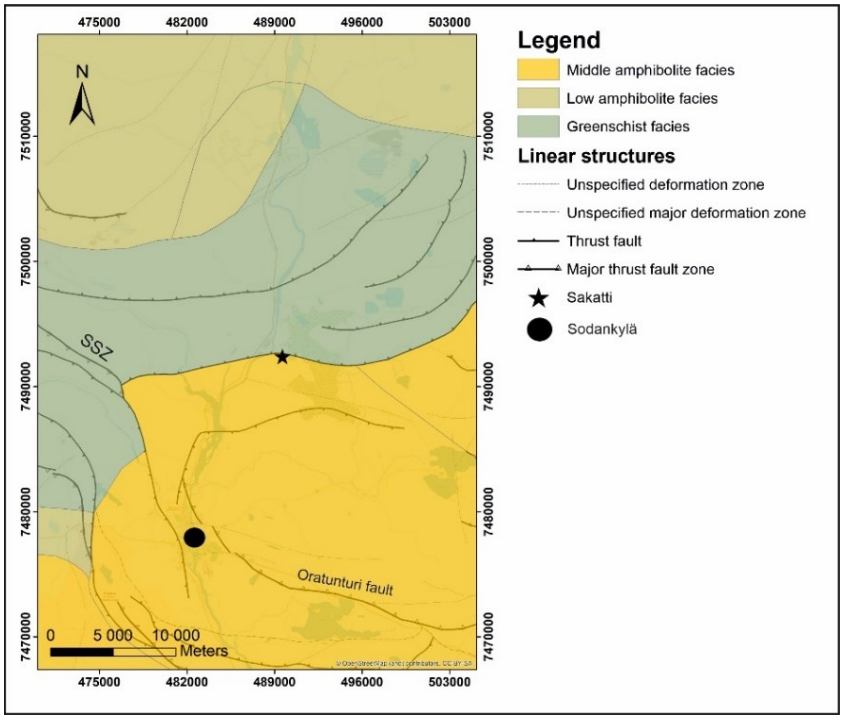

Figure 9. Major structures and metamorphic facies areas in the vicinity of the Sakatti deposit. Most of the structures have been interpreted from geophysical maps. Sakatti deposit is located in between the greenschist facies and middle amphibolite facies rocks. SSZ = Sirkka Shear Zone. Modified from publicly available maps the Bedrock of Finland 1:1 000 000 and Metamorphism 1:1 000 000. Coordinates are given in EUREF-FIN.

2.8 Metamorphism

Central Lapland has undergone extensive metamorphism, where the degree of metamorphism varies (figs. 9-10). It has been divided by Hölttä et al. (2007) into different areas where mineral assemblages in mafic and pelitic rocks differ as well.

Partly, these areas correspond to the main geological units but there is variation within them as well. The CLGB for its part represents the lowest metamorphic grade with greenschist facies rocks (fig. 10), while the surrounding geological units LGB and CLGC include higher grade amphibolite and granulite facies rocks (Hölttä et al. 2007). The highest-grade granulite facies rocks occur near the LGB (Hölttä et al. 2007). Typical mineral assemblages found in the CLGB greenschist facies rocks are muscovite-chlorite-biotite-albite-quartz assemblage in metapelites and actinolite-chlorite-epidote-albite-carbonate-quartz assemblage in metavolcanic ultramafic-mafic rocks (Hölttä et al. 2007). Pelitic schists sometimes contain primary structures that are fine grained and commonly pervasively sheared (Hölttä et al. 2007). The Sakatti deposit is located between the greenschist and middle amphibolite facies rocks (fig. 9).

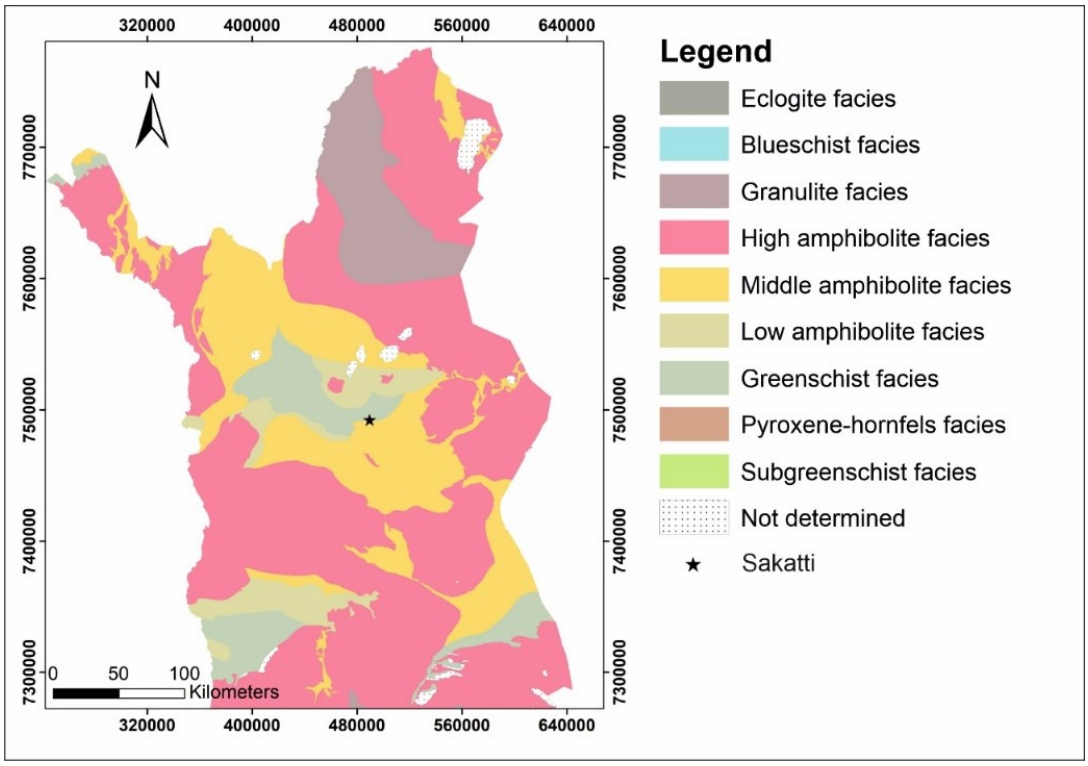

Figure 10. A metamorphic map of Northern Finland modified from publicly available map Metamorphism 1:1 000 000 (GTK, 2018). The Sakatti deposit is located within the greenschist facies rocks near middle amphibolite facies rocks. Coordinates are given in EUREF-FIN.

3. Materials and methods

The materials used in this study include structural and lithological drill core logging data and analysis of samples collected from the drill cores. The samples were prepared for thin section studies or for geochemical analyses. The structural data consisted of α-, β- and γ-angle measurements made chiefly from ductile structures during drill core logging, structures recorded in thin sections and unit continuations and stratigraphic separations observed in stratigraphic columns. The lithological data included rock types

and units observed during drill core logging, mineralogical data obtained in thin section studies and geochemical data. The lithological data was especially utilized in the stratigraphic study.

3.1 Thin sections

The thin section samples were taken from several drill cores (fig. 11 A-C) and representative drill core intervals. The samples were named with running numbering according to the Anglo American's internal thin section sampling standard in the form of TS-Hole ID-Interval (m). The most essential observations were recorded and photographed. A total of 44 thin sections were finally prepared, of which 31 were oriented. The sampling was performed by sawing a 5 cm thick rock interval and conserving the orientation line, if present, in the sample. In the laboratory of the University of Turku they were sawed into ~ 1 cm thick samples and finally polished.

Structural analysis

The samples prepared for structural analysis were taken from oriented drill core intervals. In thin section preparation, a good care was taken in saving the orientation line so that the orientation of each thin section was recorded. In addition, the direction of ground surface was marked to thin sections with an arrow. Thin sections were finally sawed perpendicular against a planar orientation for obtaining the best angle for structural investigation. Observed microstructures were photographed and their asymmetries and shear senses interpreted in sketches and recorded.

Stratigraphic study

If a purpose of a certain thin section was stratigraphical classification, the sample was taken from a drill core interval that was homogeneous and representative of the respective rock unit. The rock units that were sampled for thin section studies included schists of two varieties, mafic volcanic rocks, brecciated Ca-bearing rocks and intensively altered picrites. Rest of the rock units were mainly fault breccias without an orientation line or ultramafic/mafic rocks and they were left out from the thin section studies as their petrographic investigation was not under great interest in this study. Typical mineral assemblages, textures and metamorphic minerals were recorded and assigned finally to certain rock units. These studies supported the initial rock unit division performed during drill core logging and aided in stratigraphical classification.

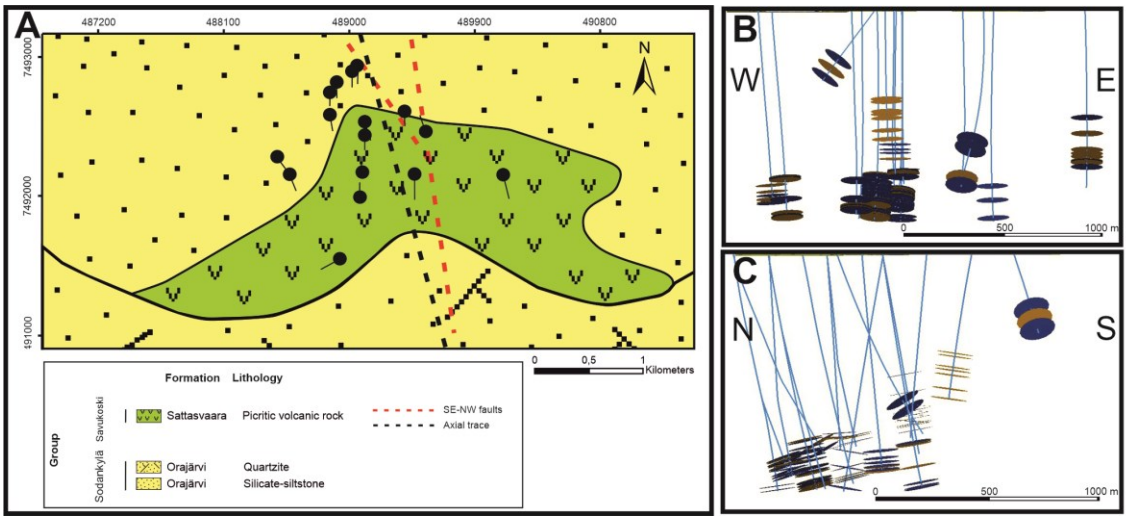

Figure 11. A: Map view of the study zone with stratigraphic units and drill core sites. Red dashed lines describe the SE-NW faults that are quite parallel to the axial trace of the large-scale open fold (black dashed line). The map is based on the publicly available map The Bedrock of Finland 1:200 000 (GTK) and coordinates are given in EUREF-FIN. B and C: Thin section (orange disks) and geochemical sampling sites (blue disks) exhibited in two cross sections in 3D-view. Drill holes are marked with blue and in figures above they reach the surface. The samples are taken from great depths and from both sides of the footwall basal thrust (figs. 21-22).

3.2 Geochemistry

Geochemical sampling and whole rock analysis were performed first to classify the rock units and correlate them to regional stratigraphic groups, and secondly to construct stratigraphic columns and enhance the stratigraphic separation study. The samples were taken from drill cores, whose drilling sites are indicated in figure 11. The sampling sites (fig. 11 B-C) concentrated on different rock units on both sides of the footwall basal thrust and in general the samples were taken from representative and homogeneous rock units. Few samples were taken from fault breccias since their investigation offered information about the hydrothermal alteration. In addition to the whole rock analysis, a micro-XRF analysis was performed for certain chosen thin section samples to study the zonation of some metamorphic minerals.

The samples weighed 200-300 g/sample. If the sampled drill core was already split to half, the core was split again, and the minimum length of the sample was determined to be 40 cm. If the sampled drill core was not split, the core was cut in half and the minimum length of the sample was 20 cm. The samples were photographed and their lithological properties were recorded. They were named with running numbering according to Anglo American's internal sampling standards in the form FMOSX (X=running numbers). In sampling the QAQC process was conducted according to Anglo American's internal QAQC standards as sample blanks, duplicates and certified

reference material (CRM) were included. The insertions of QAQC samples in general was random, and no QAQC samples were taken after another QAQC sample, except the coarse and pulp duplicates as they must be taken together according to the standards. Coarse quartz blanks and pulp blanks were both inserted at a rate of 1 in 40 original samples alternating between the two blanks. Coarse and pulp duplicates were inserted both at a rate of 1 in 20 original samples. CRMs comprised two types of CRM and their insertion was not random as one CRM should chemically resemble the original sample it is compared to. Each CRM was used at least twice, and they were inserted at a rate of 1 in 20 original samples.

A total of 84 samples including the QAQC-samples were taken and firstly shipped to Bureau Veritas Mineral Laboratory in Poland where the samples were crushed and pulverized, and then finally shipped to Bureau Veritas Mineral Laboratory in Canada, where they were analyzed by the ICP-ES (Inductively Coupled Plasma Emission Spectrometer) and ICP-MS (Inductively Coupled Plasma Mass Spectrometer) methods. Some of the samples were first treated by fire-assay, aqua regia digestion or other acid digestion, but as these treatments were done for elements not under investigation in this study, they are not explained further.

Stratigraphic study

Obtained geochemical results were plotted into several geochemical diagrams, where they were compared with regional stratigraphic groups and with each other. This facilitated their correlation in the regional perspective and offered profound comprehension of different rock units. The results were utilized in the constructions of stratigraphic columns as they usually confirmed geochemical discrepancies between different rock units.

Micro-XRF analysis

Micro-XRF (Micro X-ray Fluorescence spectrometry) is a method that can be used for non-destructive elemental analysis. The apparatus used for the analysis was M4 Tornado. The analysis was performed only for thin sections with zoned metamorphic minerals, as the zonation could provide information about the metamorphism and possible hydrothermal alteration. The measurements were thus made within very small areas of thin sections, with a very small measurement spot distance (20 μm). The analysis was performed in 20 mbar pressure and two silicon drift detectors were used. Before the analysis, these detectors were calibrated with a Zr-standard sample. Other

set-ups in the analysis included 50 kV voltage, 600 μA anode current and 10 ms/pixel measuring time. The pixel size was 25 μm.

The analysis was performed within predetermined areas of samples. The results show relative proportions of certain elements within the area of analysis, while the method is not yet able to product trustworthy absolute element contents. Thus, if an element is present homogeneously thorough a sample without any clear anomalies, it results in an evenly distributed colours in final photographs and thus does not inform much about the concentrations of elements. The method suits best for the elements that are clearly concentrated on certain minerals and for non-homogeneous samples. The results are rather descriptive than quantitative with respect to the element contents.

3.3 Core logging and data management

Drill core logging was performed only for such drill cores that penetrated or possibly reached the footwall basal thrust or for drill cores that reached depths where the thrust was expected to occur. The chosen drill cores were not investigated completely, as the investigation was performed for rock intervals ~100 m above and below the core of the footwall basal thrust. Finally, seventeen drill cores were chosen of which nine were oriented. As an orientation line is usually required for measuring planar and linear structures of drill cores, there are no structural measurements from those eight non-oriented drill holes. However, lithologies and faulted rock intervals were recorded in each chosen drill core, including the non-oriented drill cores.

Structural analysis

Five of the nine oriented drill cores were representative for structural investigation while the rest consisted of mafic or ultramafic rocks without clear ductile planar or linear structures. In total 205 α-, β- and γ-angle measurements were performed of those drill cores including axial plane, fold axis, fault plane and foliation measurements. In addition to measurements made by the author, previous measurements were used as well to support new data. The measurements were plotted in stereoplots, and they were compared with lithological unit and footwall basal thrust continuities that were drawn on several cross sections where stratigraphic separations were also searched for (fig. 2). The measurements and local stratigraphic continuities were additionally used in the footwall basal thrust 3D-modelling as it was assumed that the metasedimentary rocks and the footwall basal thrust have similar orientations. For observing systematic or sudden variations related to faulting or folding, dip and dip direction measurements were separately plotted on dipmeter-diagrams (fig. 1) against depth in drill core by

following a procedure represented by Hesthammer & Fossen (1998). The structures observed already during drill core logging stage were photographed and their asymmetries were described in detail.

Stratigraphic study

Lithological and fault interval logging formed the basis in the stratigraphic study and rock unit division. Pervasive alteration complicated rock identification, and rock units and respective field names determined during drill core logging rather describe some property of the unit than any specific rock type. Contacts of the units were carefully recorded and so were observed the colours, grain sizes, textures, minerals and structures of each unit. Crosscutting veins, faults and other structures were searched for and recorded if they were present. The widths and fillings of fault cores and respective damage zones were stored whenever possible to visually determine them. Final rock units were eventually compared with geochemistry and thin section studies to assure their correlation. When the final rock units were determined, the stratigraphic columns for each drill core were constructed.

4. Results

4.1 Petrography

Several rock units were recognized in drill core logging, which include units named during core logging as aphanite, metaperidotite, altered and sheared metaperidotite, carbonate breccia, Mg-breccia, mafic volcanic rock, basalt, schists, mafic breccia and fault breccia. As the exact rock type was commonly difficult to infer due to pervasive alteration, the names listed above are used below in rock type descriptions, while the names used by the company and more accurate rock types are shown in parentheses.

Aphanite (IT) (Si- enriched picrite)

Commonly in the central parts of the study zone appearing aphanite unit rocks consisted of black or dark-grey coloured mafic volcanic rocks with aphanitic grain size. They can be easily distinguished by the intrinsic pillow lava or flow-top breccia structure (Appendix 3) attributed to subaqueous extrusion. The rocks were commonly crosscut by carbonate veins that occurred densely in the vicinity of brittle faults that also crosscut these rocks.

Metaperidotite (1B/1Bb/1A) (Metaperidotite)

In the NW-parts of the study zone occurring metaperidotites were black or dark-grey and medium to coarse grained rock types, while fine-grained metaperidotites also

occurred occasionally. The cumulus-texture is typical for this rock type (Appendix 3), and observations of predominant orientation of minerals were referred as magmatic flow foliation. Metaperidotites were usually crosscut by carbonate veins and more seldom by Cu-mineralized, gypsum, and anhydrite veins.

Altered and sheared metaperidotite (2FM) (Intensively altered picrite)

Dominating pervasive alteration gave a characteristic greenish or brownish colour to altered and sheared metaperidotites facilitating their identification (Appendix 3). Non-altered intervals of this unit occasionally resembled the previously described metaperidotite rocks as the cumulus-texture is sometimes detected on the background. White carbonate dots were common features although not always visible or present. The grain size varied from fine to medium-grained. Porphyritic and ophitic textures were common, and the plagioclase crystals in latter ones were enclosed by amphibole minerals probably altered from pyroxenes.

The rocks were usually crosscut by carbonate veins and sometimes gypsum veins that occurred densely close to their lower contact to the footwall basal thrust. In addition, the rocks became frequently weaker close to the thrust. Presumably also the alteration is most probably related to the closeness of the thrust. Geochemical results (figs. 12 & 13) indicate that the altered and sheared metaperidotites have notably higher Al_2O_3, K_2O, Na_2O and SiO_2 contents and a lower MgO content compared to the metaperidotites. Additionally, the CaO contents are higher in altered and sheared metaperidotites than in metaperidotites (Appendix 1). The altered and sheared metaperidotites consist of tremolite, chlorite, talc, albite and phlogopite. This together with the geochemistry and present veins could refer to albitization, talc-carbonate alteration and chloritization. Andalusite porfyroblasts and syn-kinematic scapolite porfyroblasts were quite common in more aluminium and potassium rich and visibly sheared samples and provided information about metamorphism.

Fault breccia (BRE)

Fault breccia unit comprises a heterogeneous group of fault rocks and thus the abundant minerals and geochemical contents varied considerably. Characteristic for all fault breccias were angular clasts, chaotic texture and pervasive alteration with pale colour (Appendix 3). The CaO contents were high in these rocks and the fault cores were typically clayish. The specific fault rock types included especially fault breccias but also fault gouges, protocataclasite, cataclasite and protomylonite, of which the last was represented as a layer in chapter 4.3.

Basaltic vein (Basaltic trachy-andesite)

Only rarely found basaltic veins occurred solely within the footwall basal thrust, and they are not described as a separate unit. The chemistry of basaltic veins was strikingly uniform (figs. 12-13) considering the modest sampling size and the fact that they clearly deviate from other mafic rocks. They were found in three drill cores above the metasedimentary rocks as short (<40 cm) black or dark-grey coloured layers consisting of fine-grained material.

Carbonate breccia (ANBR) (Brecciated Ca-bearing rock)

Rock unit found in the northwestern and eastern parts of the study zone was the carbonate breccia, whose main minerals are calcite and anhydrite. Additionally, some minerals were dissolved in thin section preparation and are observed as empty spaces in thin sections. These dissolved minerals probably included gypsum. The distinguishable features include pink to pale-grey colour and sometimes occurring mafic/ultramafic and pelitic rock fragments. Grain size varies from very coarse to medium-grained and clasts are poorly sorted. Clasts are usually subangular or subrounded, indicating sedimentary origin and short transport distance from the original source. In addition, the texture is chaotic that is characteristic for these rocks.

Magnesite breccia (ANBR/BRE) (Brecciated Mg-bearing rock)

In association with the carbonate breccias occurring magnesite breccias were orange or brown rocks, with textures and structures similar to those of carbonate breccias. Chemically the magnesite breccias contain more Mg than Ca and more iron compared to the carbonate breccias (fig. 14), which may refer to a presence of mafic minerals in these rocks.

Mafic breccia (BRE) (Mafic breccia)

Third type of breccias found in the study zone is the mafic breccia, which was a rare and heterogeneous rock unit. With respect to the rock texture the clasts are chaotically oriented and commonly angular or subangular. This breccia unit could be interpreted as igneous breccia or fault breccia, as surrounding units are mafic volcanic rocks, but the layers are relatively thin and probably connected to faulting.

Mafic volcanic rock (2M. 6S) (Metabasalt)

Rocks situated in between the schists were mafic volcanic rocks. They did not exhibit clear foliation or folding in macroscale, while thin section studies revealed both. These rocks are fine-grained rocks with porphyritic texture, and mineralogically they consist mainly of biotite, chlorite, opaque minerals, tremolite and hornblende. However, it must

be noted that only one thin section sample from the mafic volcanic rock unit was prepared and analysed.

Schists (6S) (Ca-rich and Ca-poor schists)

The schists can be divided in two subunits: pale-grey coloured Ca-rich schists and dark-grey or brown coloured Ca-poor schists. Mineralogically the Ca-poor schists are mainly composed of quartz, chlorite, muscovite and biotite, while Ca-amphiboles and epidotes occur as well. The Ca-rich schists are consisted of calcite, quartz and chlorite in addition to Ca-amphiboles and epidote. Medium grain size, low-temperature minerals and intense foliation form the basis for the term schist. Common microstructures in both schist varieties are crenulation cleavage, microfolding, axial plane cleavage, shear bands and boudinage among others. Epidote and hornblende porfyroblasts were coarse-grained and clearly post-tectonic.

4.2 Local geochemistry and correlation to Savukoski and Sodankylä Groups

Sixty-seven rock samples excluding the QAQC samples were collected from the drill cores. The samples were divided based on the petrographic analysis into mafic/ultramafic volcanic rock units and metasedimentary or breccia units. The former comprised thirty-seven samples, while the metasedimentary and brecciated units included fifteen samples of metasedimentary rocks and fifteen of different breccias. The complete list of results from the geochemical analysis of major elements can be found in Appendices 1 and 2.

As one of the main objectives in this study was to test if the ultramafic/mafic rocks correspond to the Savukoski Group, the metaperidotites, altered and sheared metaperidotites, aphanites, mafic volcanic rock unit rocks and basaltic veins were compared with the general geochemistry of the Savukoski Group presented by Lehtonen et al. (1998). Similarly, the schists were compared with the Sodankylä Group earlier described by Lehtonen et al. (1998), Räsänen (2008, 2018), Köykkä et al. (2019) and Köykkä & Luukas (2021).

4.2.1 Major element geochemistry of ultramafic/mafic rocks

Five mafic/ultramafic volcanic rock units were finally discriminated in the geochemical classification diagrams (figs. 12-13), where each colour corresponds to a certain rock unit. In overall, the geochemical analysis seems to characterize well these units and supports the initial division made during core logging, even if the rock type classified by geochemical diagrams does not always correspond to the original field name.

Aphanite unit (IT) (Si-enriched picrite)

A total of eight samples from the aphanite unit were geochemically analysed and plotted to several geochemical plots. The aphanite unit rocks are classified as basalts or picrobasalts in the TAS-diagram due to their higher SiO_2 content (~45-50 %) and higher Na_2O and K_2O contents compared to those contents in metaperidotites (fig. 12). A high MgO content is typical as the rocks are classified as komatiitic basalts in the Jensen's cation plot, although two samples plot into the komatiite field (fig. 13). However, considering the terms komatiite or picrite they do not describe this unit well in its current state as they cannot be defined as ultramafic rocks due to SiO_2 content > 45% (Appendix 1). The term basalt is not suitable either, as the high (>18 %) MgO content prevents its use by definition. Since the extremely high MgO content refers to ultramafic origin, in this study these rocks are called Si-enriched picrites from now on. This subject will be discussed further in chapter 5.1.

Metaperidotite (1B/1Bb/1A) (Metaperidotite)

Eight metaperidotite samples exhibit extremely low SiO_2 contents and low Na_2O and K_2O contents in the Total Alkali vs. Silica (TAS)-diagram (Middlemost, 1994) that classifies these rocks even more SiO_2-poor rocks than picrobasalts (fig. 12). However, picrobasalt field in the TAS-diagram corresponds to a peridotite field in the TAS-diagram for intrusive rocks that describes these rocks better due to the relatively coarse grain size. The Jensen's cation plot (Jensen, 1976) exhibits another alternative by classifying them as komatiites (fig. 13). In this study, the rocks are named as metaperidotites due to coarse grain size, lack of clear spinifex-textures, gradual contacts and trace element geochemistry. However, since they are extremely MgO-rich and ultramafic rocks they were compared with regional stratigraphic groups and ultramafic intrusions that also include komatiites and picrites.

Altered and sheared metaperidotite (2FM) (Intensively altered picrite)

The altered and sheared metaperidotites express great deviation in the TAS-diagram as a total of fifteen samples plot into several fields, of which the basalt and tephrite fields are the most usual (fig. 12). The rocks have high Mg content as they are classified as komatiites in the Jensen's cation plot (fig. 13). These results also deviate to some extent as four samples plot into the komatiitic basalt field and one sample into the high-Mg tholeiitic basalt field (fig. 13). The one altered metaperidotite sample that deviates distinctively from other samples was originally classified as gabbro and may indeed represent a different rock type. The high silica contents sometimes observed in the

TAS-diagram may be related to the high proportion of albite in these rocks. It must be noted that the unit was visibly altered and the elevated Na_2O and K_2O contents probably reflect this alteration. Strikingly, the geochemistry of this unit seems to resemble the geochemistry of the Si-enriched picrites (Appendix 1). The relatively fine grain size and geochemical similarity with the Si-enriched picrites refer to that the term metaperidotite does not describe these rocks well, despite the cumulus-texture sometimes detected in these rocks. In addition, as the alteration is characteristic for this unit, in this study these rocks are named as intensively altered picrites.

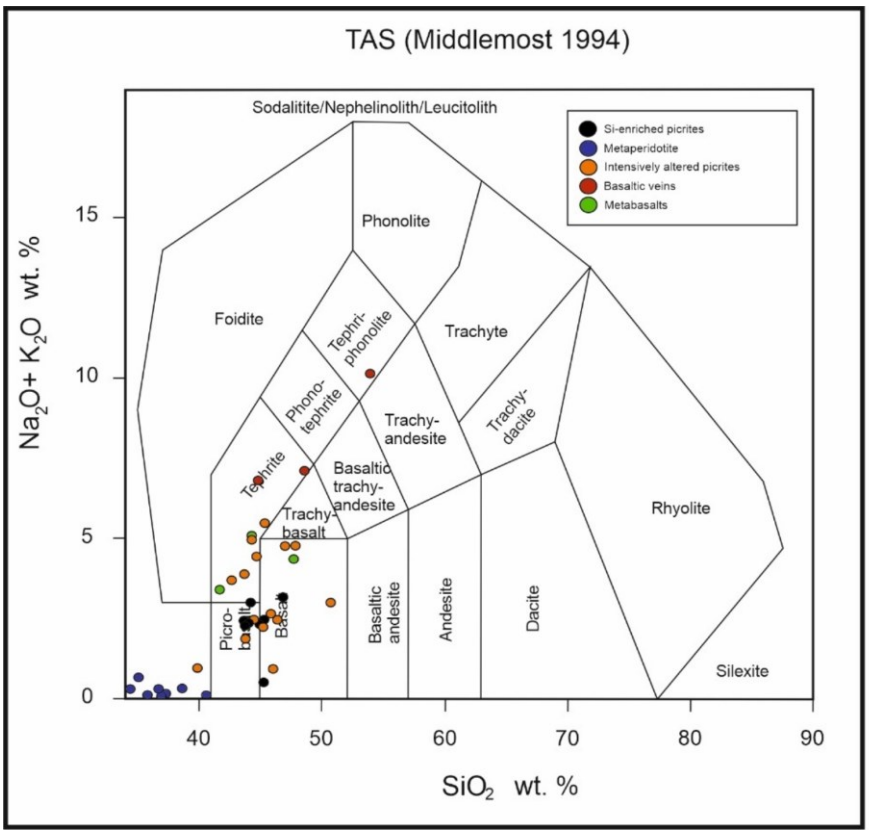

Figure 12. Geochemical classification of the mafic/ultramafic rocks of Sakatti according to the TAS-diagram (Middlemost, 1994).

Mafic volcanic rock unit and basaltic veins (metabasalts and basaltic veins)

Only three mafic volcanic rock samples and three basaltic vein samples were taken for geochemical analysis. These samples exhibit high Na_2O and K_2O contents and the geochemical classification diagram of Middlemost (1994) classifies mafic volcanic rocks as tephrites or basalts and basaltic veins as tephrites or tephri-phonolites (fig. 12). Higher Na_2O+K_2O contents probably indicate alteration and for simplicity these units are named as metabasalts and basaltic veins, respectively. The Na_2O+K_2O contents are higher in basaltic veins compared to the metabasalts that makes them geochemically distinct (fig. 12). Both units usually plot into the High-Mg tholeiitic basalt field in the

Jensen's cation plot due to high Al_2O_3 content and low Fe^T and TiO_2 contents. Only one basaltic vein sample shows elevated Fe^T values and plots into the High-Fe tholeiite basalt field (fig. 13). These veins typically occur within the footwall basal thrust and the elevated Na_2O and K_2O values possibly reflect alteration related to it.

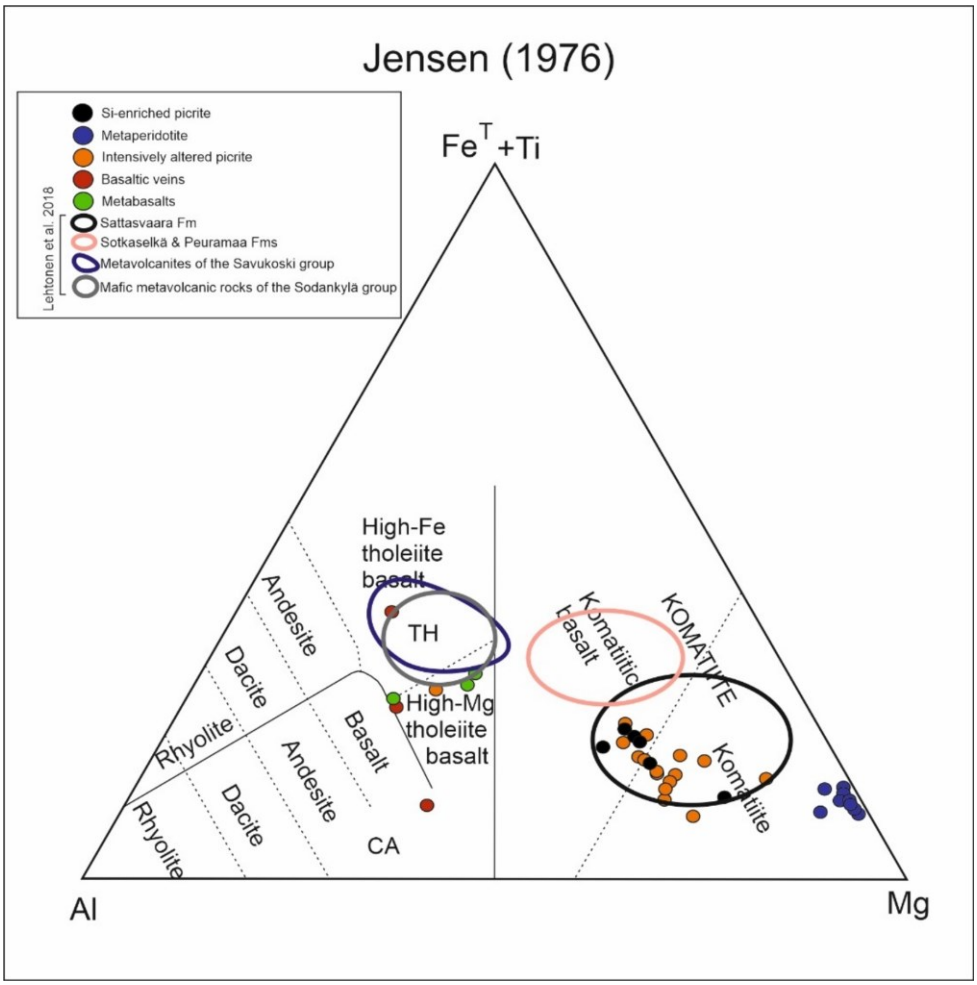

Figure 13. Geochemical classification of the mafic volcanic rock units in Sakatti according to the Jensen's cation plot (1976). The local rock units are compared with the Savukoski and Sodankylä Group rocks that are marked with different coloured circles.

Correlation to Savukoski and Sodankylä Group rocks

Lehtonen et al. (1998) characterized the Savukoski Group komatiites and picrites and the mafic metavolcanic rocks of the Sodankylä and Savukoski Groups. The results of their study included several geochemical diagrams of which the results of the Jensen's cation plot were added in figure 13 for facilitating comparison with the studied rocks. It seems that the Si-enriched picrites and intensively altered picrites plot close to the komatiites of the Sattasvaara Formation, while the metaperidotites are much more enriched in MgO. The basaltic vein and metabasalt samples plot close to the field to where the mafic metavolcanic rocks of the Savukoski and Sodankylä Groups are plotted

(fig. 13). The Si-enriched picrites, intensively altered picrites and metaperidotites deviate significantly from all of them, while the picrites only slightly from the rocks of the Sotkaselkä and Peuramaa Formation (fig. 13). Thus at least based on the Jensen's cation plot the Si-enriched picrites and intensively altered picrites could resemble the Sattasvaara komatiites and perhaps also the Sotkaselkä and Peuramaa picrites, while the metaperidotite unit rocks do not correlate with any of these rocks.

4.2.2 Major element geochemistry of metasedimentary and brecciated rock units

Five metasedimentary or breccia units were recognized in drill core investigation and sampled for geochemical analysis. The results were plotted in geochemical binary plots where major element contents are compared with SiO_2 contents. A complete list of major element results is in Appendix 2.

Fault breccia (BRE)

The fault breccia unit shows great deviation in chemistry and only three fault breccia samples were analysed. The Al_2O_3 and K_2O+Na_2O contents are quite high (fig. 14) which makes sense considering that they were situated within fault zones. The samples were taken from different faults with different surrounding lithological units that strongly influences their varying chemical composition. The sample with highest CaO content was taken within the footwall basal thrust and could represent filling material and wall rock alteration between the footwall basal thrust and surrounding units.

Carbonate breccia (ANBR) (Brecciated Ca-bearing rock)

The geochemical analysis of carbonate breccias included five samples. According to the results the extremely high CaO and MgO concentrations are typical for these rocks and the chemistry closely resembles the chemistry of Ca-rich schists excluding the elevated MgO values (fig. 14). The Na_2O and K_2O contents are low (<1,5 %) except for one sample with notably higher contents. Carbonate breccia unit mainly consists of CaO and MgO that together with SiO_2 practically form the rock. Since this unit is interpreted as a sedimentary unit that brecciated after its deposition, the unit is named as the brecciated Ca-bearing rock unit.

Magnesite breccia (ANBR/BRE) (Brecciated Mg-bearing rock)

Magnesite breccia unit occurred together with the carbonate breccia unit, and it is geochemically distinguished from the latter by the lower CaO contents and higher Fe_2O_3 and MgO contents (fig. 14). The close connection and similarity with sedimentary carbonate breccias refer to similar origin for this unit, and thus the unit is named correspondingly as the brecciated Mg-bearing rock unit. Four samples of this unit were

analysed and show quite uniform results, although one sample exhibited an elevated CaO content with reduced Fe_2O_3 and MgO contents (fig. 14).

Mafic breccias (BRE)

Three mafic breccia samples were geochemically analysed, and the results show significant deviation (fig. 14). The mafic breccias were considerably rarer than the carbonate and magnesite breccias and they seemed to have a strong mafic trace as the MgO content is high and the SiO_2 content is higher compared to the contents in carbonate and magnesite breccias. The rocks were commonly sheared and contained relatively high amounts of Al_2O_3 and Na_2O+K_2O that is related to alteration as the rocks were located close to bottom of drill holes and possible faults.

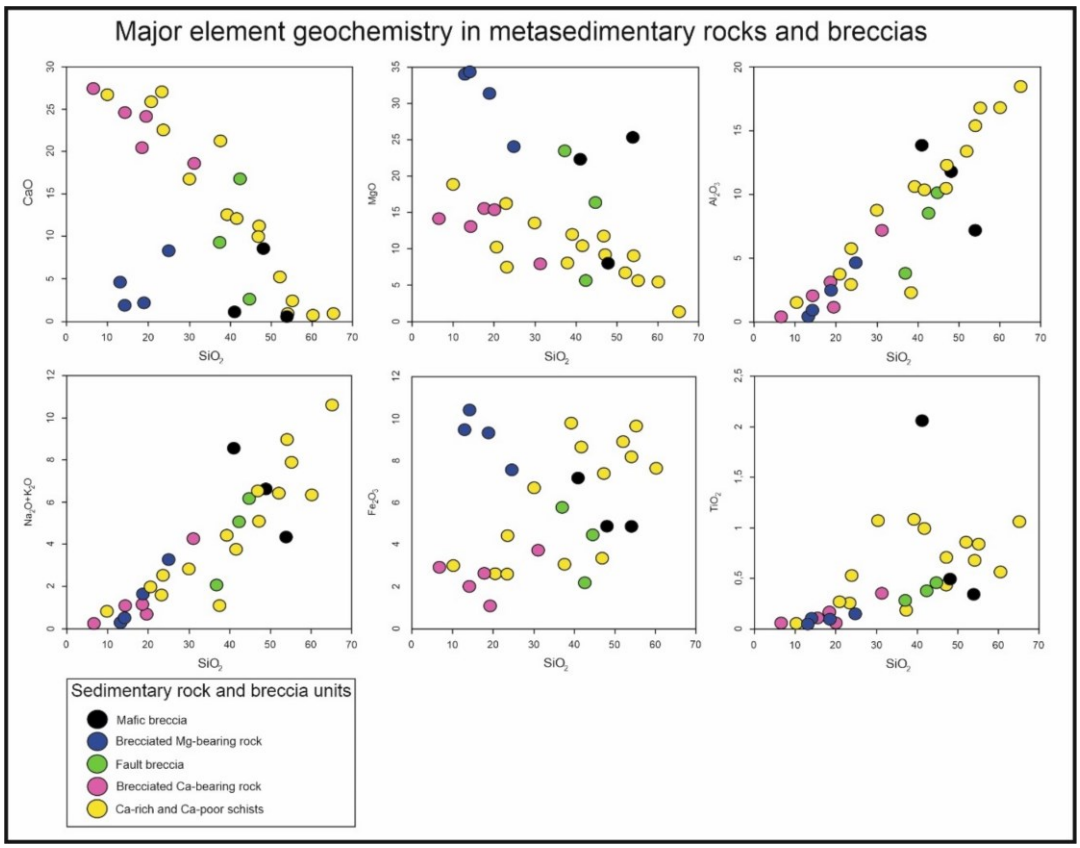

Figure 14. Major element vs silica diagrams for the metasedimentary rock and breccia samples.

Schists (6S) (Ca-rich and Ca-poor schists)

A total of fifteen schist samples were taken for geochemical analysis. The samples exhibit a clear continuum of Na_2O+K_2O and Al_2O_3 contents that increase as SiO_2 increases, while CaO and MgO show negative correlation with the SiO_2 (fig. 14). The two types of schists usually alternated from one type to another without sharp contacts. The chemical variation between the two members is well seen in the binary plots as the

Ca-rich schists for instance are characterized by an extremely high Ca content with smaller SiO_2, Al_2O_3, Fe_2O_3, Na_2O, K_2O and TiO_2 contents than Ca-poor schists while the MgO content is higher in Ca-rich schists.

Correlation to Savukoski and Sodankylä Group rocks

The rocks of the Honkavaara and Orakoski Formations of the Sodankylä Group were compared with the schists in the ternary diagram of $CaO+Na_2O$-Al_2O_3-K_2O that describes the CIA (Chemical Index of Alteration)-index (fig. 15) used for estimating paleoclimate and paleoweathering of sediment source areas (in e.g., Köykkä et al. 2019). The diagram shows that the Ca-rich schists deviate from the rocks of the Orakoski Formation while the Honkavaara Formation rocks appear quite similar. The Ca-poor schists instead show similar patterns to the rocks of the Orakoski Formation, as they both get higher CIA-index values than the Ca-rich schists indicating a greater degree of weathering (fig. 15).

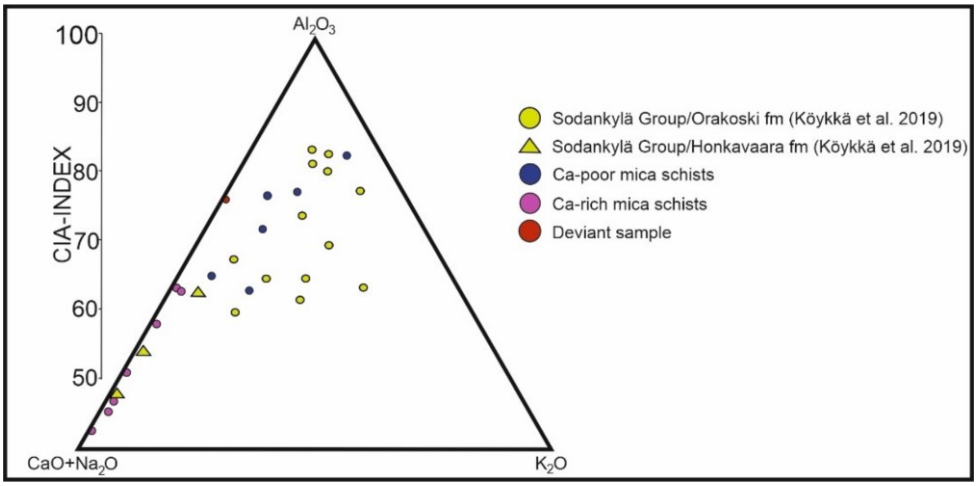

Figure 15. CIA-ternary diagram indicating parallel values for the Ca-poor schists and the rocks of the Orakoski formation. Ca-rich schists show similar patterns with the rocks of Honkavaara formation. Higher CIA-index indicates greater degree of weathering.

A discriminant-function diagram (fig. 16) shows similar outcomes, as the Ca-poor schists plot relatively close to the Orakoski Formation rocks, both plotting into the continental rift field (fig. 16). In turn, the Ca-rich schists plot into the island arc/continental arc field as do the Honkavaara Formation rocks (Köykkä et al. 2019), even if they are not plotted into this discriminant-function diagram due to too high SiO_2 content. The discriminant-function diagrams describe the tectonic setting for deposition and are proven to be quite robust against later chemical changes (in e.g., Köykkä et al. 2019). Thus, at least based on the previous geochemical diagrams the schists correlate quite well with the Sodankylä Group rocks. Since the Ca-rich and Ca-poor schist are

distinctively different even though they commonly occur as rapidly alternating layers, it is possible that alteration has taken part in forming the present chemical composition.

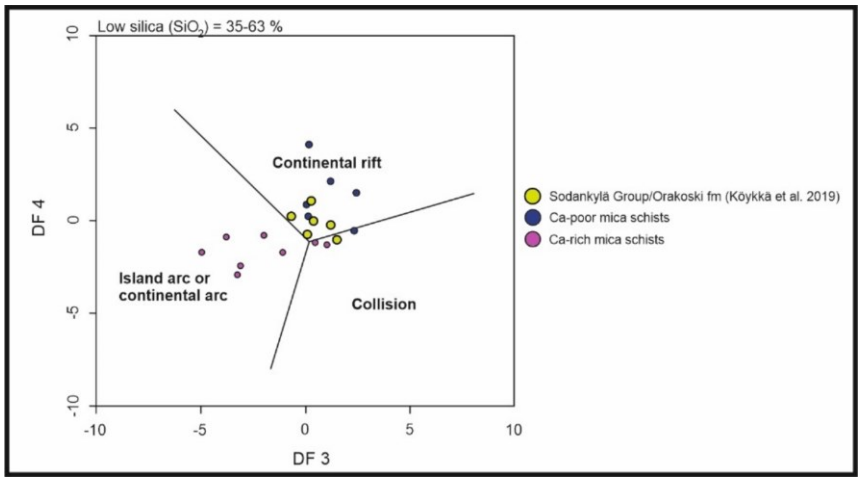

Figure 16. A discriminant-function multi-dimensional diagram of low-silica content for Sakatti schists and rocks of the Orakoski Formation (Köykkä et al. 2019) modified after Bhatia (1983) and Verma & Armstrong-Altrin (2013). Formulas for calculating the DF3 and DF4 are after Verma & Armstrong-Altrin (2013).

4.2.3 Trace elements

Mafic/Ultramafic volcanic rocks

Spider diagrams show distinct LREE (Light Rare Earth Elements) and HREE (Heavy Rare Earth Elements) patterns for ultramafic and mafic volcanic rock units (fig. 17). The amount of certain coloured curves in the diagram is not the number of samples of respective rock unit. The coloured curves rather depict the extreme values of the unit in question. Most of the units show a decreasing pattern for LREEs, while also HREEs decrease although more gently. The intensively altered picrites, one basaltic vein sample, two metabasalt samples and metaperidotite samples instead exhibit a flat pattern for HREEs (fig. 17). The intensively altered picrite unit has distinct negative Eu-anomaly that other units do not have. One Si-enriched picrite and one metabasalt sample show smoothly increasing LREE pattern. The metaperidotite unit has extremely low LREE and HREE values in general (fig. 17). Interestingly, the LREE and HREE patterns do not exhibit any clear anomalies, excluding the negative Eu-anomaly of the intensively altered picrite unit.

The chondrite normalized spider diagrams of the Sattasvaara komatiites and Sotkaselkä and Peuramaa picrites were published by Lehtonen et al. (1998). Those picrites in general exhibit decreasing patterns with respect to both LREEs and HREEs, while LREEs in Sattasvaara komatiites have an increasing trend and HREEs exhibit gently

decreasing trend with a positive Lu-anomaly. La and Ce negative anomalies are distinct and characteristic for komatiites (Hanski et al. 2001). The Si-enriched picrites do not show any anomalies, and the LREE contents in general are greater than those of the Sattasvaara komatiites (fig. 17). The Si-enriched picrites and intensively altered picrites closely resemble the LREE and HREE patterns of the Sotkaselkä and Peuramaa picrites. Picrites of the Sotkaselkä and Peuramaa formations have LREE contents of ~15-50 and corresponding values for studied ultramafic/mafic volcanic rocks would be ~8-45 if metaperidotite samples and one basaltic vein sample are excluded (fig. 17). Thus, the trace element contents and LREE and HREE patterns are quite similar between the picrites. With respect to the metaperidotite rock samples, the LREE and HREE contents differ greatly. In addition, there is no increasing trend in the LREEs either. The trend seems to be closer to the one of picrites, but the contents are much lower (fig. 17). It could be possible that secondary alteration has influenced these trends by decreasing both LREE and HREE values.

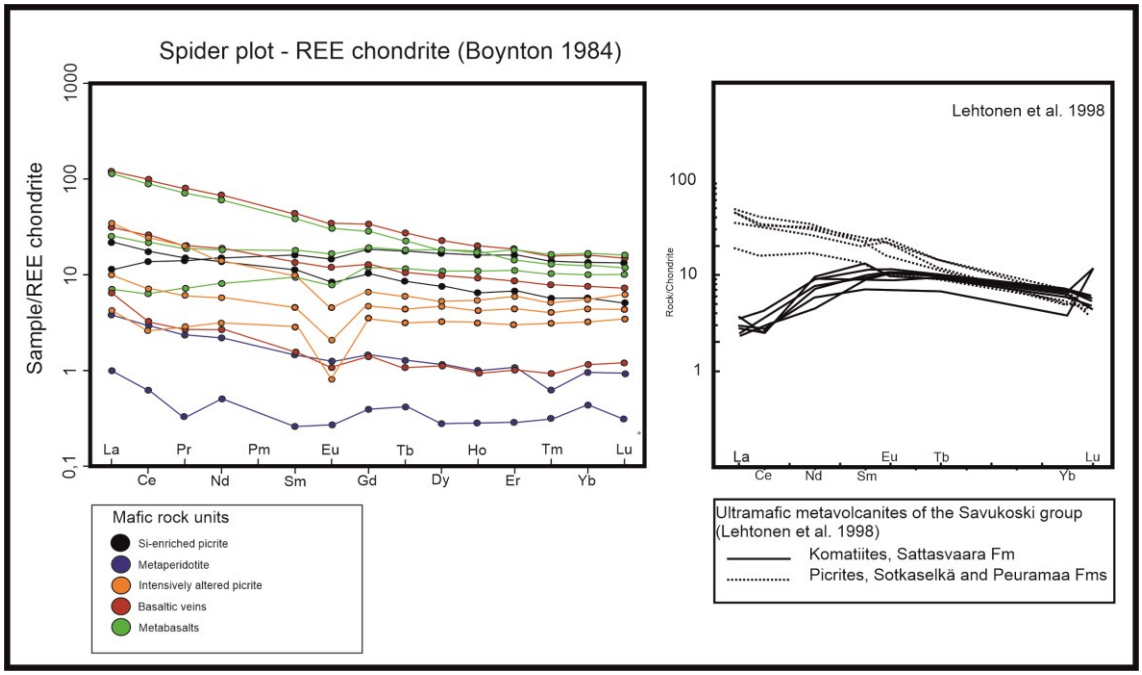

Figure 17. Left: chondrite normalized spider diagrams for mafic/ultramafic metavolcanic rocks of the study zone after Boynton (1984). Right: chondrite normalized spider diagrams for the ultramafic metavolcanic rocks of the Savukoski Group modified after Lehtonen et al. 1998.

Metasedimentary rocks and breccias

Trace element geochemistry of schists was investigated by constructing chondrite normalized spider diagrams where LREE and HREE patterns are presented (fig. 18). They were not built for breccia units as they were commonly quite heterogeneous. Strikingly, the patterns in general look like the patterns of the ultramafic/mafic volcanic

rocks, as the trend for LREEs seems to decrease for both schist varieties while HREEs exhibit a smoothly decreasing or almost a flat pattern (fig. 18). One Ca-poor schist shows a steeply decreasing LREE trend and an increasing HREE trend. However, this sample was slightly different from other schists and located within the footwall basal thrust. The Ca-rich schists have similar patterns with the Ca-poor schists but the REE contents in general are lower. The sample marked with red colour is a clearly sheared metasedimentary rock sample that was not a schist and deviates greatly from others (fig. 18). There is no clear anomaly in the LREE and HREE patterns. Again, the number of coloured curves in spider diagrams describes the extreme values for each rock unit and not the exact number of samples.

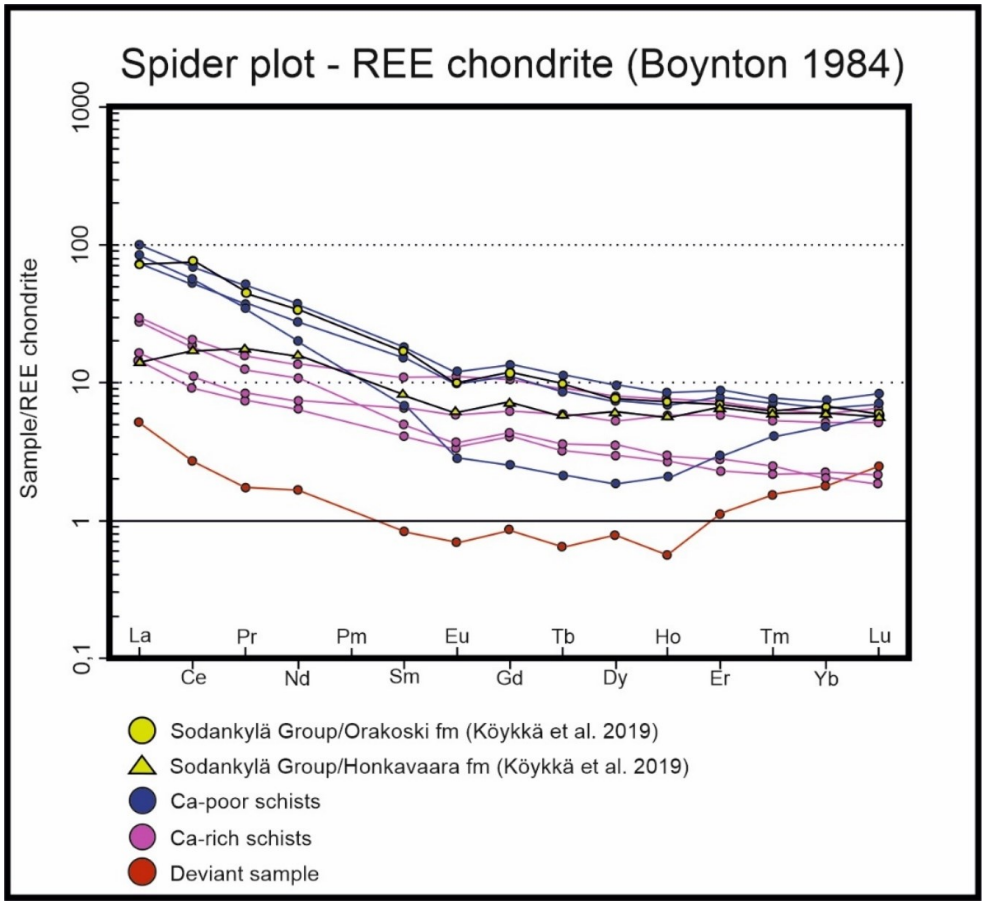

Figure 18. Chondrite normalized spider diagrams for the schists in the study zone after Boynton (1984). General curves for Orakoski and Honkavaara Formation rocks of Sodankylä group are modified after Köykkä et al. 2019.

Köykkä et al. (2019) represented spider diagrams of several stratigraphic groups found from the CLGB, KB and PB, of which the ones of the Sodankylä Group are shown in figure 18 together with the spider diagrams of the schists. The rocks of the Orakoski Formation follow strikingly well the patterns of Ca-poor schists and exhibit decreasing LREE patterns and smoothly decreasing or flat HREE patterns without any clear

anomalies. The only readily distinguishable differences are the modest positive Ce-anomaly in Orakoski formation rocks and one different Ca-poor schist sample (fig. 18). The Honkavaara formation rocks have an increasing trend initially for lightest lanthanoids that turns to a decreasing pattern towards Eu. The HREE pattern is flat in overall for the Honkavaara formation rocks, which follows quite well one Ca-rich schist sample (fig. 18). However, the spider diagrams point slightly different LREE and HREE patterns for Ca-rich schists and Honkavaara formation rocks.

4.2.4 Summary of the geochemical correlation to Sodankylä and Savukoski Groups

Ultramafic/mafic volcanic rocks

The Si-enriched picrites were quite similar to the Sotkaselkä and Peuramaa picrites with respect to trace element geochemistry (fig. 17), while they are more similar to the Sattasvaara komatiites with respect to major element geochemistry (fig. 13). The metaperidotites do not resemble the geochemistry of the Sotkaselkä and Peuramaa picrites or the Sattasvaara komatiites at all (figs. 13 & 17). Thus, the geochemistry does not support well any correlation between the Savukoski Group rocks and the studied ultramafic/mafic rocks, although in overall the geochemistry of the Si-enriched picrites does not deviate significantly of the Sotkaselkä and Peuramaa picrites.

Köykkä & Luukas (2021) described a new stratigraphic formation called the Visasaari Formation, which lies in the upper parts of the Sodankylä Group in the stratigraphic column and consists of mafic Fe and Mg-tholeiitic subaerial volcanic rocks that could well be represented here by the studied metabasalts. The rocks of the Visasaari Formation were not compared with the studied rocks in geochemical diagrams since there is no published data about their geochemistry. Unlike the other ultramafic/mafic volcanic rocks, the metabasalts were deformed and their typical occurrence within the schists would support the contemporaneous deformation and similar age with the Sodankylä Group schists.

Metasedimentary rocks and breccias

The geochemical results support the hypothesis according to which the schists could correspond to the Sodankylä Group, as the trace element and major element geochemistry are consistent (figs. 15-16, 18). The only clear difference is the SiO_2 content that is much lower for Ca-poor schists (46-65 %) than it is for the Orakoski formation rocks (52-96%, Köykkä et al. 2019). Still, only one sample does not yield to the range unlike all the other Ca-poor schist samples (Appendix 2). There is not much available data about the common mineralogy in the rocks of the Orakoski Formation,

but according to Räsänen et al. (2018) quartz, plagioclase and biotite are the most common minerals in the rocks of the Tepsanniemi member of the Orajärvi Formation. In addition, the Orajärvi Formation is defined as calcareous and scapolite bearing pelitic rocks (Räsänen et al. 2018). Both descriptions are in concordance with the results of studied schists. As the Orajärvi Formation is found in the upper parts of the Sodankylä Group, while the Orakoski Formation belongs to the lowermost parts, the Orajärvi Formation matches better with the studied rocks. The discovery of anhydrite within the thick sedimentary brecciated Ca-bearing rock unit above the schists provides strong support for classification these rocks as Sodankylä Group rocks, as evaporites and collapse-type breccias have been indirectly evidenced in the uppermost parts of the Sodankylä Group (Köykkä et al. 2019). Kyläkoski et al. (2012) suggested origin for the recorded collapse-type breccias in the Petäjäskoski formation in PB to be related to the dissolution of evaporites. Similar proposition was made by Vanhanen (2001) for the origin of breccias found in the KB and Vaimojärvi, Petäjävaara and Hukkavaara formations, of which the Vaimojärvi formation is a correlative unit to the Orajärvi formation (Räsänen, 2018). These formations in the Kuusamo Belt and Peräpohja Belt could correspond to the brecciated Ca-bearing rock unit described in this study.

Pelitic metasediments are also found in lower parts of the Savukoski Group (in e.g., Hanski & Huhma, 2005), but as there are no detailed geochemical data of the rocks, they were not taken into comparison here. Black schists, greywackes and phyllites are the most typical rocks for the lower parts of the Savukoski Group, and the two first ones were not observed in this study, and phyllites would probably have even smaller grain size than the studied schists had. However, if pelitic metasediments of the Savukoski Group would geochemically and petrologically resemble the studied schists, it would be consistent with the regional stratigraphy as they should be overlain by the ultramafic/mafic volcanic rocks (fig. 7).

4.3 Stratigraphy

In this chapter, the stratigraphic columns of certain drill cores are presented with a purpose of compare them and detect repeated or missing sections. The stratigraphic units are primarily built based on the petrography and geochemistry, and secondarily based on structural heterogeneities such as fault or mylonite zones. The stratigraphic columns are drawn on several variably oriented cross sections (figs. 19, 21-22) and they are simplified in figure 20.

Si-enriched picrite unit

The Si-enriched picrite unit was typically the uppermost layer overlying the intensively altered picrites (fig. 20), and it occurred widely in the study zone. The unit was not observed as continuous through the study zone, but it occurs especially close to the E-W and SE-NW faults 1 and 2 in figures 21 and 22. The contact with underlying intensively altered picrites was usually gradual. As the drill holes were not investigated entirely, the upper contacts were not recorded. Thus, the absolute thickness of this unit cannot be estimated based on this study. However, based on the previous data and this study the maximum thickness is ~200 meters. Interestingly, these rocks were not found together with the metaperidotites or brecciated Ca or Mg-bearing rocks that typically occur in the northwestern part of the study zone (figs. 20-22). However, according to previous data the Si-enriched picrites sometimes appear together with metaperidotites as repeated layers with gradual contacts. The petrographic and geochemical studies supported a strong connection between this unit and the intensively altered picrite unit.

Metaperidotite unit

Metaperidotites were found exclusively in the northwestern part of the study zone (fig. 21). It is typically the uppermost unit in areas where the Si-enriched picrite unit is not present and can cover a thickness of ~150 meters. The lower contact with the brecciated Ca-bearing rock unit is sharp and tectonic, while the nature of the upper contact is in turn unknown as it was not observed in the study. Within this unit dolomite and Mg-rich metaperidotite layers occur together as relatively thin and sharp layers and they are commonly associated with pyrite mineralizations. Dolomites are crosscutting veins, while the Mg-rich peridotites probably represent the alteration halo between the metaperidotites and dolomite veins. Other crosscutting veins include calcite, gypsum and seldomly anhydrite veins.

Intensively altered picrite unit

Present widely in the study zone and recorded in almost every logged drill core, the intensively altered picrite unit typically underlies the Si-enriched picrite unit and overlies the schists (figs. 20-22). The intensively altered picrite unit occurs sometimes as sheared above the footwall basal thrust indicating the influence of the latter. The sheared varieties of the intensively altered picrites are also included in the stratigraphic columns (fig. 21-22). Few samples from the sheared intensively altered picrites were geochemically analysed and the results corresponded to the chemistry of non-sheared

intensively altered picrites, thus being considered here as the same rocks but with shearing. The northwestern part of the study zone lacks the intensively altered picrites, while the metaperidotite unit is present there (figs. 21-22). Otherwise, the intensively altered picrite unit is continuous and seems to dip moderately towards northwest (fig. 21, sections 4 and 6). The lower contact with the schists was determined by the footwall basal thrust and related fault breccias. It was estimated that the intensively altered picrite unit covers a thickness varying between 60 to over 100 meters.

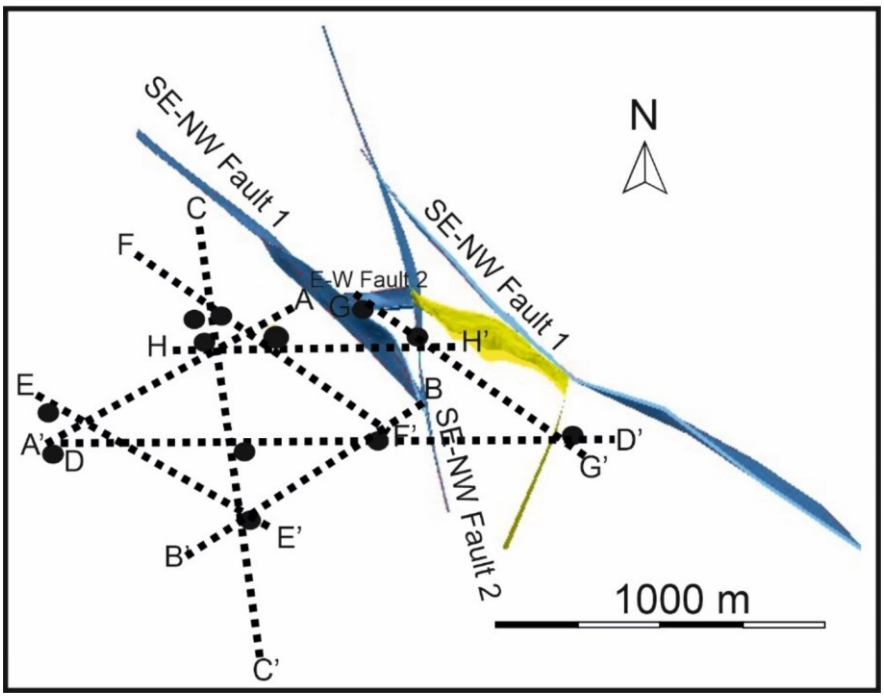

Figure 19. Horizontal projections of cross sections used in constructing the stratigraphic columns. Yellow faults are not described further as they were used mainly for scaling. Black circles are drilling sites.

Fault breccias

The fault breccias typically occur within the footwall basal thrust or other faults. In the footwall basal thrust they determine the core together with clayish rubble zone and characterize the nature of the thrust in later stages of deformation. Other fault breccias were especially located close to the SE-NW directed fault 2 and vertically oriented protomylonites. The thickness of fault breccia layers within the footwall basal thrust is ~10 meters varying from a minimum of 4 meters to a maximum of 20 meters.

Brecciated Ca and Mg-bearing rock units

The actual brecciated Ca and Mg-bearing rock units were found in the northwestern and eastern parts of the study zone (fig. 21) as ~35-55 meters thick units situated between

the overlying metaperidotites and underlying schists. In addition, these rocks occur as repeated thinner layers, from a few meters to almost 20 meters in thickness. Some of these thinner layers were located within the metaperidotite unit. The contact to underlying schists seems to be tectonic as it is usually characterized by brittle faults, shearing and fault breccias. As these units (i) are exceptionally thick layers compared to typical fault breccias, (ii) contain mainly subrounded or subangular clasts, (iii) do not exhibit clear signs of shearing or faulting excluding their contacts, and (iv) form a quite homogeneous units compared to typical fault breccias, they are interpreted as sedimentary breccias. Strikingly, the brecciated Ca and Mg-bearing rocks were not found in any place together with the footwall basal thrust at least in its regular form. However, in drill hole 12MOS8118 there is a very short and faulted interval, located at the underlying contact with the schists, that could be comprehended as the footwall basal thrust. However, the modest interval thickness and quite different faulting pattern in its neighbour drill hole 12MOS8105 led to its omission. Strikingly, in drill holes 12MOS8105 and 12MOS8118 this unit repeats in general in addition to repetitions within the metaperidotite unit (fig. 21). This repetition in almost vertical drill holes could be caused by reverse faulting.

Mafic breccia

Mafic breccia unit was found in a quite limited area from the central part of the study zone. This breccia type occurred typically below the intensively altered picrite unit and could be interpreted as either fault breccias or igneous breccias. The latter is supported by the observation according to which the overlying contact seems to be concordant and gradual. Their lower contact was not found as drill holes were ended probably due to drilling problems related to confronted fault, and thus there is no certainty about the breccia type. The extent and thicknesses of this unit were modest in drill cores, and thus this unit is not shown in the stratigraphic columns.

Schists (Ca- rich and Ca-poor schists)

Stratigraphically the lowermost rocks in the study zone are the Ca-rich and Ca-poor schists. They are overlain by the footwall basal thrust and related fault breccias and thus have a tectonic contact with the intensively altered picrite unit. Their lower contact was not reached by drilling, and so the complete unit thickness is unknown. However, the minimum thickness of the unit including both schist varieties and the metabasalt unit is ~40 meters. The thickest layers were found in the southernmost parts of the study zone where they were located closer to surface. The rocks were found across the study zone

except for one small area between the SE-NW faults 1 and 2 and the E-W fault 2 (figs. 19 & 22). The absolute contact between the different schist varieties is difficult to determine as the sedimentary layers are very thin and their contact is continuous and gradual rather than abrupt. This unit is folded and exhibits several deformation stages, where planar orientations in general dip to NW with ~30-50° angle.

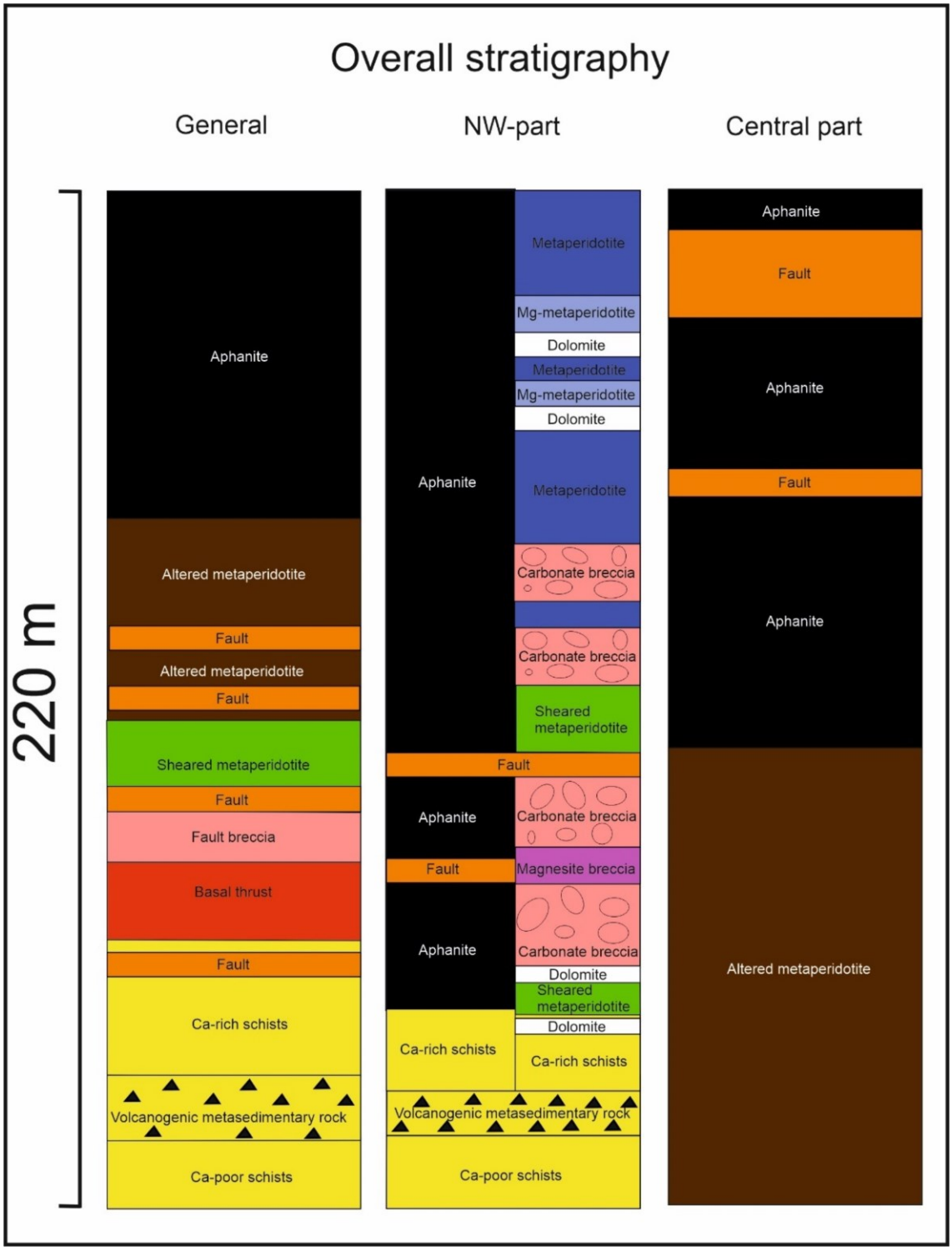

Figure 20. Generalized stratigraphy in different parts of the study zone. Unit thicknesses are not in exact scale.

Due to uniform orientations of planar structures, the initial hypothesis was that the complete metasedimentary unit had similar orientation to them. However, figure 21 reveals clear variation. If the schist unit would dip subhorizontally to NW, the apparent dip direction of the unit when viewed from the south would be almost horizontal with a modest dip to west, which seems to be the case (section 4, fig. 21). Similarly, the apparent dip direction of the unit when viewed from the southwest would be the true dip, thus dipping subhorizontally to NW. Sections 5 and 6 in figure 21 seem to support this dip direction. However, section 2 indicates ~40º dip towards NE, that does not fit to the idea about a constant dip direction of the schist unit towards NW. This section terminates to the SE-NW fault 2 that may influence this different dip direction. Interestingly, section 1 instead would support the NW dip direction as the schists dip almost horizontally towards NE that is close to the expected apparent dip according to the hypothesis. Section 3 is viewed from the west, and it indicates steep dip towards N for the footwall basal thrust and the schists although the latter seems to curve to almost flat in the north close to the E-W faults. This steep dip towards north is not expected either considering the hypothesis. Thus, it seems that the schist unit does not have a constant orientation dipping to NW, as there is some variation close to the SE-NW fault 2 and E-W faults. Despite the varying unit continuity, the dip and dip direction measurements taken from the drill cores in these areas indicate NW-dipping foliation with ~40º angle.

Metabasalt unit

The sheared metabasalts comprise a mafic unit situated between the Ca-rich and Ca-poor schists. Its position between the two schist varieties, moderate unit thickness, fine grain size and apparently concordant contact between the overlying Ca-rich schists and underlying Ca-poor schists would support extrusive origin and partly coeval genesis with the schists. Other option could be a sill-like intrusion. If it is an extrusive rock, it would also belong to the Sodankylä Group. Thin section studies revealed sheared micaceous layers that were not observed during core logging and that other mafic/ultramafic rocks did not exhibit, which is one reason why this unit is comprehended as a separate unit. In drill cores this unit was ~5-10 meters thick and it was found around the study zone except for one domain bordered by the SE-NW faults 1 and 2 and E-W fault 2 (figs. 21-22).

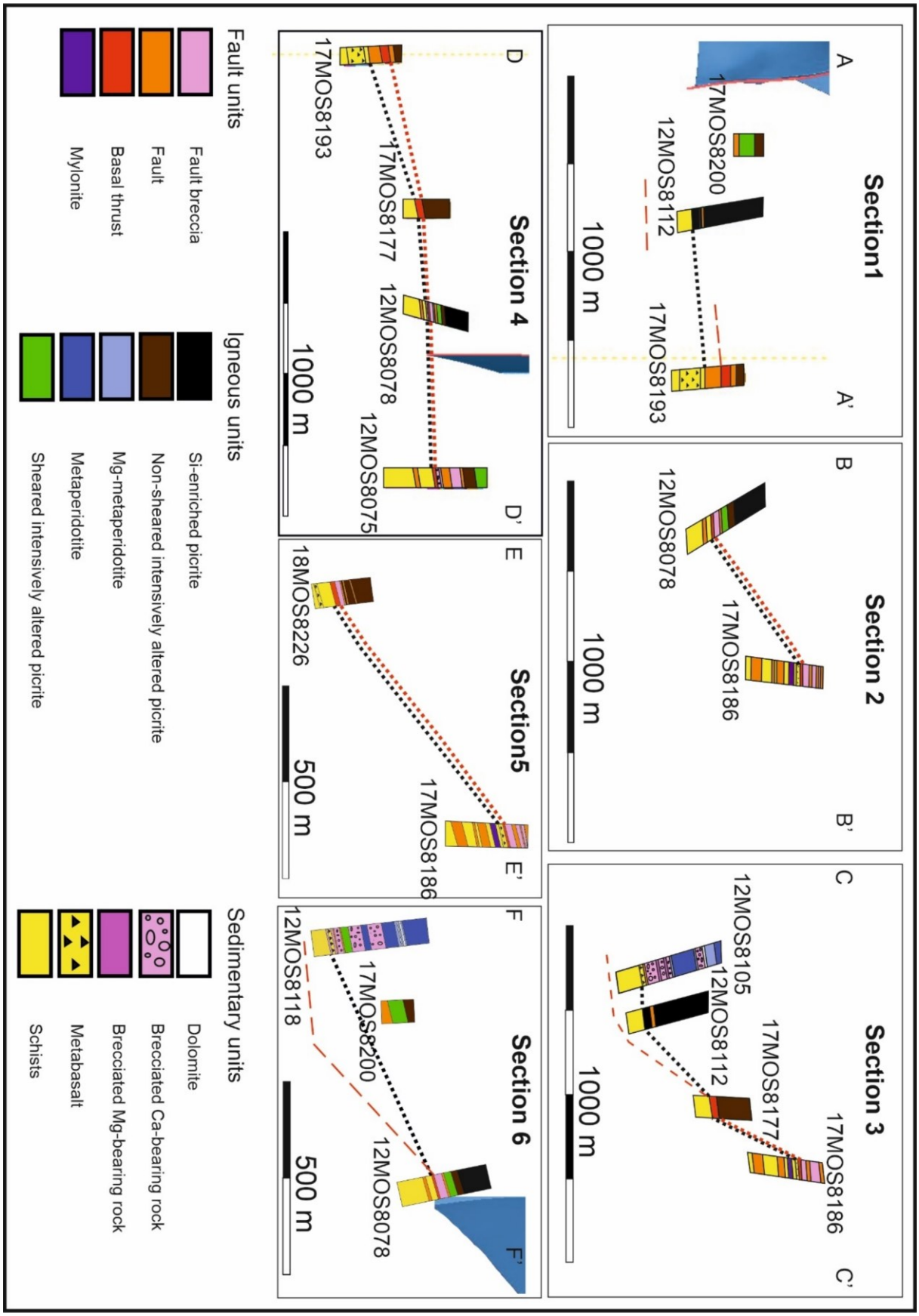

Figure 21. Stratigraphic columns depicting current stratigraphy in the study zone. Figure 19 indicates the locations of each section. The red dotted lines describe continuation of the basal thrust and black dashed lines indicate corresponding continuity for the metasedimentary rocks. Sections 3 and 6 show suggested continuations for the footwall basal thrust (red dashed lines). Each unit was geochemically sampled.

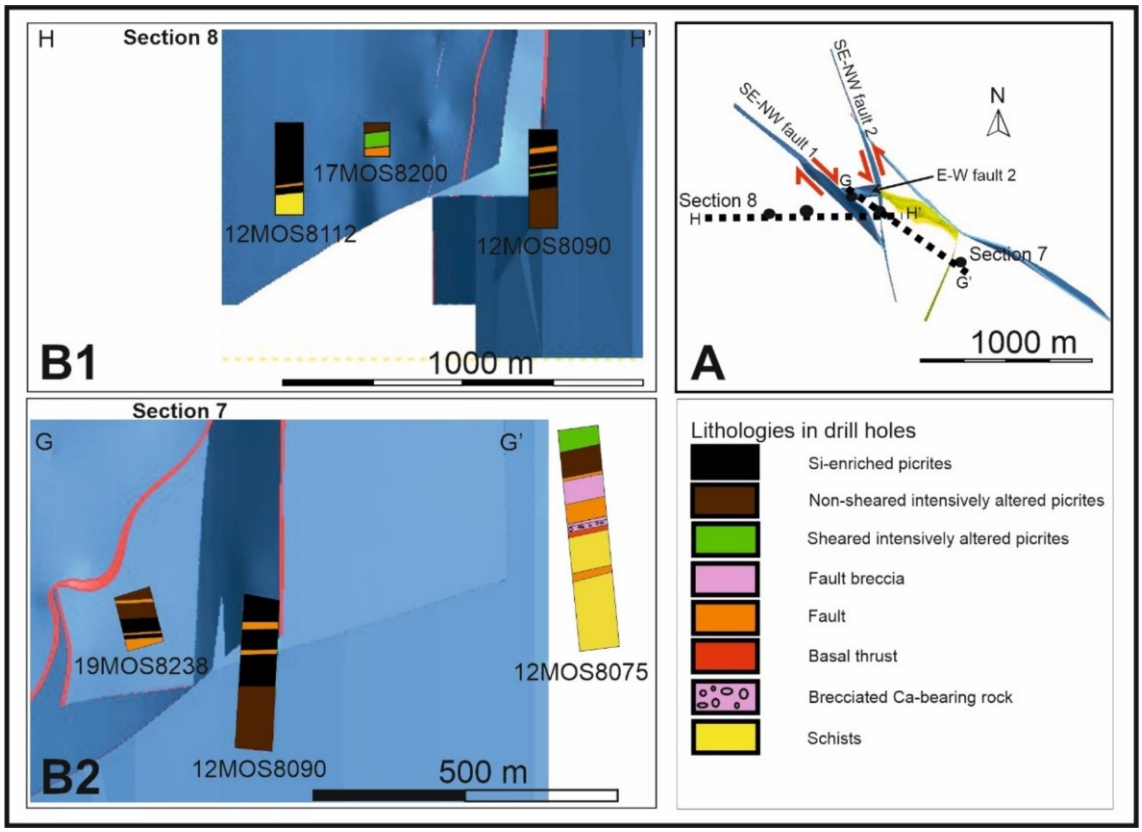

Figure 22. A: Cross sections 7 and 8 and major faults in map view. B1 and B2: Stratigraphic columns depicting current stratigraphic order in the sections 7 and 8. The domain where the schists and footwall basal thrust are absent is bordered by the SE-NW faults 1 and 2 and E-W fault 2. However, in both sides of the domain the schists occur (12MOS8075 and 12MOS8112).

The footwall basal thrust

The footwall basal thrust is a tectonic contact between the schists and intensively altered picrites. It is overprinted by brittle deformation that is observed sometimes as dozens of meters thick rubble zones that include fault breccias and metasedimentary rock and metaperidotite fragments. It is a high-strain zone, as folding, fracturing, alteration and schistosity get more intense towards it. In general, it occurs widely in the study zone and exhibits similar continuities as the schist unit usually dipping to NW. Thus, it is located closer to the surface in southern parts of the study zone, while in north it is found almost 1 kilometer below the surface. The original hypothesis of the footwall basal thrust was that it had the same orientation with the rock units and planar structures, and as observed in sections 1, 4, 5 and 6 this seems to be the case in most areas. Close to the SE-NW fault 2 it seems to fold a bit as it dips towards NE as did also the schists (fig. 21, sections 1-2). The SE-NW fault 2 appears as a structure located close to the curvature or axial trace of a proposed large-scale open fold represented by the Sattasvaara volcanic rocks (fig. 11 A) and possibly the footwall basal thrust and other rock units. The footwall basal thrust was not found in the domain delimited by the SE-NW faults 1 and 2 and the E-W fault 2, and not in the northwestern parts of the

study zone either (figs. 21-22). Its thickness varied greatly being usually ~20-80 meters thick if the fault breccias are included. Sections 3 and 6 (fig. 21) propose an alternative interpretation for the continuation of the footwall basal thrust, where it seems to turn to almost flat in the NW of the study zone, where it does not follow the upper sedimentary contact anymore. The flat part could represent a detachment fault that is connected to the footwall basal thrust. However, there are many other options. In general, the red dotted lines describe the continuation of the thrust.

4.4 Structures and tectono-metamorphic history

Structural core logging and thin section studies offered useful information about the deformation history of the study zone and metamorphism. The deformation history is presented below in chronological order. Previously presented stratigraphic separations and unit continuations supported the interpretations.

4.4.1 Early stages

The deposition of sediments initiated the development of the stratigraphic units recorded in this study. High Ca content of the schists require an abundant source of calcium that could be available for instance in a marine setting. The change from schists to overlying brecciated Ca-bearing rocks and evaporites in the NW-parts of the study zone reflects a change in the depositional environment to a system with more restricted circulation of water and high levels of salinity. However, as detailed stratigraphic or petrographic studies were not performed, these matters will be discussed further in chapters 5.2 and 5.3.

4.4.2 Overthrusting and metamorphic peak

After deposition, the sedimentary layers lithified and were finally subjected to regional compression and overthrusting that resulted in tilting of the sedimentary layers. The striking homogeneity of NW-dipping foliation values (fig. 23) could refer to SE-vergent thrusting along NW-dipping thrust fault. The initial thrusting along NW-dipping thrust fault thus determines the first deformation event (D_1) and caused the NW-dipping foliation (S_1) that no longer represents primary bedding (S_0).

Continued SE-vergent overthrusting and progressive deformation (D_2) created asymmetric SE-vergent folding (F_2) that was observed in drill core logging, thin section studies and dipmeter-data analysis (fig. 24 B-C). Fold axis and axial plane measurements support SE-vergent overthrusting, as the axial planes in general dip to NW and fold axes are horizontal or subhorizontal dipping slightly towards NE or SW (fig. 23). Some of the steepest axial planes were measured from the southernmost parts

of the study zone from protomylonite zones that cut the metasedimentary rocks and represent later tectonic event. The steeply and SE-dipping axial planes may represent parasitic folding in front limbs of SE-verging major folds, which was sometimes observed in thin sections. Figure 24 shows few examples of folding observed during core logging. Figure 24 A exhibits kink-band folds that form by differences in layer competences reacting differently to stress. The Ca-rich and pelitic layers have folded while the mafic more competent layers have faulted instead. In addition to asymmetric folding, boudinage structures were found in schists, which indicates layer parallel extension (fig. 24 D). These are common structures in folds and describe extension in fold limbs that could be generated during overthrusting.

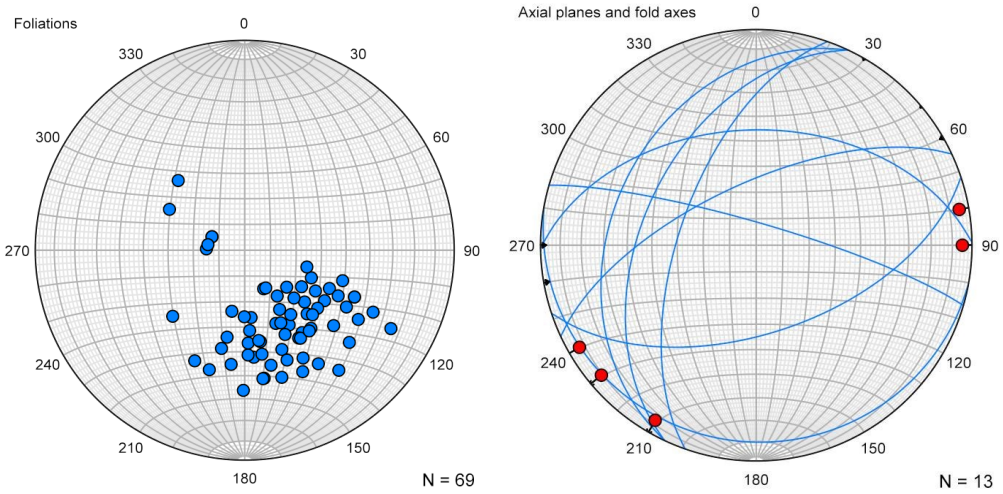

Figure 23. Left: Foliation measurements plotted on a stereoplot as poles. They indicate average dip direction to NW with ~40° angle. Right: Axial plane and fold axis measurements plotted on a stereoplot. Most of the axial planes dip to NW with horizontal fold axis. Few axial planes dip to SE that may represent parasitic folding.

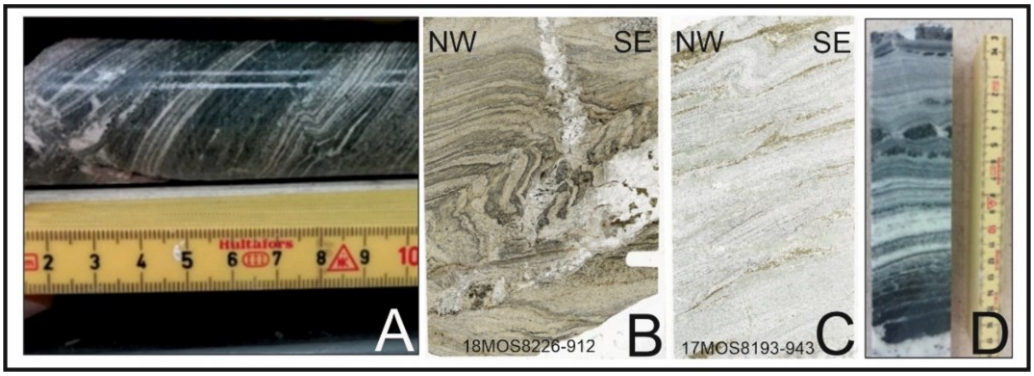

Figure 24. A: Kink-band folds in a schist with faulted green coloured mafic layers, B: Reverse and overturned asymmetric folding in a schist, C: Ca-rich schist with reverse asymmetric overturned folding. D: Ca-rich schist with boudinage.

Uniform foliation data was investigated more accurately, as it was odd that the folding was observed in centimeter-scale, but not in meter-scale during core logging. On this purpose, the foliation values were plotted into dipmeter-diagrams, where both dip and

azimuth values are shown separately in relation to z-axis denoting depth along the drill core. Figure 25 shows the dipmeter-diagrams and related sketches about general folding pattern in three representative drill cores. It was discovered that the azimuth was relatively constant in all three drill cores while the dip fluctuated repeatedly and quite rapidly. The black dots are foliation measurements, which were connected to adjacent measurements with black lines describing the folding (fig. 25). According to the dipmeter-data, the general azimuth of structures in drill cores is towards NW, although in drill core 17MOS8193 there is some variation as NNE directed azimuth values are present as well. However, dip fluctuates quite distinctively in all three drill cores and indicates tight, SE-vergent overturned folding where both fold limbs dip to NW. The absolute dips are different in each drill core, as in 18MOS8226 they are between ~20-50º, in 17MOS8193 ~25-60º and in 17MOS8200 ~40-65º. The stereoplots also show calculated fold axis orientations, indicating a NE-SW strike and almost horizontal dip that are consistent with the measurements.

Thus, even if the foliation was considered initially as homogeneous and uniform, it exhibits variation. Some of the faults observed and measured during drill core logging are added to the folding sketches with red lines and suggested kinematics (fig. 25). The one fault in 18MOS8226 was interpreted as S-C shear structure with a normal sense of shear due to continuously curving and anomalous foliation values observed in one depth interval (fig. 25, 2. population in drill hole 18MOS8226). However, it must be noted that there are other options as well, while this presents one of them.

Thin section studies revealed folding patterns similar to those presented above but also provided information about the sense of shearing and metamorphism. Crenulation cleavage was present within the microfolds, and its intensity increases towards the axial planes to where the highest strain is localized (fig. 26 A & C). Its orientation is commonly parallel to the axial planes of microfolds, and it resembles the axial plane cleavage (S_2) observed as micaceous foliation that cuts the S_1 foliation (fig. 26 B). The crenulation cleavage was common in schists where the amount of mica minerals was extremely high. Its dip depends on the location within the microfold, as in longer backlimbs they dip to NW, while in shorter forelimbs it varied but on average dip more steeply to SE or NW (fig. 26 A & C). The crenulation cleavage most probably formed during the deformation peak and overthrusting. In general, the crenulation cleavage and folding were more intense closer to the footwall basal thrust that in larger scale refers to a high strain zone represented by the thrust.

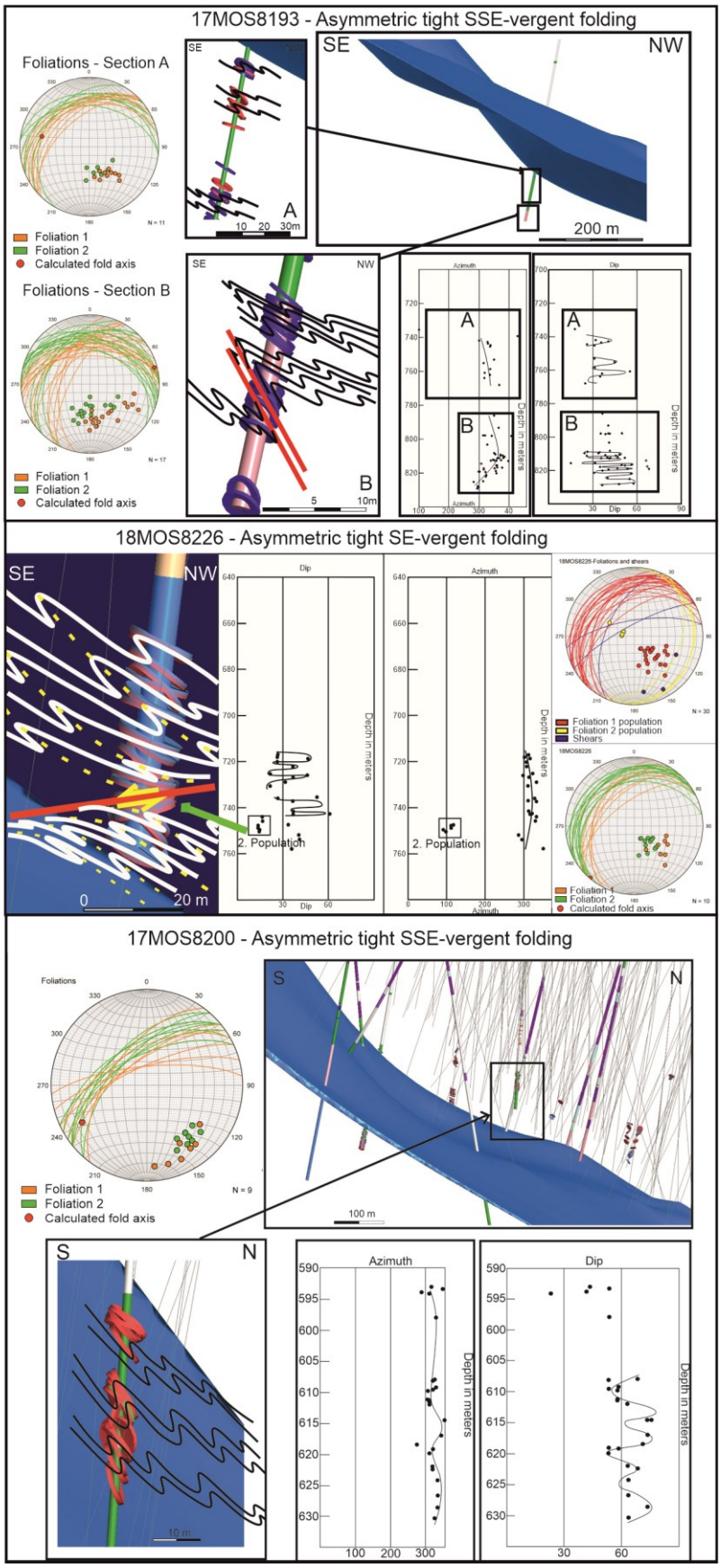

Figure 25. Dipmeter-data analysis and fold sketches drawn based on the dipmeter-data, logging observations and thin section observations. The results support SE-vergent folding and thrusting. The absolute dip and azimuth values vary a bit between different drill cores. The azimuth remains relatively constant in each drill core, while the dip fluctuates.

In addition to the above-mentioned structures, S-C structures, stair-stepping structures and mica fishes were observed, and they usually exhibit reverse kinematics towards southeast, thus being consistent with the SE-vergent overthrusting (fig. 26 B, D, E & F). This vergence is consistent with the previously presented results about the asymmetric folding and thus support the observations made in macroscale.

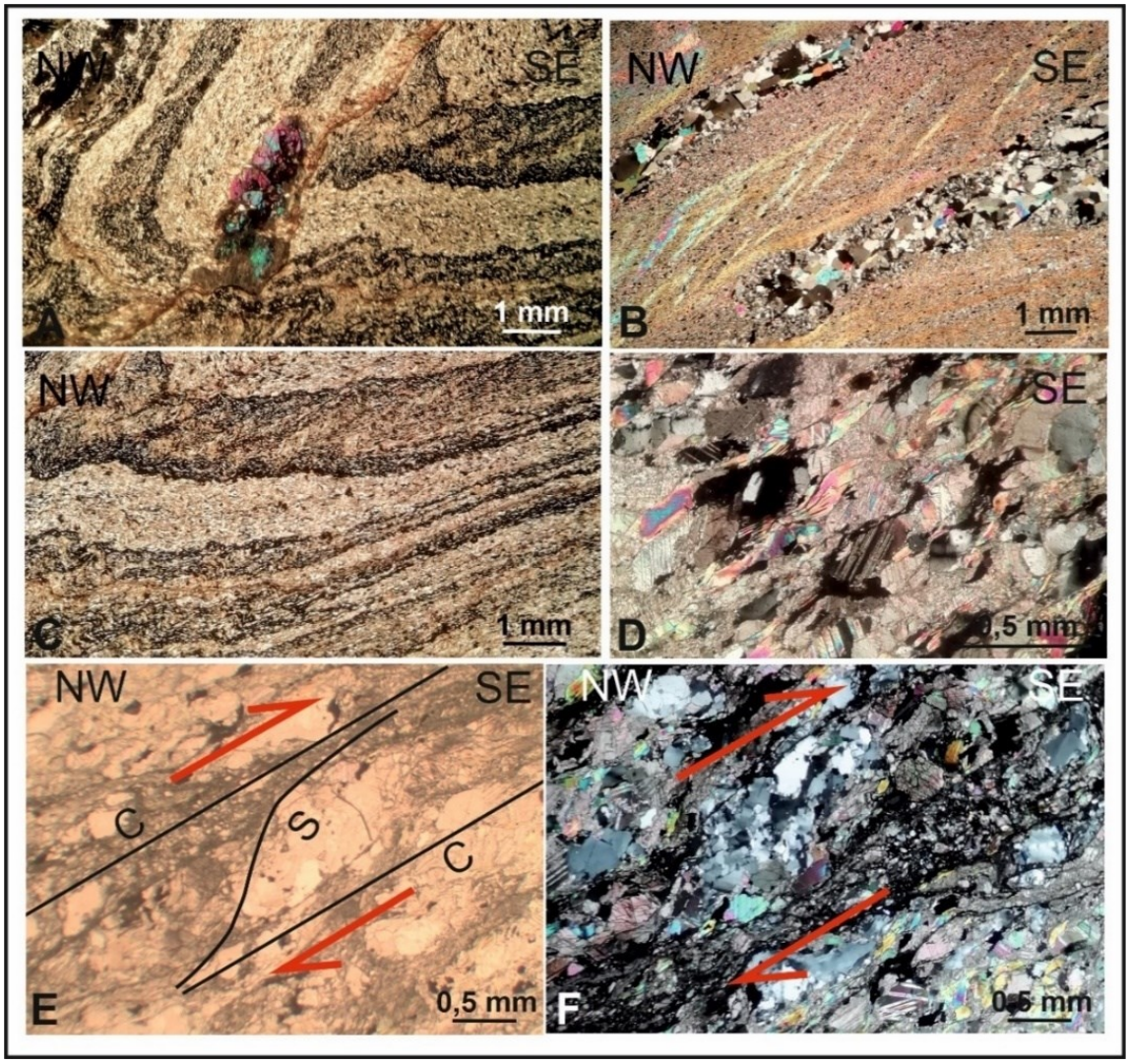

Figure 26. Microtextures from thin sections. The thin sections are oriented vertical sections of thin section samples. A: Overturned folding in a schist. The crenulation cleavage is parallel to the orientation of axial plane. Amphiboles and fractures are also concentrated on the axial planes and have parallel orientation to them. B: Dextral S-C structure developed in a schist. Dynamical recrystallization of elongated quartz ribbons shows subgrain rotation. C: The crenulation cleavage is more intense closer to the axial plane. D: Dextral mica fishes in a schist. E&F: Dextral S-C structure developed in a schist and around dynamically recrystallized quartz ribbons. The type of dynamical recrystallization is grain boundary migration.

The deformation peak was also the metamorphic peak, which conditions were estimated based on the syn-kinematic andalusite and scapolite (marialite) porphyroblasts (fig. 27) and dynamically recrystallized quartz grains (fig. 26 B & F). Both minerals indicate relatively low pressure and temperature. A study of Vanko & Bishop (1982) about evaporite related marialites suggests their growths at ~400 ºC that refers to greenschist

facies conditions and is the estimated minimum temperature for the deformation and metamorphic peak. This temperature is consistent to the ~400º-500º C estimated based on the type of dynamic recrystallization of quartz, which was usually of subgrain rotation- type (Stipp et al. 2002). Close to the footwall basal thrust, however, also grain boundary migration type of dynamic recrystallization exists, referring to a temperature >500º C, which is the estimated peak temperature.

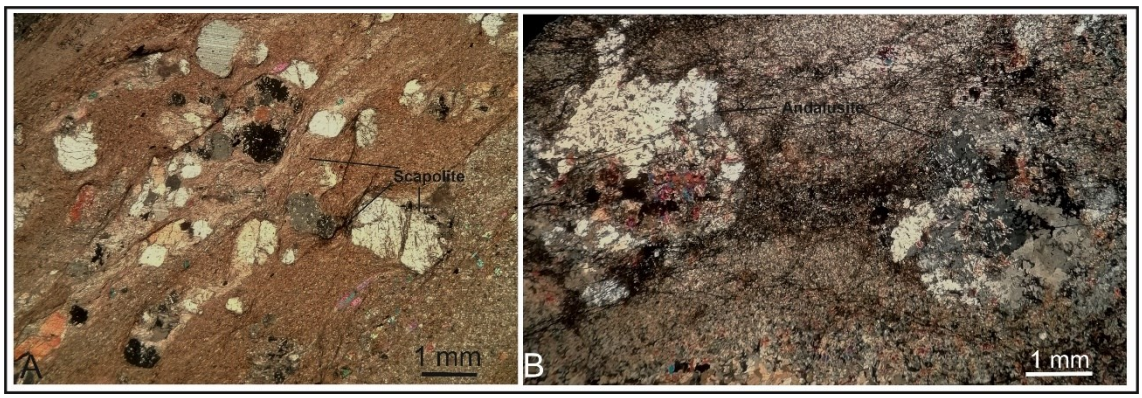

Figure 27. A) Syn-kinematic scapolite porphyroblasts in sheared and intensively altered picrites and B) andalusite porfyroblasts close to the intensively altered picrite-schist contact.

4.4.3 Post-metamorphic metasomatism

Thin section observations included porphyroblastic minerals that depict post-tectonic mineral growth and metasomatism (fig. 28). The post-tectonic growth concerns the poikiloblastic epidote porphyroblasts in which the inclusions are oriented parallel to the overall schistosity that is not deflected around the porphyroblasts. The schistosity is not observed within the amphibole porphyroblasts, which only contain randomly oriented opaque crystals. The surrounding schistosity is not deflected around these porphyroblasts either, unlike the crenulation that is created by a shortening orthogonal to the earlier schistosity (fig. 28, 18MOS8226-943). This crenulation is observed within a very small area of the thin section, and thus may represent a local response to the shortening active after the formation of schistosity and the porphyroblasts.

The micro-XRF analysis offered useful information about the zonation within the porphyroblasts and metamorphism. According to the analysis, Ca seems to be the most characteristic element that is enriched on the amphibole and epidote porphyroblasts compared to the rock matrix (fig. 28). However, Fe is the most common element, although it was not detected readily in micro-XRF studies since it is also a common element in the matrix. Fe and Mn are concentrated on the rims of the porphyroblasts and represent the zonation (fig. 28). It seems that the centers of the epidote porphyroblasts are geochemically quite similar to the matrix as they do not exhibit any distinct element

anomalies. Other common elements within all porphyroblasts were Al and Si, which do not show anomalies in the micro-XRF analysis as their content within the porphyroblasts is almost the same as in the matrix.

The micro-XRF analysis support the initial mineral identification since the distinct Ca-anomalies and high Fe content are typical for Fe-rich epidotes and calcic amphiboles. The chemical composition in the rims of epidotes with higher Mn and Fe contents could refer to piemontite, while the Mn and Fe-poor centers could correspond to clinozoisite as the former can be derived from the latter via substitution of Al to Mn. These elements could create the zonation, while the identification of exact mineral of the epidote group is not certain. According to the study of Holdaway (1972), in lower temperatures the solid-solution series of epidotes become more immiscible and there are many factors that control the crystallization. However, the study of Keskinen & Liou (1979) concluded that the crystallization of piemontite refers to high oxygen fugacity and that its stability is restricted to low temperatures if the oxygen fugacity is lower as well. Thus, changes in either of these factors during crystal growth or afterwards could be responsible for the zonation in epidotes.

In addition to the epidote porphyroblasts, the calcic amphibole porphyroblasts exhibit zonation where the Fe and Mn are enriched in the rims. Their enrichment could indicate higher oxygen fugacity and slightly lower temperature (Spear, 1981) compared to the time of crystallization of the cores. Respect to the identification of the amphibole minerals, the high Ca and Fe content, low Mg and Al contents and green colour and pleochroism would refer to hornblende or ferrohornblende.

Since the porphyroblasts mainly occurred close to the footwall basal thrust, were post-tectonic and exhibit clear positive Ca anomalies, they have most probably formed as a result of metasomatism after peak pressure conditions but when the temperatures were still enough high. Surrounding minerals are mainly quartz, muscovite or opaque minerals, which do not contain Ca and are thus unlikely minerals to derive Ca for the porphyroblasts. The opaque minerals are not used by the porphyroblasts and are thus left as inclusions. The likely source of Ca is probably external and related to the footwall basal thrust.

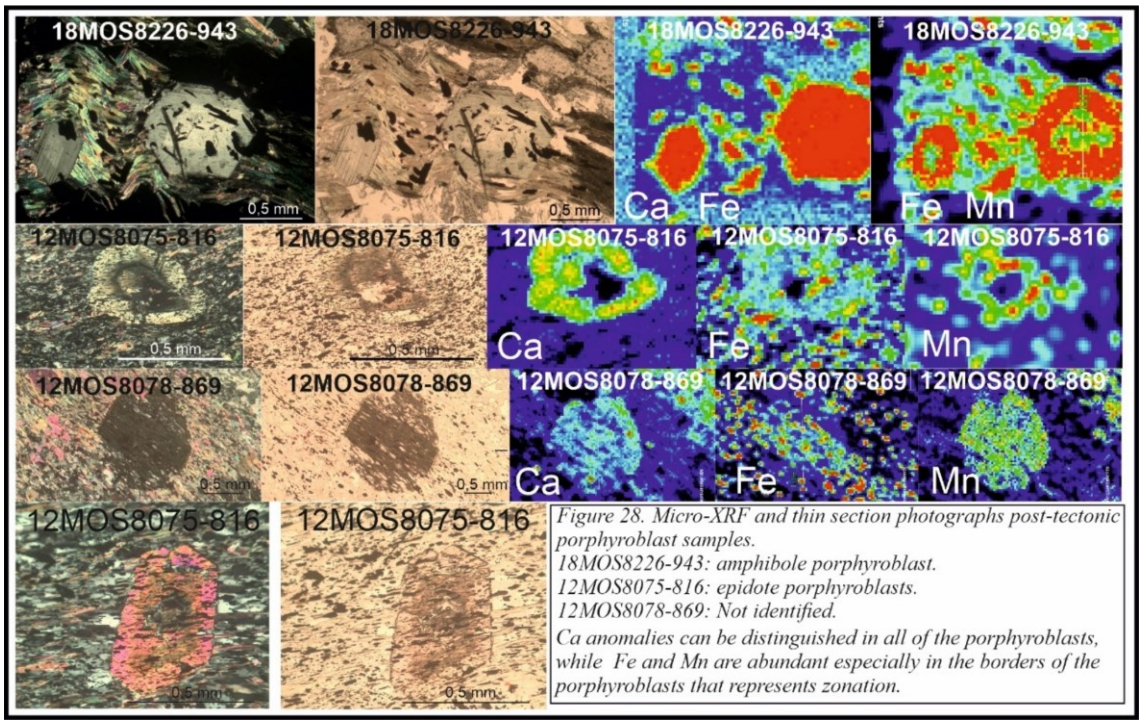

Figure 28. Micro-XRF and thin section photographs post-tectonic porphyroblast samples.
18MOS8226-943: amphibole porphyroblast.
12MOS8075-816: epidote porphyroblasts.
12MOS8078-869: Not identified.
Ca anomalies can be distinguished in all of the porphyroblasts, while Fe and Mn are abundant especially in the borders of the porphyroblasts that represents zonation.

4.4.4 Cooling stage and brittle structures

Brittle faults, fractures and protomylonites crosscut the earlier ductilely deformed rocks, thus being younger than the foliation (D_2) and the rocks. The most significant fault with brittle overprint is the footwall basal thrust, whose core is consisted of fault rocks and rubble zone. In addition, the drill hole 17MOS8186 was extremely faulted and exhibited varying results in dipmeter-diagrams (fig. 29). The fault zones were almost vertical NNW or SSE dipping ductilely deformed zones, which were characterized as protomylonites due to high proportion of coarse-grained clasts. The drill hole is located in the southernmost parts of the study zone and exhibits at least two protomylonite zones that include folding, where axial planes are steep and fold axes horizontal (fig. 23). In these shear zones, the steeply dipping foliation has two opposite dip directions, which may reflect transposing of foliation across the shear zone in NNW-SSE horizontal compression. The absolute kinematics of the protomylonite shears were not recorded due to the absence of trustworthy kinematic indicators in thin sections. The maximum thickness of these shear zones was ~ 15 m. These shear zones represent the D_3 phase, which is interpreted as being responsible of creating the large-scale fold (fig. 11) formed by buckling of the Sattasvaara Fm rocks, the footwall basal thrust and the schists. The large-scale folding is observed as NW-dipping structures and units in the western side of the axial trace of the fold and as NE-dipping structures in the eastern side of it (figs. 11 A & 21). The SE-NW fault 2 is a later fault interpreted in this study as having developed to the axial plane of the large-scale fold. The actual age of this deformation phase cannot be determined, but as they exhibit ductile structures, they are

probably related to a tectonic stage between the main overthrusting stage and brittle stage.

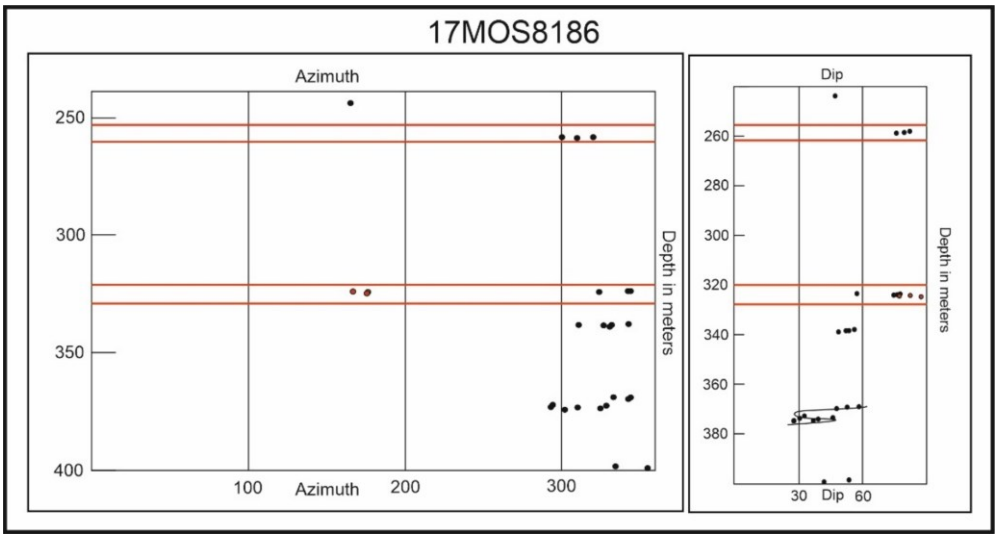

Figure 29. Dipmeter-diagram describing foliation variation in drill hole 17MOS8186. Folding cannot be interpreted based on this diagram, while it reveals locations of vertical faults marked with red lines.

The stratigraphic study revealed stratigraphic separations in a domain that lacked metasedimentary rocks and the footwall basal thrust, while in its neighbour domains both were present, indicating a missing section in this domain (figs. 21-22). The domain (Domain A) is delimited by the SE-NW faults 1 and 2 (fig. 30) and the E-W fault 2. The drill cores that penetrate the domain contain only Si-enriched picrites and intensively altered picrites in depths where the footwall basal thrust and schists are expected. Thus, the picrites are located deeper than expected (fig. 22). This would indicate that the domain A and the structures and rocks within have been faulted and displaced.

One possible explanation for the displacement of the domain A is given in figure 30 (A-B), which is a modified 3D-fault model of the Sakatti deposit. The model follows the riedel fracture theory (fig. 30 C), according to which the R and R' fractures are shear and conjugate fractures that define the maximum stress direction σ^1 (in e.g., Bartlett et al. 1981). T-fractures are tension fractures and define the minimum stress direction σ^3. In the model, the SE-NW faults are conjugate fault planes where the σ^1 would be horizontal with ~NNW-SSE direction. The SE-NW fault 2 has a sinistral sense of shear while the SE-NW fault 1 would have a dextral sense of shear. According to the model, the footwall basal thrust and the rock units in domain A moved towards S-SSE along these SE-NW faults. The real displacements along the vertical SE-NW faults would be horizontal although the apparent displacement of the domain A appeared in cross sections as vertical. Unfortunately, as the schists or the footwall basal thrust were not reached in drilling of this domain, the magnitude of the displacement is unknown. Also,

as the drill cores penetrating the domain A were not oriented, the absolute kinematics of the faults could not have been recorded in thin section studies and the previously presented explanation can not be confirmed.

The deformation phase that is related to the displacement of the domain A would comprise either a new D_4 phase or being contemporaneous with the D_3 phase, which is possible as the D_3 phase comprised vertically oriented shear zones also formed during horizontal NNW-SSE compression. This does not contradict with the result according to which the domain A was displaced towards S-SSE. As no clear signs of ductile deformation with strike-slip kinematics were observed, this phase is however comprehended here as a brittle D_4 phase. The previously explained model gives one alternative explanation for the missing section in the domain A, according to which the domain A would have displaced laterally towards SSE. It is possible that the current brittle overprint in the footwall basal thrust was generated during this stage. With respect to the fault model, it must be noted that only one drill core in the domain A was deep enough to be investigated in the study, and that its drilling orientation influences on observations performed during core logging.

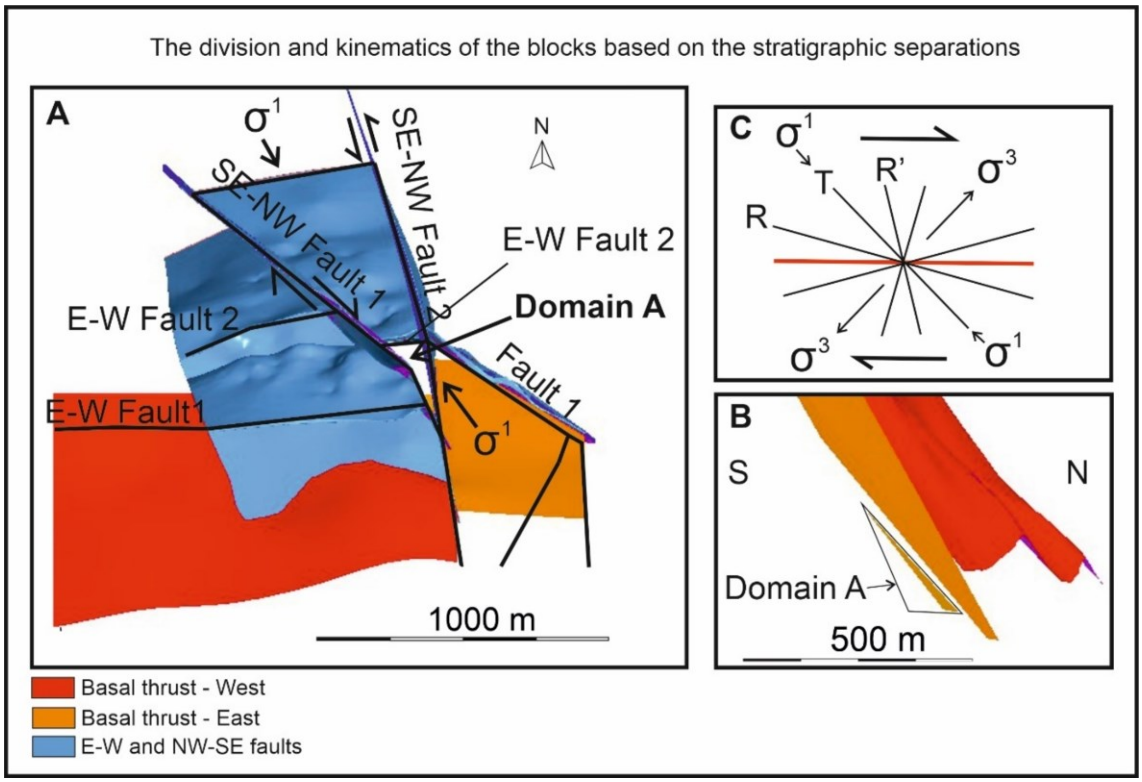

Figure 30. A: SE-NW fault kinematics and domain movements in the study zone. E-W faults and the footwall basal thrust are displaced. No metasedimentary rocks or the footwall basal thrust were observed within the domain A. σ^1 points the orientation of maximum shear stress. B: Sketch of the displacement of the footwall basal thrust along SE-NW faults 1 and 2. C: Riedel fractures and T- fractures indicate the maximum and minimum shear stress directions. R and R' fractures are conjugate fault planes. Modified after Bartlett et al. (1981).

Other structures observed in core logging were veins, slickensides and fractures. Most of the veins that cut rock units and foliation were carbonate veins, although gypsum, anhydrite and Cu-mineralized carbonate veins occurred commonly as well. Many of these veins were parallel to foliation. Considering the possible sources for the veins, especially the brecciated Ca-bearing rock unit seems possible as it contained calcium, gypsum and anhydrite. The unit was commonly faulted in its contacts evidenced by fault breccias in borders. Faulting creates open space that was probably filled by the carbonate minerals mobilized by either the high temperature and pressure conditions both or by the decrease in pressure. However, as these veins usually cut the rock units and ductile structures, the latest deformation phase that influenced the overprinting veining was probably the brittle D_4 phase or even later.

5. Discussion

5.1 Volcanism

Ultramafic melts are produced in unusually hot conditions in unusual depths or in very volatile rich conditions where the degree of melting is extremely high (in e.g., Arndt, 2003). The observed metaperidotites indicate a period of ultramafic volcanic activity during the development of the CLGB. The studied Si-enriched picrites correspond to the rocks of the aphanite unit described in the study of Brownscombe (2015), who named them as plagioclase-rich picrites. According to his study the plagioclase-rich picrites were not altered, their high SiO_2 content reflects the original composition, and they are more mafic than ultramafic rocks. In this study, this view is adopted and the Si-enriched picrites are interpreted as mafic rocks high in MgO. Since the intensively altered picrites were defined as altered rocks of the Si-enriched picrites in the study of Brownscombe (2015), which is supported by the geochemical results presented in this study, the intensively altered picrites are interpreted as altered forms of the Si-enriched picrites. According to the data offered by the company, the Si-enriched picrite and metaperidotite layers sometimes occur together as with gradual contacts. This supports their close relationship and at least partly common genesis. Brownscombe presented a theory according to which the metaperidotites (olivine cumulate unit sensu Brownscombe, 2015) intruded the Si-enriched picrite (aphanitic) unit in a conduit possibly related to the same magmatic event but a different magmatic phase. In the same study it was shown that the ultramafic body has experienced several phases of magmatic activity. The results of this study do not conflict with Brownscombe's theory. Thus, the Si-enriched picrites and metaperidotites may represent different magmatic phases, of which the former erupted in a subaqueous environment indicated by their

common pillow texture and aphanitic grain size, while the metaperidotites intruded these rocks in a later phase.

The intensively altered picrites deviated from the Si-enriched picrites mainly by their higher Na, K and Mg contents, while Ca content was locally higher as well. The lower contact to the footwall basal thrust and the geochemistry refer to alteration related to the thrust. The dominating alteration types include talc-carbonate alteration and chloritization. The observation of an occasionally occurring cumulate-texture in the intensively altered picrite rocks and the higher MgO content challenges the assumption according to which these rocks are altered Si-enriched picrite rocks exclusively. It is possible, that the intensively altered picrite unit better describes the overprinting alteration caused by the footwall basal thrust than neither of these rock units alone.

It has been under discussion whether the ultramafic rocks in Sakatti could represent komatiite flows. Considering this term for the Si-enriched picrites and metaperidotites, a few remarks must be given: (i) The TiO_2 contents correspond to general contents in komatiites (Hanski et al. 2001); (ii) The observed pillow breccia textures in the Si-enriched picrites could represent flow-top breccias commonly present in uppermost layers of komatiites (Arndt, 1986); and (iii) The observed cumulus-texture is commonly found in lower layers of komatiites (Arndt, 1986). In addition, there are documented observations of the olivine spinifex texture in Sakatti. These details would support the use of the term komatiite, which is the favoured term in the studies of Halkoaho (2014, 2015 & 2019, Anglo American internal reports). However, the significant deviation in LREE and HREE trends from the typical trends observed in komatiites (fig. 17) conflicts with their classification as such. In addition, the lack of olivine spinifex texture observations made in this study, which is considered as the most critical evidence of komatiites (Arndt, 2003), does not support their classification as komatiites in this study. However, the lack of documented olivine spinifex textures does not exclude the existence of komatiites. According to Halkoaho (2014, 2015 & 2019), the increased LREE patterns result from strong crustal contamination caused by felsic material. However, as presented in chapter 4.2 the metaperidotites are rather depleted in HREEs and LREEs both than enriched in LREEs (fig. 17).

Stratigraphic correlation of ultramafic/mafic volcanic rocks

From regional perspective, the geochemical discrepancies between the studied ultramafic/mafic rocks and the Sattasvaara komatiites, Sotkaselkä and Peuramaa picrites and other mafic metavolcanic rocks of the Sodankylä and Savukoski Groups (figs. 13 &

17) are striking and raise questions about the origin of the studied rocks. Considering the possible stratigraphic groups that could correlate with the studied rocks, the only stratigraphic groups in the CLGB with records of ultramafic volcanism are the Kuusamo and Savukoski Groups (Hanski & Huhma, 2005; Brownscombe, 2015). In addition, ultramafic intrusions such as the 2.4-2.5 Ga Koitelainen, the 2.2 Ga sills (in e.g., Haaskalehto type) and the 2.05 Ga Kevitsa intrusion are reported near Sakatti (in e.g., Lehtonen et al. 1998; Brownscombe, 2015). Since the studied metasedimentary rocks are probably much younger than the Kuusamo Group rocks and Koitelainen, it is unlikely that the overlying studied volcanic rocks would belong to them.

The fact that gypsum, anhydrite and carbonate veins crosscut the ultramafic/mafic rocks points that the veins are younger than the ultramafic/mafic rocks. The brecciated Ca-bearing unit of the Sodankylä Group was presented as a potential fluid source for these veins. In addition, as the footwall basal thrust sometimes contained calcite, gypsum and anhydrite, it is possible that it was a pathway for these fluids that intruded the overlying ultramafic/mafic rocks during the D_4 phase or later that opened space for the fluids. It is probable that the fluids would have propagated to surrounding lithological units at the time of the faulting. Thus, the ultramafic/mafic rocks were probably already situated close and above the brecciated Ca-bearing rocks before the late faulting of the footwall basal thrust. If the ultramafic/mafic rocks were older than the underlying Sodankylä Group rocks, they should have been brought upwards by thrusting already before this faulting event. The older Kuusamo Group rocks and Koitelainen intrusion are located deep below the uppermost parts of the Sodankylä Group according to the regional stratigraphy, and thus are unlikely to have been crosscut by these veins and thrusted above the Sodankylä Group rocks during the same tectonic event. Thus, it is more likely that the ultramafic/mafic rocks should be younger or roughly of the same age as the brecciated Ca-bearing rock unit but older than the veins and the displacement that opened space to the fluids.

The Savukoski Group and Kevitsa intrusion are both younger than the Sodankylä Group rocks and exhibit ultramafic magmatism, therefore being possible correlative units for the studied Si-enriched picrites and metaperidotites. Additionally, the 2.2 Ga gabbro-wehrlite associations crosscut the Sodankylä Group rocks and include ultramafic rocks in their base (Hanski & Huhma, 2005; Brownscombe, 2015). As mentioned above, there was no clear geochemical correlation between the studied ultramafic rocks and the Savukoski Group rocks, which does not support the original hypothesis about their

correlation (figs. 13 & 17). Furthermore, Brownscombe (2015) showed that the ε_{Nd} values of the Savukoski Group rocks and the 2.2 Ga intrusions deviate clearly from those of Sakatti, and that the Savukoski Group rocks were not affected by crustal contamination, unlike the ones of Sakatti (fig. 31). Based on the geochemical diagrams represented by Lehtonen et al. (1998), the Haaskalehto type 2.2 Ga sills could be characterized as komatiites as they sometimes plot to that field in the Jensen's cation plot. However, the chondrite normalized diagrams for trace elements (Lehtonen et al. 1998) show quite different LREE and HREE patterns compared to the patterns of the studied ultramafic/mafic rocks. On the contrary, the Kevitsa deposit instead has similar ε_{Nd} values (fig. 31) in addition to other shared characteristics, such as the trace element geochemistry when comparing the chondrite normalized diagrams (Lehtonen et al. 1998). Although the Kevitsa intrusion includes mainly Fe-tholeiites that are more evolved rocks than the ones in Sakatti (Lehtonen et al. 1998), their common characteristics and close spatial relation would support a common or similar origin (Brownscombe, 2015). Age determination studies indicate 2.05 Ga age for the Kevitsa intrusion (Mutanen & Huhma, 2001), thus representing the same period as the Savukoski Group. This would indicate that the displacement of the footwall basal thrust that created evaporitic fluid activity within the ultramafic and mafic rocks would be posterior to the formation of the Kevitsa intrusion.

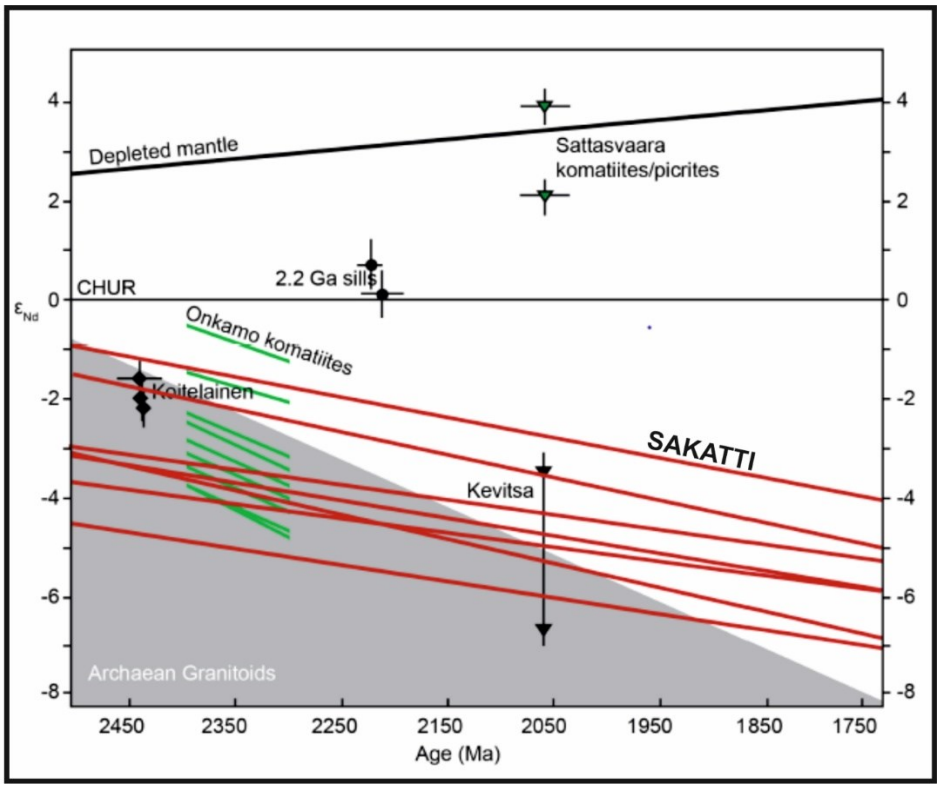

Figure 31. ε_{Nd} values of Sakatti and other ultramafic lithologies in the CLGB in comparison modified after Hanski & Huhma (2005, and references therein); Peltonen et al. (2014); Brownscombe (2015).

5.2 Depositional history

The schists are the oldest rocks deposited in the study zone and their correlation with the Orajärvi Formation of the Sodankylä Group was suggested in the Results chapter. According to unit description (Räsänen, 2018) they were deposited in a shallow marine setting indicated by well sorting, ripple-laminations and graded bedding. Beach face, beach bars and dunes are included as possible deposition environments for these rocks that were originally sandstones or siltstones (Räsänen, 2018). Confirmed sedimentary structures were not found in this study, but the high Ca content, geochemistry, grain size and its variation and mineralogy do not conflict with those deposition environments. The deposition of the schists of the Sodankylä Group corresponds to the syn-rift or syn-rift to early post-rift stages described by Köykkä et al. (2019). This is supported by the discrimination function diagram, where the Ca-poor schists were plotted into the continental rift field (fig. 16). The Ca- rich schists were plotted in the island arc/continental arc field, which may reflect a transition in tectonic setting towards syn-rift to early post-rift stage. During the deposition of schists, the metabasalts of the Visasaari Formation extruded on top of sediments, thus indicating a stage of volcanic activity that could correspond to the coeval volcanism reported during syn-rift stage and the deposition of the rocks of the Sodankylä Group (Köykkä et al. 2019).

After the deposition of sandstones and siltstones of the Orajärvi Formation, the evaporitic brecciated Ca-bearing rocks, also inferred as part of the Sodankylä Group, were probably deposited in a shallow tidal influenced marine setting or epeiric sea setting where water circulation was restricted (Köykkä et al. 2019). These originally evaporitic successions were possibly dissolved afterwards that could have led to a collapse of overlying units and to a formation of collapse-type breccias found from KB, PB and other sites of CLGB as well (Friedman, 1997; Kyläkoski et al. 2012; Köykkä et al. 2019). This would also explain the dominated subrounded-subangular clasts that do not closely resemble typical clasts in fault breccias, the unit thickness and the observed chaotic texture with anhydrite matrix. Another option for the formation of this unit could be that they really are fault breccias and that the evaporites were derived from somewhere else.

Clear indicators about the environment where the precipitation of evaporites took place were not found in this study, but their occurrence together with the Sodankylä Group schists related to marine setting would support their precipitation in a marine setting as well. According to Warren (2010), evaporites form by concentration of a nearsurface or surface brine driven by solar energy. Large and thick deposits have usually marine

origin and require epeiric conditions facilitated by the vicinity of continents, which is why recently opened rifts or parts of collision suture belts commonly express these deposits (Warren, 2010). Evaporites can be accumulated in several different tectonic environments including convergent, divergent and intracratonic settings, of which the divergent setting is favoured for the deposition of the brecciated Ca-bearing rock unit, as previously deposited schists were deposited during syn-rift stage. Syn-rift and post-rift sedimentation types in divergent setting are the most common alternatives for their deposition (Warren, 2010), but as the complete geometry and continuity of the unit is unknown, it is not possible to decide which alternative is more plausible. The post-rift stage could indicate basin closure, which would correlate well with the findings of Haverinen (2020) who focused on the evaporites of the Savukoski Group. However, since these rocks were correlated with the Sodankylä Group rocks deposited during syn-rift or syn-rift to early post rift stage, the deposition of the evaporites probably took place during these stages as well. In any case, the close common occurrence of schists and brecciated Ca-bearing rocks indicates fluctuation in water level during the time of deposition and clear change in the deposition environment or conditions (Köykkä et al. 2019). If the Sodankylä Group calc-silicate rocks were deposited in shallow marine setting, the change that would lead to a deposition of evaporites could be related to water regression. If this is the case, this regression would have taken place during syn-rift to post-rift tectonic stage.

The brecciated Ca-bearing rock unit occurred commonly as several repeated tens of meters thick layers that in combined were almost 100 m thick (figs. 20-21). It is possible that these layers were originally connected, but as evaporites are easily deformed and are mechanically weak (Warren, 2010), these repetitive layers in drill cores could represent reverse thrusting (figs. 2, 21). This is supported by the fault breccias commonly bordering the brecciated Ca-bearing rock unit. Recent finding of a similar setting within the CLGB (Haverinen, 2020) further supports the idea of evaporite layers acting as slip surfaces for displacements observed here as several repeated evaporite sections above the footwall basal thrust. Another area, where evaporite layers have been related to faulting, was reported by Piippo et al. (2019) who discovered a detachment fault zone within the Petäjäskoski formation in the Peräpohja belt. Thus, the brecciated Ca-bearing rock layers of this study may represent several slip surfaces for reverse faults that were active simultaneously with the footwall basal thrust during D_1-D_2 stage. It is however also possible that they represent splaying continuation

of the footwall basal thrust in the NW parts of the study zone, which would indicate fault termination (Fossen, 2010).

Brownscombe (2015) discussed further the relation between the evaporites and sulphides and their $\delta^{34}S$ geochemistry within the main ultramafic body and metaperidotites. He concluded that as anhydrite occurs as intergrown with pyrite, it is likely that the signature of anhydrite would be reflected in surrounding sulphides, if the anhydrite had a sedimentary origin (Brownscombe, 2015). Since this reflection was not detected, the anhydrite was assumed to be related to alteration and oxidation of sulphides or to unknown external source (Brownscombe, 2015). However, as described above especially the rock textures and considerable unit thickness support sedimentary origin. It is possible, that the anhydrite present in veins and as fragments within the ultramafic body is an alteration product via reaction with calcite veins and sulphides. However, this does not exclude a possibility that the brecciated Ca-bearing rock unit had sedimentary origin, and that the calcite veins within the ultramafic body were related to it. Some of the present anhydrite in veins and fragments may have recrystallized and formed later than the anhydrite within the brecciated Ca-bearing rock unit. Most of the fragments and veins within the ultramafic/mafic rocks were located close to their lower contact with the metasedimentary rocks, which is probably related to faulting.

The Si-enriched picrites, intensively altered picrites and metaperidotites were the following rocks that erupted or intruded into the study zone. As discussed above, there is no certainty on which stratigraphic group or intrusion they are related to, but as the rocks and geochemistry of the Kevitsa intrusion seems the most likely alternative, in this study the studied ultramafic/mafic rocks are linked to their genesis. They were intruded at ~2.05 Ga (Mutanen & Huhma, 2001) during the time of deposition of the Savukoski Group rocks in a deepened sea during passive margin stage at 2.1-1.92 Ga (Köykkä et al. 2019).

Hemipelagic sedimentary rocks, gravity driven sandstones and subaqueous volcanic rocks of the Savukoski Group were not detected in this study, and thus it seems that these rocks have been either moved by thrusting or by intrusion, of which the latter could be represented by the studied ultramafic/mafic body. The footwall basal thrust, as positioned between the metasediments and picrites, could have displaced the picrites above the metasediments and/or possibly also the rocks of the Savukoski Group beyond the original contact between the Savukoski and Sodankylä Group metasediments.

However, as there are no recorded and published evidence about whether some rocks in the Sakatti or in its direct vicinity belong to the Matarakoski Formation, excluding the geological maps, the reason for its absence remains unsolved. It could, however, be related to the overthrusting. If the lowermost schists were successfully correlated to the Matarakoski Formation, the brecciated Ca-bearing rock unit would correlate well with the evaporites described by Haverinen (2020).

5.3 Tectonic history

After the deposition or emplacements of rock units, the area was subjected to compression that corresponds to the 1.92 Ga SW-NE shortening event described by Lahtinen & Huhma (2019). The previously interpreted local deformation history of the study zone consisted of at least four phases: D_1) SE-vergent thrusting along NW-dipping thrust resulted in foliation of metasediments dipping to NW; D_2) Continued progressive SE-vergent thrusting led to overturned folding of metasediments and metabasalts, which culminated in the development of crenulation cleavage. This stage comprises the peak deformation and metamorphism stage under greenschist facies conditions in ~400-500ºC; D_3) NNW-SSE compression that created vertically oriented protomylonite shear zones and buckled previous structures and rock units; D_4) NNW-SSE compression that possibly created strike-slip displacements along SE-NW directed conjugate faults, where each previous rock unit and structure, including the footwall basal thrust, displaced towards SSE within the domain A. The post-tectonic epidote group porphyroblasts were most probably crystallized after peak deformation and metamorphism stage after cessation of deformation, possibly corresponding to the D_3 stage or to a later stage.

The initial NW-SE compression presented in the interpretation does not correlate well with the results presented by Lahtinen & Huhma (2019), according to which NE-SW shortening took place first and was followed by renewed parallel shortening. However, the third regional stage with NNW-SSE shortening (Lahtinen & Huhma, 2019) correlates well with the local interpreted D_3 phase. It is possible, as the tectonic history described by Lahtinen & Huhma (2019) depict regional events, that the observed structures in the study zone only represent a local response to regional stress. On the other hand, one could envisage that the metasedimentary rocks were in fact first thrusted progressively towards SW during the D_1-D_2 phases that resulted in overthrusting and overturned folding. The regional D_3 phase with NNW-SSE compression could have buckled the metasediments and the footwall basal thrust against the competent ultramafic body (fig. 32), which would appear as NW-dipping and SE-vergent

structures presented in the Results chapter. The D_3 phase represented by Lahtinen & Huhma (2019) also included buckling that was observed as bended pre-orocline fabrics and gentle folding, which could support this theory presented also in chapter 4.4.4 where the large-scale fold was formed when the metasediments and the footwall basal thrust were buckled. This stage would thus have a ductile nature. Since the above-mentioned explanation is possible, fits to the tectonic history described by Lahtinen & Huhma and explains well the formation of the observed large-scale fold, it is the favoured explanation for the D_1-D_2 phases in this study instead of the NW-SE shortening presented in chapter 4.4.2. The interpreted local tectonic history and the tectonic history described by Lahtinen & Huhma (2019) are shown and compared in figure 32. However, the original interpretation with SE-vergent thrusting is also recognized as possible.

As mentioned above, the large-scale gentle and open fold could have been generated by buckling of the earlier structures and units in NNW-SSE compression, if there was some competent counterpart against which to compress (fig. 32). The ultramafic/mafic body could provide this counterpart since these rocks are quite competent and together comprise a quite voluminous mass. However, as the Kittilä allochthon was thrusted eastwards at 1.92 Ga during the Lapland-Savo orogeny (Hanski & Huhma, 2005), it could also form the large-scale fold that would indicate E-W compression. Nonetheless, as the Lapland-Kola orogeny deformed the Kittilä allochthon (for references, see Lahtinen et al. 2015a), the structures related to E-W compression should be overprinted by later deformation phases of the Lapland-Kola orogeny, which was not observed. Thus, in this study the buckling scenario with NNW-SSE compression is better supported by the data.

The final D_4 phase was not under careful examination, but it had a brittle nature and could correspond to the regional NNE-SSW shortening event during 1.79-1.76 Ga that created E-W, NNW-SSE and ENE-WSW trending extensional faults and fractures. The SE-NW faults 1 and 2 in Sakatti have been before connected to these structures and as they cut the deposit, it is possible. However, as it was pointed out these SE-NW faults clearly mark the boundaries for a domain that has displaced during the D_4 phase (fig. 30), thus being older or synchronous with the displacement. Additionally, if they are conjugate faults as proposed in the model (fig. 30), they rather support NNW-SSE directed compression and displacement instead of the NNE-SSW regional compression. If the SE-NW faults were directly related to the NNE-SSW shortening, these faults

would not be conjugate faults and the displacements would be slightly different. In this study, the SE-NW faults are interpreted as having formed and displaced during the D_4 phase in NNW-SSE compression that took place earlier than the regional NNE-SSW shortening during 1.79-1.76 Ga and shortly after the D_3 phase (fig. 32).

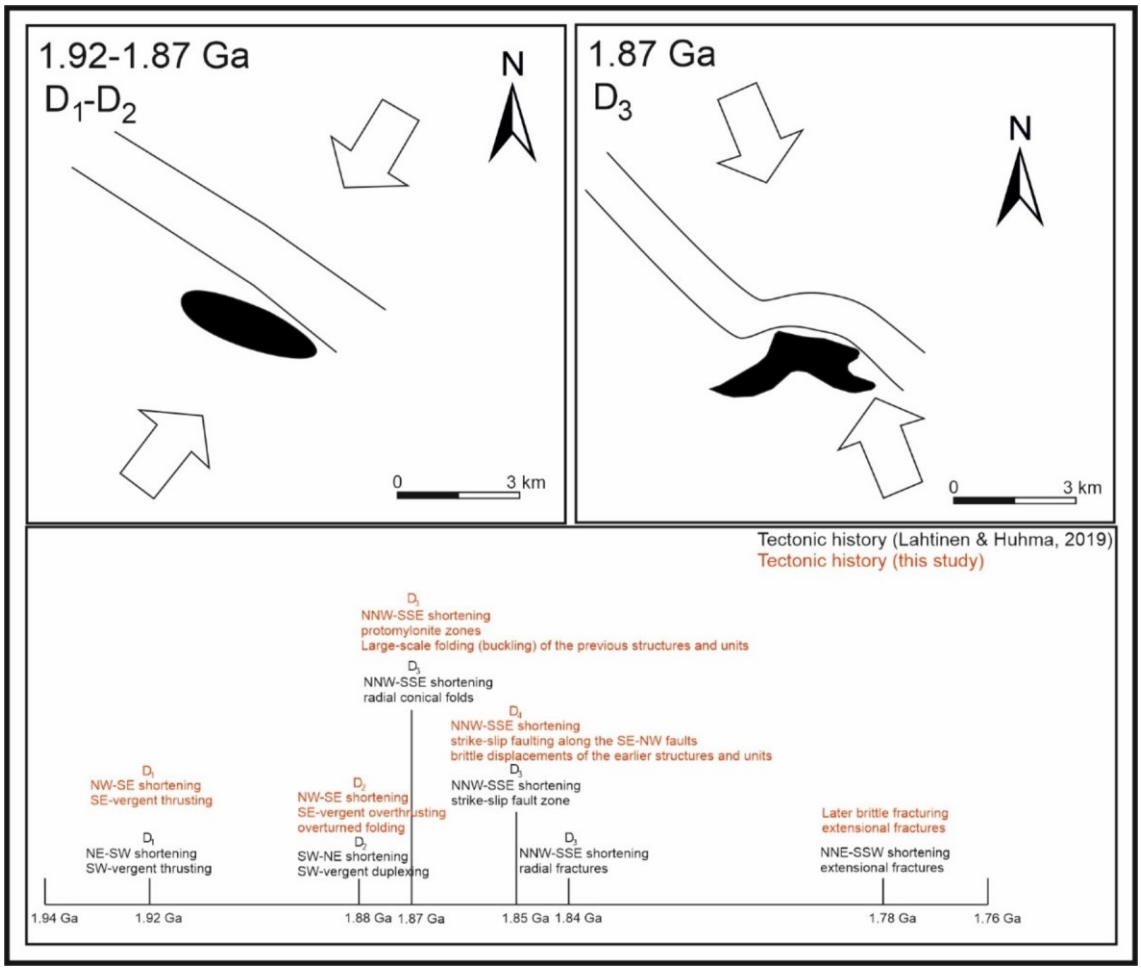

Figure 32. The interpreted D_1-D_3 phases describe the buckling of the earlier structures and rock units against the Sakatti intrusion. Black lines are form lines of rock units. Sakatti intrusion is shown in black. Lower photo represents the timelines of tectonic events represented by Lahtinen & Huhma (2019) and this study.

In overall, the SW-vergent thrusting stage and overturned folding could correspond well to the structural interpretation of the Sodankylä nappe complex presented by Evins & Laajoki (2002). In their proposed model and cross section (fig. 8 C) the study zone would be located in the northernmost end north to the Oratunturi fault, and would be controlled by duplex thrusting, where the thrusts dip to north and the folds are S-vergent. Since the observations of overturned folding and fold vergences are parallel to the results presented in the study of Evins & Laajoki, it is possible that the Sodankylä nappe complex extends further north. In addition, the footwall basal thrust may be one of its thrust sheets. With respect to duplex thrusting, it is recognized as possible mechanism to form the observed type of thrust faulting, since the repeated evaporite

sections above the footwall basal thrust are mechanically weak and support reverse faulting. They were initially located above the schists, which were originally more competent sandstones and could represent the lowermost detachment. However, also other thrust geometries are possible.

5.4 Footwall basal thrust

It was pointed out earlier that the SE-NW faults cut the footwall basal thrust, which indicates that the footwall basal thrust is older than those faults. According to the fault model (fig. 30) the E-W faults 1 and 2 are crosscut by the SE-NW faults and are thus older than these faults. Although the E-W faults were not under investigation in this study, according to the data offered by the company they represent mylonite shear and curve near the contact of the footwall basal thrust with reverse kinematics, which would indicate that they are older than the footwall basal thrust. Since the footwall basal thrust contains fragments from the underlying schists and from the overlying intensively altered picrites, both units are older than the thrust or at least older than the latest stage when the thrust was active. Since these rocks were assigned to the Sodankylä Group and Kevitsa intrusion, of which the latter is younger ~2.05 Ga, the maximum age of the latest time of activity is ~2.05 Ga. However, since the fragments within the thrust represent the brittle deformation phase D_4, it is probable that the latest time of activity was after the ductile phase 1.92-1.87 Ga. The absolute age of the footwall basal thrust cannot be estimated by the data gained in this study, and it is probable that it has been reactivated several times during tectonic history.

With respect to reactivations, it can be assumed that the footwall basal thrust has been active at least three times. The first of these had ductile nature as it is probable that the footwall basal thrust took part in deforming the underlying schists. This is especially supported by the folding intensity that increased closer to the thrust. Kinematic indicators, such as the observed S-C structures, mica fishes and asymmetric folding indicated reverse ductile displacement for the footwall basal thrust, active during the progressive D_1-D_2 phases during the Lapland-Kola orogeny. The second time was also ductile and occurred during the D_3 phase when the protomylonite zones were formed and the footwall basal thrust was buckled. The latest time of activity was during the brittle D_4 phase that was observed as rubble zones, fault breccias and crushed rock fragments.

To form the observed kind of overthrusting, overturned folding and shearing, another counterpart probably exists underneath the footwall basal thrust and below or within the

schist unit, such as a similarly oriented thrust. Otherwise, some variation in the orientations of structures would be expected, contrary to observations. Thus, an existence of a second footwall basal thrust-type thrust is inferred below the schists and the footwall basal thrust that has not yet been reached by drilling.

5.5 Metasomatism and hydrothermal alteration

Post-tectonic epidote group porphyroblasts were referred to be formed by metasomatism and according to Franz & Liebscher (2004) this could be done by mass transport where Ca, Fe and Al-rich schists could have transported these elements to form the epidote group minerals. As mentioned above, especially Ca is enriched in these porphyroblasts while matrix does not show any signs of Ca-enrichments (fig. 28). This mass transfer could have been realized with $CaCl_2$-bearing fluid as transporting agent, although $CaCO_3$ and fluorine are also possible (Franz & Liebscher, 2004). However, the syn-tectonic marialite porphyroblasts, which require NaCl to be stable, could infer that there were free $CaCl_2$ in the system. Additionally, as epidote group minerals and marialite have been recorded to occur commonly together and that in part their thermal stabilities coincide (Vanko & Bishop, 1982), the $CaCl_2$-bearing fluid could well be the transporting agent. The increased Fe and Mn contents in the rims of the porphyroblasts may refer to changes in temperature or oxygen fugacity during the crystallization of the porphyroblasts or afterwards (Keskinen & Liou, 1979). One suitable pathway for the fluids could have been the footwall basal thrust, since the porphyroblasts are located close to it and the core is Ca-rich.

Considering the likely source of Na and Cl required by the marialites, the brecciated Ca-bearing rock unit is considered as an option. The fact that the rocks hosting the marialite porphyroblasts belonged to the intensively altered picrite unit, which was crosscut by anhydrite and gypsum veins previously connected to the underlying brecciated Ca-bearing rock unit, favours this assumption. The origin of marialite may be related to hydrothermal alteration in the vicinity of calcite, anhydrite and gypsum veins and possibly to Na-metasomatism. This type of metasomatism and source of salts have been recorded before in other greenstone belts in Finland as well when they are linked to evaporite deposits (for references, see Köykkä et al. 2019). In addition, Vanko & Bishop (1982) presented a similar genesis for marialite, whose source of salts were evaporites and Na-metasomatism was one of the factors in hydrothermal alteration. According to their study, scapolite occurred as replacements of plagioclase, in veins and in scapolite dikes. Also, in this study the porphyroblasts could represent the replacements of plagioclase.

5.6 Possible sources of error

The performed structural analysis on drill cores contains uncertainties that must be considered in interpretations. The study is based on the very limited amount of oriented drill cores, which represent only a small proportion of the bedrock of the study zone. The number of oriented drill cores that finally penetrated the footwall basal thrust was even smaller. There were not any 2D-sections of the study zone that are typically performed in mapping projects and that would facilitate interpretations. In addition, the drilling orientation influences strongly on observed rock units and drill core intactness (if drilled along fault for instance). Moreover, the stage when the orientation line is drawn on the drill hole includes uncertainties.

6. Conclusions

- The footwall basal thrust is a dominating structure below the ultramafic/mafic main body in the Sakatti deposit, and it mainly follows the contact of ultramafic/mafic rocks and schists, although not in the NW parts of the study zone.
- The footwall basal thrust and the rock units form a large-scale fold, where they dip towards NW west of the large-scale fold's axial trace and towards NE east of it. At the axial trace they dip towards N steeper compared to fold's limbs.
- Kinematic indicators point SE-vergent overthrusting and reverse kinematics for the footwall basal thrust and overturned folding. These structures formed during the D_1-D_2 phases. According to the interpretation the overthrusting was initially SW-vergent, but the later D_3-phase buckled the previous structures and rock units that are now observed as NW-dipping and SE-vergent structures and units west of the axial trace of the large-scale fold. The large-scale fold formed during the D_3 phase.
- The footwall basal thrust has been active at least three times. During the two first times it was ductile and corresponds to the D_1-D_3 phases. The last event was brittle and is related to the D_4 phase. It is probable that the footwall basal thrust has been active several times more.
- The D_4 phase displaced the footwall basal thrust and the rock units in domain A towards SSE along vertical SE-NW conjugate faults in NNW-SSE compression. These displacements indicated strike-slip kinematics.
- Repeated sections of the brecciated Ca-bearing rocks observed in the stratigraphic columns support reverse faulting related to the D_1-D_3 phases.

- Based on this study, the schists, metabasalts and the brecciated Ca- and Mg-bearing rock units correlate well with the Sodankylä Group. The schists could belong to the rocks of the Orajärvi Formation.
- According to geochemistry, the ultramafic/mafic rocks do not correlate well with the Savukoski Group. They correlate much better with the Kevitsa intrusion, which is the suggested correlative unit for these rocks.

7. Acknowledgements

Firstly, I would like to express my gratitude for the AA Sakatti Mining Oy and Anglo American Ltd. for funding this project. I would like to thank the technicians working at AA Sakatti Mining Oy for assisting in drill core sampling, sawing and in other logistical problems related to drill cores. Furthermore, I am grateful to Tuomas Väliheikki and Janne Siikaluoma for their support and ideas of conducting the study, which assisted in planning the work. Additionally, I would like to thank Annukka Torvinen and Outi Ahvenjärvi for their guidance in the QAQC-sampling protocol and data management. Particular thanks to my supervisors Timo Kilpeläinen (University of Turku), Jouni Luukas (GTK) and Olli Räisänen (AA Sakatti Mining Oy) for their expertise and vital guidance in planning the study and in the thesis writing process. Additionally, I would like to thank laboratory technician Arto Peltola for thin section preparation and Timo Saarinen for guidance in micro-XRF analysis. I am truly grateful also to Pietari Skyttä and Jussi Mattila for their advice in drill core investigation and management, which provided many ideas of how to proceed and analyze the drill core data. Lastly, I would like to thank Susanna Metso for her ideas and peer support in drill core logging.

8. References

Arndt, N. 1986: Differentiation of komatiite flows. Journal of Petrology, 27 (2), 279–301.

Arndt, N. 2003: Komatiites, kimberlites, and boninites. J. Geophys. Res., 108, 2293 pp.

Bartlett, W. L., Friedman, M., & Logan, J. M. 1981: Experimental folding and faulting of rocks under confining pressure. Part IX. Wrench faults in limestone layers. Tectonophysics, 79, (3–4), 255-277.

Berthelsen, A., & Marker, M. 1986: 1.9-1.8 Ga old strike-slip megashears in the Baltic Shield, and their plate tectonic implications. Tectonophysics, 128 (3-4), 163-181.

Bhatia, M. R. 1983: Plate tectonics and geochemical composition of sandstones. The Journal of Geology, 91(6), 611-627.

Bogdanova, S. V., Bingen, B., Gorbatschev, R., Kheraskova, T. N., Kozlov, V. I., Puchkov, V. N., & Volozh, Y. A. 2008: The East European Craton (Baltica) before and during the assembly of Rodinia. Precambrian Research, 160 (1-2), 23-45.

Brownscombe, W. 2015: The geology and geochemistry of the Sakatti Cu-Ni-PGE deposit, N. Finland. Doctoral dissertation. Imperial College London, 247 pp.

Brownscombe, W., Ihlenfeld, C., Coppard, J., Hartshorne, C., Klatt, S., Siikaluoma, J. K., & Herrington, R. J. 2015: The Sakatti Cu-Ni-PGE sulfide deposit in northern Finland. In Mineral deposits of Finland (211-252). Elsevier.

Daly, J. S., Balagansky, V. V., Timmerman, M. J., Whitehouse, M. J., De Jong, K., Guise, P., Bogdanova, S., Gorbatschev, R., & Bridgwater, D. 2001: Ion microprobe U-Pb zircon geochronology and isotopic evidence for a trans-crustal suture in the Lapland–Kola Orogen, northern Fennoscandian Shield. Precambrian Research, 105 (2-4), 289-314.

Evins, P. M., & Laajoki, K. 2002: Early Proterozoic nappe formation: an example from Sodankylä, Finland, Northern Baltic Shield. Geological magazine, 139 (1), 73-87.

Fossen, H. 2010: Structural geology. Cambridge University Press. Cambridge. 463 pp.

Franz, G., & Liebscher, A. 2004: Physical and Chemical Properties of the Epidote Minerals–An Introduction-. Reviews in mineralogy and geochemistry, 56 (1), 1-81.

Friedman, G. 1997: Dissolution-collapse breccias and paleokarst resulting from dissolution of evaporite rocks, especially sulfates. Carbonates and Evaporites, 12 (1), 53-63.

Gaál, G., & Gorbatschev, R. 1987: An outline of the Precambrian evolution of the Baltic Shield. Precambrian research, 35, 15-52.

Gorbatschev, R., & Bogdanova, S. 1993: Frontiers in the Baltic shield. Precambrian Research, 64 (1-4), 3-21.

Hanski, E., Huhma, H., Rastas, P., & Kamenetsky, V. S. 2001: The Palaeoproterozoic komatiite–picrite association of Finnish Lapland. Journal of Petrology, 42 (5), 855-876.

Hanski, E. & Huhma, H. 2005: Central Lapland greenstone belt. The Precambrian Geology of Finland-Key to the Evolution of the Fennoscandian Shield. (Vol. 14, pp. 139-193). Elsevier.

Haverinen, J. 2020: Evaporites in Central Lapland Greenstone Belt. 73 pp.

Heaman, L. M. 1997: Global mafic magmatism at 2.45 Ga: Remnants of an ancient large igneous province? Geology, 25 (4), 299-302.

Hesthammer, J., & Fossen, H. 1998: The use of dipmeter data to constrain the structural geology of the Gullfaks Field, northern North Sea. Marine and Petroleum Geology, 15 (6), 549-573.

Holdaway, M. J. 1972: Thermal stability of Al-Fe epidote as a function of fO_2 and Fe content. Contributions to Mineralogy and Petrology, 37 (4), 307-340.

Huhma, H., Hanski, E., Kontinen, A., Vuollo, J., Mänttäri, I., & Lahaye, Y. 2018: Sm-Nd and U-Pb isotope geochemistry of the Palaeoproterozoic mafic magmatism in eastern and northern Finland. Geological Survey of Finland, Bulletin 405, 150 pp.

Hölttä, P., Väisänen, M., Väänänen, J., & Manninen, T. 2007: Paleoproterozoic metamorphism and deformation in Central Lapland, Finland. Geological Survey of Finland, Special Paper, 44, 9-58.

Hölttä, P., Heilimo, E., Huhma, H., Kontinen, A., Mertanen, S., Mikkola, P., Paavola, J., & Sorjonen-Ward, P. 2012: The Archaean of the Karelia province in Finland. Geological Survey of Finland, Special Paper, 54, 9-20.

Hölttä, P. & Heilimo, E. 2017: Metamorphic Map of Finland. Bedrock of Finland at the scale 1:1000 000 – Major stratigraphic units, metamorphism and tectonic evolution. Geological Survey of Finland, Special Paper, 60, 77-128.

Kerr, A. C., Marriner, G. F., Arndt, N. T., Tarney, J., Nivia, A., Saunders, A. D., & Duncan, R. A. 1996: The petrogenesis of Gorgona komatiites, picrites and basalts: new field, petrographic and geochemical constraints. Lithos-Amsterdam, 37 (2), 245-260.

Keskinen, M., & Liou, J. G. 1979: Synthesis and stability relations of Mn-Al piemontite, $Ca_2MnAl_2Si_3O_{12}$ (OH). *American Mineralogist*, *64* (3-4), 317-328.

Kyläkoski, M., Hanski, E., & Huhma, H. 2012: The Petäjäskoski Formation, a new lithostratigraphic unit in the Paleoproterozoic Peräpohja Belt, northern Finland. Bulletin of the Geological Society of Finland, 84, 85-120.

Köykkä, J., Lahtinen, R., & Huhma, H. 2019: Provenance evolution of the Paleoproterozoic metasedimentary cover sequences in northern Fennoscandia: age distribution, geochemistry, and zircon morphology. Precambrian Research 331, 105364.

Köykkä, J., & Luukas, J. 2021: Keski-Lapin litostratigrafia ja paleoproterotsooisen Sodankylän ryhmän kivilajiyksiköiden määrittely. Geological Survey of Finland, Open File Research Report 13/2021. 63 pp.

Lahtinen, R., Korja, A., & Nironen, M. 2005: Paleoproterozoic tectonic evolution. In Developments in precambrian geology,14, 481-531.

Lahtinen, R., Garde, A. A., & Melezhik, V. A. 2008: Paleoproterozoic evolution of Fennoscandia and Greenland. Episodes, 31 (1), 20.

Lahtinen, R., Korja, A., Nironen, M., & Heikkinen, P. 2009: Palaeoproterozoic accretionary processes in Fennoscandia. Geological Society, London, Special Publications, 318 (1), 237-256.

Lahtinen, R., Hölttä, P., Kontinen, A., Niiranen, T., Nironen, M., Saalmann, K., & Sorjonen-Ward, P. 2011: Tectonic and metallogenic evolution of the Fennoscandian Shield: Key questions with emphasis on Finland. Geological Survey of Finland, Special Paper, 49, 23-33.

Lahtinen, R., Huhma, H., Lahaye, Y., Jonsson, E., Manninen, T., Lauri, L. S., Bergman, S., Hellström, F., Niiranen, T., & Nironen, M. 2015a: New geochronological and Sm–Nd constraints across the Pajala shear zone of northern Fennoscandia: Reactivation of a Paleoproterozoic suture. Precambrian Research, 256, 102-119.

Lahtinen, R., Sayab, M., & Karell, F. 2015b: Near-orthogonal deformation successions in the poly-deformed Paleoproterozoic Martimo belt: Implications for the tectonic evolution of Northern Fennoscandia. Precambrian Research, 270, 22-38.

Lahtinen, R., & Huhma, H. 2019: A revised geodynamic model for the Lapland-Kola Orogen. Precambrian Research, 330, 1-19.

Lehtonen, M., Airo, M. L., Eilu, P., Hanski, E., Kortelainen, V., Lanne, E., Manninen, T., Rastas, P., Räsänen, J., & Virransalo, P. 1998: Kittilän vihreäkivialueen geologia. Geological Survey of Finland, Report of investigation 140. 144 pp.

Manninen, T. 1991: Sallan alueen vulkaniitit. Geological Survey of Finland, Report of Investigation 104. 97 pp.

Manninen, T., & Huhma, H. 2001: A new U-Pb zircon constraint from the Salla schist belt, northern Finland. Geological Survey of Finland, Special Paper, 33, 201-208.

Melezhik, V. A., Fallick, A. E., Hanski, E. J., Kump, L. R., Lepland, A., Prave, A. R., & Strauss, H. 2005: Emergence of the aerobic biosphere during the Archean-Proterozoic transition: challenges of future research. GSA Today, 15 (11), 4-11.

Melezhik, V. A. 2006: Multiple causes of Earth's earliest global glaciation. Terra Nova, 18 (2), 130-137.

Molnár, F., Middleton, A., Stein, H., Hugh, O., Lahaye, Y., Huhma, H., ... & Johanson, B. 2018: Repeated syn-and post-orogenic gold mineralization events between 1.92 and 1.76 Ga along the Kiistala Shear Zone in the Central Lapland Greenstone Belt, northern Finland. *Ore Geology Reviews*, *101*, 936-959.

Mutanen, T. 1997: Geology and ore petrology of the Akanvaara and Koitelainen mafic layered intrusions and the Keivitsa-Satovaara layered complex, northern Finland. Geological Survey of Finland, Bulletin 395. 233 pp.

Mutanen, T., & Huhma, H. 2001: U-Pb geochronology of the Koitelainen, Akanvaara and Keivitsa layered intrusions and related rocks. Geological Survey of Finland, Special Paper 33, 229-246.

Niiranen, T., Poutiainen, M., & Mänttäri, I. 2007: Geology, geochemistry, fluid inclusion characteristics, and U–Pb age studies on iron oxide–Cu–Au deposits in the Kolari region, northern Finland. Ore Geology Reviews, 30 (2), 75-105.

Nikula, R. 1988: Palaeosedimentology of Precambrian tidal Virttiövaara and fluvial Värttiövaara quartzite formations in Sodankylä, Northern Finland. Geological Survey of Finland, Special Paper 5, 177-188.

Nironen, M. 2017: Structural interpretation of the Peräpohja and Kuusamo belts and Central Lapland, and a tectonic model for northern Finland. Geological Survey of Finland, Report of Investigation 234, 53 pp.

Patison, N. L. 2007: Structural controls on gold mineralization in the Central Lapland Greenstone Belt. Geological Survey of Finland, Special Paper, 44, 107-124.

Peltonen, P., Huhma, H., Santaguida, F., & Beresford, S. 2014: U-Pb zircon and Sm-Nd isotopic constraints for the timing and origin of magmatic Ni-Cu-PGE deposits in northern Fennoscandia. SEG 2014 Conference: Building Exploration Capability for the 21st Century.

Piippo, S., Skyttä, P., & Kloppenburg, A. 2019: Linkage of crustal deformation between the Archaean basement and the Proterozoic cover in the Peräpohja Area, northern Fennoscandia. Precambrian Research, 324, 285-302.

Poli, S., & Schmidt, M. W. 2004: Experimental subsolidus studies on epidote minerals. Reviews in mineralogy and geochemistry, 56 (1), 171-195.

Rastas, P., Huhma, H., Hanski, E., Lehtonen, M. I., Härkönen, I., Kortelainen, V., Mänttäri, I., & Paakkola, J. 2001: U-Pb isotopic studies on the Kittila greenstone area, central Lapland, Finland. Geological Survey of Finland, Special Paper 33, 95-141.

Räsänen, J. 2008: Keski-Lapin liuskevyöhykkeen geologinen kehitys Sodankylän liuskealueella. Geological Survey of Finland, Report of Investigation, Rovaniemi. 22 pp.

Räsänen, J. 2018: Orajärvi formation. Geological unit report. Bedrock of Finland at a scale 1: 200 000. Geological Survey of Finland.

Sorjonen-Ward, P., Nironen, M., & Luukkonen, E. J. 1997: Greenstone associations in Finland. Oxford Monographs on Geology and Geophysics, 35 (1), 677-698.

Spear, F. S. 1981: An experimental study of hornblende stability and compositional variability in amphibolite. *American Journal of Science*, *281* (6), 697-734.

Stipp, M., Stünitz, H., Heilbronner, R., & Schmid, S. M. 2002: Dynamic recrystallization of quartz: correlation between natural and experimental conditions. Geological Society, London, Special Publications, 200 (1), 171-190.

Vaasjoki, M., Korsman, K., Koistinen, T., 2005: Chapter 1: Overview. In: Lehtinen, M., Nurmi, E.A. The Precambrian Geology of Finland- Key to the Evolution of the Fennoscandian Shield. Elsevier B.V., Amsterdam, 1-18.

Vanhanen, E. 2001: Geology, mineralogy and geochemistry of the Fe-Co-Au-(U) deposits in the Paleoproterozoic Kuusamo schist Belt, northeastern Finland. Geological Survey of Finland, Bulletin 399. 229 pp.

Vanko, D. A., & Bishop, F. C. 1982: Occurrence and origin of marialitic scapolite in the Humboldt Lopolith, NW Nevada. Contributions to Mineralogy and Petrology, 81 (4), 277-289.

Verma, S. P., & Armstrong-Altrin, J. S. 2013: New multi-dimensional diagrams for tectonic discrimination of siliciclastic sediments and their application to Precambrian basins. Chemical Geology, 355, 117-133.

Väisänen, M. 2002: Structural features in the central Lapland greenstone belt, northern Finland. Geological Survey of Finland, archive report K 21, 3. 20 pp.

Warren, J. K. 2010: Evaporites through time: Tectonic, climatic and eustatic controls in marine and nonmarine deposits. Earth-Science Reviews, 98 (3-4), 217-268.

Appendix 1. Major element geochemical analysis results of mafic volcanic rocks

Sample	Hole ID	Unit	From	To	SiO2	Al2O3	Fe2O3	MgO	CaO	Na2O	K2O	TiO2	P2O5	MnO	Cr2O3
FMOS135252	19MOS8238	Altered metaperidotite	903,98	904,33	47,33	8,77	8,8	21,52	5,7	1,03	0,1	0,82	0,03	0,11	0,262
FMOS135254	18MOS8226	Altered metaperidotite	860,49	860,69	42,86	7,6	7,03	17,98	4,2	4,15	0,01	0,71	0,03	0,1	0,291
FMOS135264	17MOS8193	Altered metaperidotite	828,71	828,91	44,85	9,2	7,04	20,26	5,27	2,13	0,11	0,83	0,03	0,1	0,226
FMOS135265	17MOS8193	Altered metaperidotite	834,92	835,12	47,26	9,62	12,8	17,68	2,11	2,52	2,61	0,88	0,06	0,09	0,243
FMOS135270	17MOS8177	Altered metaperidotite	699,31	699,71	49,43	9,76	9,15	20,9	6,05	2,52	0,1	0,64	0,02	0,12	0,268
FMOS135272	17MOS8177	Altered metaperidotite	657,45	657,84	42,69	5,47	11,06	31,83	4,46	0,9	0,28	0,42	0,04	0,17	0,557
FMOS135273	17MOS8177	Altered metaperidotite	682,43	682,83	47,93	9,54	9,78	18,52	7,75	2,19	0,22	0,75	0,04	0,15	0,263
FMOS135274	17MOS8177	Altered metaperidotite	729,25	729,65	43,86	7,13	10,7	23,28	3,41	0,63	3,23	0,6	0,04	0,23	0,394
FMOS135309	12MOS8075	Altered metaperidotite	531,78	531,98	49,64	10,09	6,35	21,64	1,15	1,6	1,26	0,92	0,09	0,02	0,288
FMOS135315	18MOS8233	Altered metaperidotite	798,44	798,64	45	8,03	10,77	21,4	4,96	0,82	1,03	0,73	0,02	0,11	0,334
FMOS135316	18MOS8233	Altered metaperidotite	825,23	825,43	46,64	9,68	9,74	19,27	2,49	2,01	3,56	0,9	0,03	0,08	0,234
FMOS135317	17MOS8200	Altered metaperidotite	780,12	780,52	47,53	9,65	10,54	17,05	8,65	2,3	0,16	0,86	0,03	0,13	0,236
FMOS135318	17MOS8200	Altered metaperidotite	796,48	796,88	45,34	8,34	11,51	17,91	4,81	2,18	1,89	0,59	0,03	0,14	0,217
FMOS135330	12MOS8078	Altered metaperidotite	751,32	751,52	47,4	9,88	5,37	25,06	0,84	0,54	4	0,94	0,05	0,01	0,278
FMOS135332	12MOS8090	Altered metaperidotite	1032,09	1032,49	49,23	13,95	12,35	7,46	10,05	4,49	0,26	0,78	0,07	0,07	0,024
FMOS135253	19MOS8238	Aphanite	943,66	944,06	48,35	9,79	9,65	20,01	6,47	2,49	0,09	0,86	0,03	0,11	0,234
FMOS135301	18MOS8231B	Aphanite	997,39	997,81	45,4	7,55	7,99	26,01	5,41	0,35	0,34	0,23	0,02	0,09	0,353
FMOS135321	17MOS8190	Aphanite	305,08	305,28	49,26	10,22	9,71	15,62	7,61	2,72	0,54	0,77	0,07	0,09	0,213
FMOS135324	12MOS8112	Aphanite	851,41	851,61	48,42	9,56	11,58	18,74	7,33	2,36	0,05	0,87	0,04	0,15	0,287
FMOS135325	12MOS8112	Aphanite	947,65	947,85	47,86	9,55	12,19	17,58	7,85	2,32	0,14	0,87	0,09	0,16	0,256
FMOS135329	12MOS8078	Aphanite	703,36	703,56	48,16	9,37	11,79	18,36	7,93	2,34	0,09	0,86	0,04	0,15	0,288
FMOS135333	12MOS8090	Aphanite	942,74	942,94	46,99	8,7	10,61	17,55	9,26	1,81	1,38	0,89	0,05	0,07	0,272
FMOS135334	12MOS8090	Aphanite	872,3	872,5	47,92	9,52	11,48	17,73	8,07	2,22	0,17	0,91	0,06	0,12	0,266
FMOS135289	12MOS8118	Basalt	1016,46	1016,66	50,39	13,56	15,53	4,64	3,92	6,49	1,06	2,5	0,36	0,05	0,007
FMOS135297	18MOS8231B	Basalt	934,17	934,57	55,18	16,94	4,46	9,24	0,55	6,71	3,87	0,62	0,06	0,01	0,021
FMOS135312	12MOS8075	Basalt	692,86	693,06	50,73	14,7	10,26	6,07	6,13	6,41	0,82	0,81	0,09	0,08	0,027
FMOS135293	19MOS8237	Mg-peridotite	917,91	918,32	28,33	0,69	9,77	34,09	0,13	0,09	0,26	0,06	0,02	0,12	0,761
FMOS135300	18MOS8231B	Mg-peridotite	975,68	976,08	28,92	1,08	9,05	33,92	0,24	0,11	0,53	0,09	0,02	0,13	0,744
FMOS135276	12MOS8118	Metaperidotite	855,29	855,69	37,14	1,11	9,53	42,72	0,71	0,02	0,13	0,09	0,02	0,12	0,646
FMOS135283	12MOS8118	Metaperidotite	916,6	917	37,38	0,91	9,12	45,9	0,67	0,01	0,01	0,07	0,03	0,12	0,919
FMOS135304	18MOS8231B	Metaperidotite	910,95	911,34	35,57	1,01	10,66	42,83	0,24	0,01	0,01	0,07	0,02	0,12	1,284
FMOS135306	18MOS8231B	Metaperidotite	986,5	986,9	38	3,26	7,67	36,58	0,86	0,02	0,01	0,12	0,02	0,08	0,36
FMOS135307	18MOS8231	Metaperidotite	1026,75	1027,15	37	1,63	10,29	41,23	1,26	0,2	0,1	0,14	0,02	0,13	0,823
FMOS135308	18MOS8231	Metaperidotite	1044,07	1044,47	39,32	2,13	10,81	37,36	2,61	0,28	0,11	0,18	0,02	0,13	0,843
FMOS135262	18MOS8226	Metavolcanic rock	948,37	948,57	50,87	15,61	9,39	6,18	8,9	3,69	0,67	2,8	0,27	0,08	0,006
FMOS135266	17MOS8193	Metavolcanic rock	937,14	937,34	46,49	13,58	14,64	9,46	8,6	3,24	0,64	1,51	0,15	0,15	0,083
FMOS135267	17MOS8193	Metavolcanic rock	1008,32	1008,52	48,86	13,86	13,68	9,18	6,37	3,97	1,57	0,99	0,08	0,14	0,041

Appendix 2. Major element geochemical analysis results of metasedimentary rocks and breccias

Sample	Hole ID	Unit	From	To	SiO2	Al2O3	Fe2O3	MgO	CaO	Na2O	K2O	TiO2	P2O5	MnO	Cr2O3
FMOS135275	12MOS8118	Carbonate breccia	827,84	828,24	14,31	2,03	2	13,02	24,55	1,07	0,03	0,1	0,03	0,04	0,008
FMOS135279	12MOS8118	Carbonate breccia	880,17	880,57	6,45	0,01	2,92	14,09	27,49	0,01	0,01	0,01	0,07	0,08	0,002
FMOS135282	12MOS8118	Carbonate breccia	898,57	898,97	18,4	2,86	2,61	15,53	20,52	1,15	0,05	0,14	0,06	0,07	0,011
FMOS135287	12MOS8118	Carbonate breccia	1005,18	1005,38	31,2	7,19	3,75	7,91	18,62	3,89	0,37	0,35	0,06	0,04	0,011
FMOS135294	19MOS8237	Carbonate breccia	938,33	938,53	19,43	1,14	1,07	15,56	24,11	0,64	0,01	0,04	0,02	0,03	0,002
FMOS135255	18MOS8226	Fault breccia	891,57	891,77	42,34	8,52	2,18	5,63	16,81	5,03	0,04	0,38	0,11	0,13	0,024
FMOS135286	12MOS8118	Fault breccia	964,29	964,49	36,98	3,61	5,78	23,68	9,4	0,54	1,56	0,28	0,01	0,08	0,49
FMOS135305	18MOS8231B	Fault breccia	927,07	927,47	44,68	10,14	4,41	16,33	2,45	5,06	1,07	0,46	0,22	0,06	0,013
FMOS135295	19MOS8237	Mafic breccia	962,96	963,16	40,95	13,65	7,17	22,35	0,88	0,94	7,64	2,06	0,02	0,03	0,016
FMOS135296	19MOS8237	Mafic breccia	958,13	958,33	53,91	7,12	4,87	24,9	0,06	0,45	3,92	0,34	0,01	0,01	0,031
FMOS135310	12MOS8075	Mafic breccia	611,23	611,63	48,08	11,81	4,88	8,04	8,64	6,49	0,16	0,49	0,06	0,06	0,022
FMOS135278	12MOS8118	Magnesite breccia	872,51	872,91	14,11	0,85	10,41	34,85	1,85	0,47	0,02	0,1	0,07	0,19	0,016
FMOS135284	12MOS8118	Magnesite breccia	945,57	945,77	18,74	2,58	9,39	31,4	2,18	1,52	0,01	0,09	0,06	0,17	0,014
FMOS135285	12MOS8118	Magnesite breccia	950,22	950,42	13,16	0,28	9,53	34,65	4,62	0,14	0,02	0,01	0,18	0,2	0,006
FMOS135299	18MOS8231B	Magnesite breccia	953,61	954,02	24,78	4,61	7,58	24,04	8,36	0,14	3,15	0,16	0,04	0,07	0,01
FMOS135256	18MOS8226	Schist	910,48	910,68	37,59	2,3	3,07	8,08	21,4	0,68	0,42	0,2	0,09	0,14	0,008
FMOS135259	18MOS8226	Schist	926,2	926,4	23,74	5,73	4,42	16,45	22,48	2,32	0,25	0,52	0,08	0,21	0,008
FMOS135260	18MOS8226	Schist	942,37	942,57	39,25	10,66	9,84	11,87	12,5	3,75	0,7	1,08	0,08	0,13	0,023
FMOS135263	18MOS8226	Schist	949,98	950,15	52,02	13,46	8,93	6,66	5,24	3,35	3,05	0,86	0,13	0,03	0,018
FMOS135268	17MOS8193	Schist	1031,29	1031,49	46,8	10,48	3,36	11,81	9,99	2,03	4,53	0,43	0,1	0,05	0,016
FMOS135269	17MOS8193	Schist	1025,46	1025,58	53,97	15,64	8,21	9,46	0,44	5,25	3,72	0,68	0,05	0,03	0,026
FMOS135288	12MOS8118	Schist	1003,82	1004,02	9,98	1,41	2,97	18,92	26,73	0,83	0,03	0,07	0,26	0,15	0,002
FMOS135290	12MOS8118	Schist	1034,67	1034,87	23,09	2,97	2,63	7,41	27,03	1,04	0,53	0,25	0,05	0,08	0,007
FMOS135292	12MOS8118	Schist	1025,41	1025,61	47,07	12,04	7,39	8,77	11,16	3,08	2	0,71	0,11	0,08	0,024
FMOS135313	12MOS8075	Schist	752,38	752,58	29,89	8,76	6,71	13,55	16,78	2,52	0,3	1,07	0,08	0,18	0,018
FMOS135314	12MOS8075	Schist	779,01	779,21	41,55	10,34	8,69	10,36	12,08	3,52	0,26	0,98	0,1	0,12	0,021
FMOS135320	17MOS8190	Schist	417,92	418,12	60,16	16,84	7,64	5,08	0,3	1,44	4,92	0,56	0,1	0,02	0,021
FMOS135326	12MOS8112	Schist	983,07	983,27	65,17	18,49	0,77	1,23	0,93	10,61	0,01	1,06	0,02	0,02	0,015
FMOS135327	12MOS8112	Schist	991,69	991,89	55,08	16,84	9,68	5,62	2,27	5,45	2,45	0,84	0,18	0,01	0,021
FMOS135328	12MOS8112	Schist	1003,08	1003,28	20,61	3,75	2,61	10,25	25,83	1,47	0,45	0,26	0,13	0,13	0,022

Appendix 3. Photographs of rock types

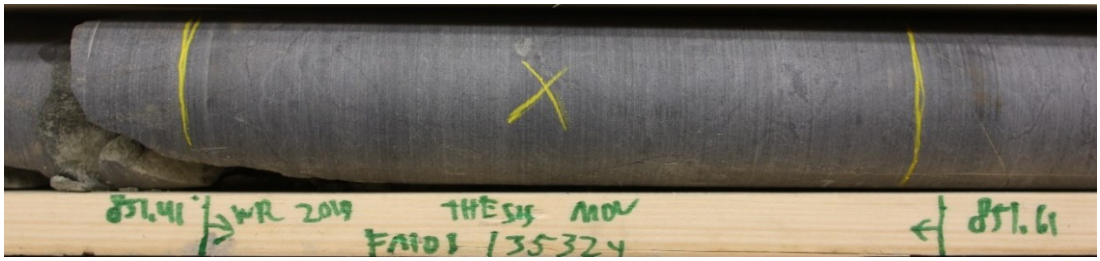

Aphanite rock with characteristic flow-top breccia structure.

Metaperidotite with typical cumulus-texture and of medium-coarse grain size. Cu-mineralized carbonate vein crosscuts the metaperidotite.

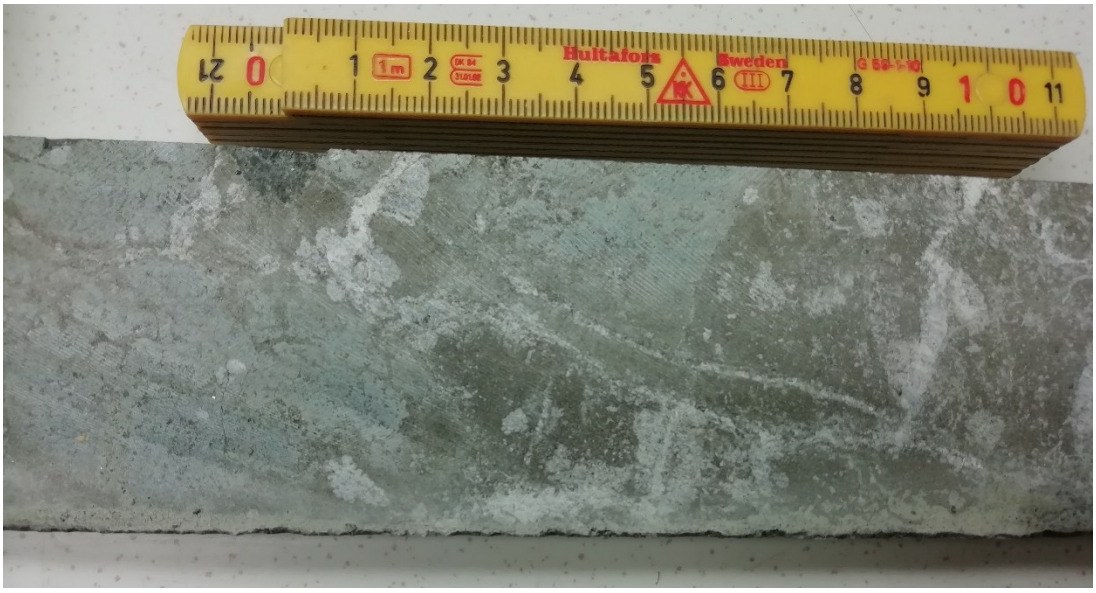

Intensively altered non-sheared picrite and characteristic greenish and brownish coloured pervasive alteration. Carbonate veins crosscut the altered peridotite rocks. The cumulus-texture weakly seen in the background.

Intensively altered and sheared picrite and characteristic greenish and brownish coloured pervasive alteration. Carbonate veins are oriented mainly parallel to overall foliation.

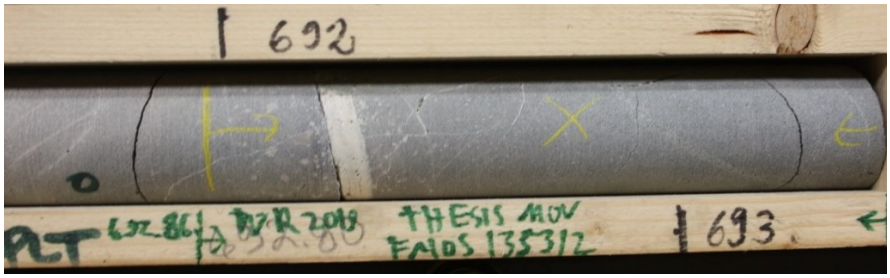

Basalt vein within the footwall basal thrust.

Example of fault breccia found within the footwall basal thrust. Note the angular clasts accompanied with poor sorting and chaotic texture.

Typical carbonate brecciated Ca-bearing rock with sub-rounded and subangular clasts.

Brecciated Mg-bearing rock with characteristic yellow colour in matrix.

Mafic breccia with chaotic texture and mainly mafic clasts.

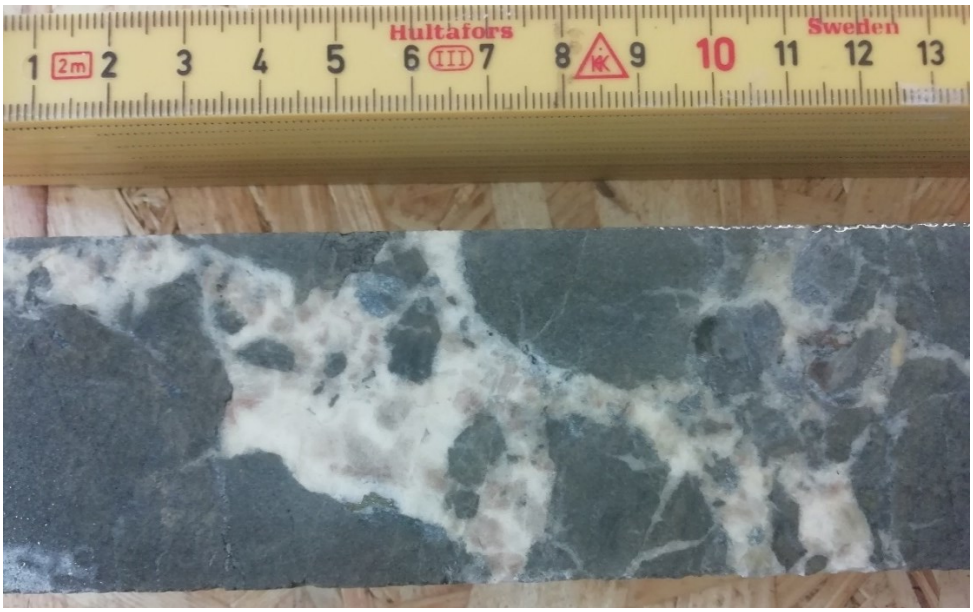

Ultramafic fragments within brecciated Ca-bearing rock close to the upper contact.

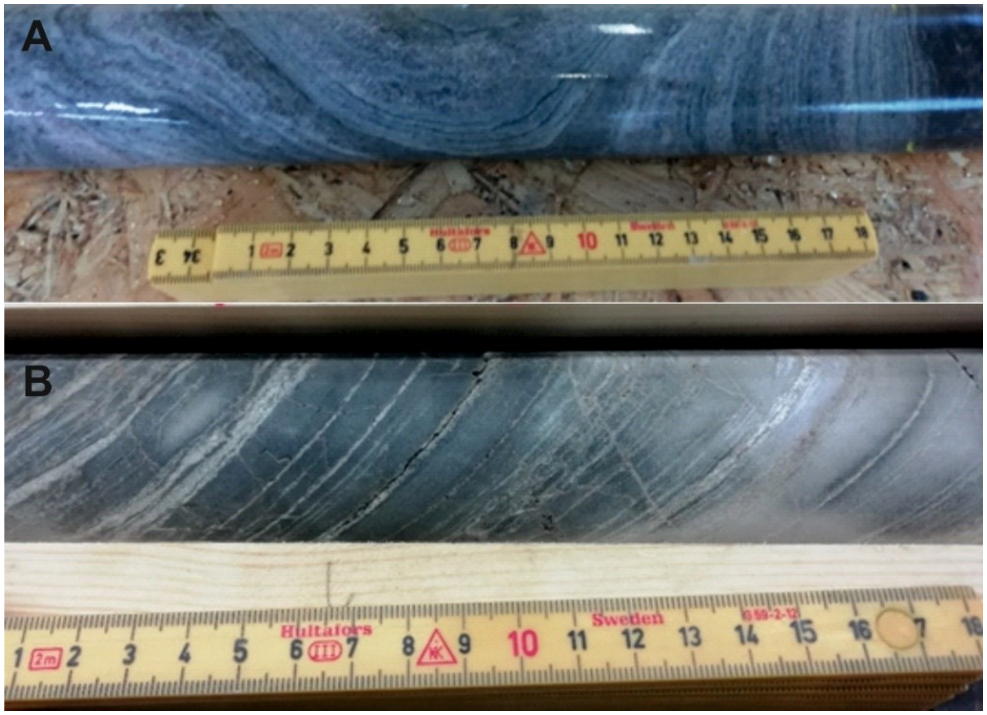

Two subunits of schists; A: Folded Ca-rich schist and B: Intensively sheared Ca-poor schist.

Metabasalt in drill hole 17MOS8193.